Development of Extracellular and Intracellular Gene Delivery System for Cancer-selective Polymeric Nanocarrier

中村, 雄太

出版情報：九州大学, 2016, 博士（工学）, 課程博士
バージョン：
権利関係：

Development of Extracellular and Intracellular Gene Delivery System for Cancer-selective Polymeric Nanocarrier

Graduate School of Systems Life Sciences

Kyushu University

2017

Yuta Nakamura

Abstract

Development of Extracellular and Intracellular Gene Delivery System for Cancer-selective Polymeric Nanocarrier

Yuta Nakamura

Doctor of Philosophy
Graduate School of System Life Sciences
Kyushu University
2017

The author group has developed polymeric nanocarriers for a cancer-specific gene delivery system. Previous studies achieved the cancer-selective gene expression and the principle design of peptide-polymer conjugates. Development of peptide-polymer conjugates provided the activation of gene expression in a cancer tissue compared to a normal tissue. However, previous peptide-polymer conjugates had a lot of challenges in clinical use. Firstly, previous developed polymers showed low stability of a polyplex in blood, although systemic administration like intravenous injection is a desirable administration technique for *in vivo* DNA delivery. Secondly, multiple synthetic route of a peptide-polymer conjugate is another disadvantage for practical use requiring of reproducible mass production. Thirdly, the key factors to secure cancer-selective gene expression remain to be completely elucidated. Thus, the author examined following three categories; 1) stabilization of the polyplex in blood, 2) synthesis scheme for practical use, and 3) principle design of peptide-polymer conjugates for the goal of this cancer-selective gene expression system.

In chapter 1, the author introduced a possibility of nanocarriers and gene delivery to cancer therapy. Numerous efforts have been made to exploit to cancer-targeted technology and multiple functions nanocarriers for safe and efficient gene delivery. Then the author described the cancer-selective gene expression system and the target of this system, protein kinase Cα (PKCα).

In chapter 2, the author developed a new technique to stabilize a polyplex composed of plasmid DNA (pDNA) and a linear polyetheleneimine (LPEI) by serum albumin coating. Serum albumin has been utilized as a drug carrier due to inherent stability and function as a blood protein. However, previous reported ternary complexes including pDNA, LPEI, and serum albumin were not applicable for intravenous injection. In this study, the author modified a stearoyl group on LPEI as a specific ligand for serum albumin. As the result, the ternary complex has excellent stability under physiological saline condition with keeping the original diameter and prevented aggregation of red blood cells. The ternary complex has equivalent transfection ability to LPEI while the cytotoxicity is significantly lower than LPEI itself. Therefore, the ternary complex is potentially useful for *in vivo* DNA delivery with high blood stability.

In chapter 3, the author examined *in vitro* performance of branched polyethylenimine (BPEI)-based gene carriers which respond to cancer-specific activation of PKCα to express pDNA. The carriers were synthesized straightforward by using amide bond formation between a peptide terminal carboxyl and a primary amine group of BPEI. To examine the effect of the peptide contents in the carrier, the author prepared several carriers with various peptide contents. As the results, the optimum content of the peptides was demonstrated to the clear-cut response to PKCα.

In chapter 4, the author investigated the effect of linker length between peptide and polymer backbone for cancer-selective gene expression responding to PKCα. The

linker was composed of hydrophilic segments and the linker length was controlled by repeated coupling of the segment in solid-phase peptide synthesis. The author synthesized some peptide-polymer conjugates with various length of the linker moieties. The linker enhanced the stability of polyplex against anionic exchange between pDNA and heparin. The carriers with critical linker length increased PKCα responsiveness by 10 times. Thus, linker length is one of the important factors for cancer-selective gene expression system.

In chapter 5, the author summarized these techniques and application for cancer specific gene delivery system.

Table of contents

1. Introduction

Gene therapy is a simple and powerful tool of medicine because transduction of therapeutic genes to diseased cells can treat intractable diseases with their genetic level. The first clinical trial in 1990 for treatment of adenosine deaminase deficiency (ADA), which has the risk of a serious complication, demonstrated the potential of gene therapy. In the last few decades, over 2,400 clinical trials covered the treatment of cancers, genetic disorders, and infections (**Figure 1.1**) [1]. Recently, development of gene delivery technology has been investigated intensively and combined with wide variety of material sciences, focusing on the development of gene carriers due to its importance. Although this technology has not realized ideal carriers satisfying the practical application, many types of promising carriers have been demonstrated.

In this thesis, I tried to develop some gene delivery systems using nanocarriers. Nanocarriers are one of non-virus vectors and can be prepared chemically so that the quality control and mass production are much easier in manufacture process than virus vectors. This chapter introduces background information of nanocarriers and previous researches.

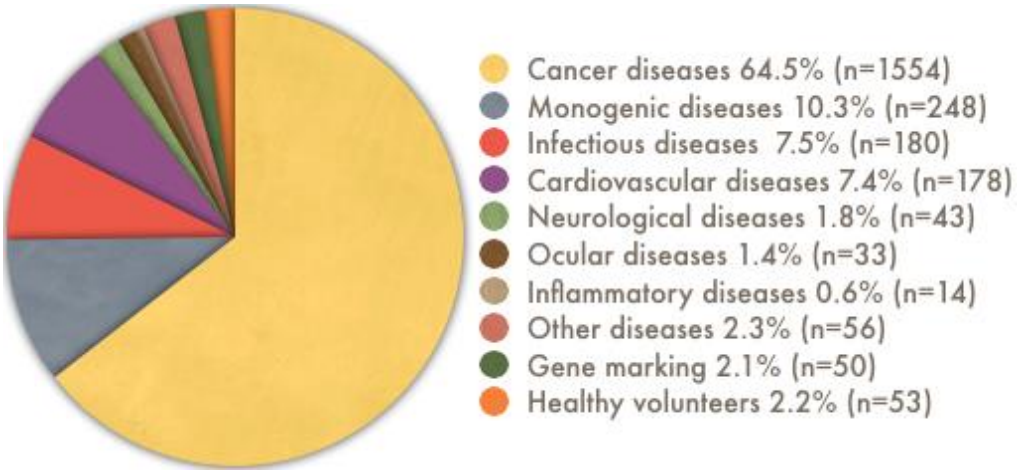

Figure 1.1. Clinical targets for gene therapy. Reproduced with permission from [1] Copyright © 2016 John Wiley and Sons Ltd.

1.1. Nanocarriers for advanced gene delivery

Development of nanocarriers has been extensively studied as the nano-sized medical device which is capable of delivering drugs, DNA, RNA, proteins, and imaging agents into diseased cells with high efficiency [2-4]. Because nanocarriers are similar in size to biologic molecules, delivery system using nanocarriers have potential for stable circulation in blood stream and easiness to reach to target tissues and cells by means of utilizing pathophysiological function [5-7]. In addition, other functions to decrease drug degradation and to control bio-distribution can be designed in nanocarriers to achieve both maximum therapeutic effects and minimum side effects. Thus, nanocarriers have been adapted for leading-edge medical care.

Although gene therapy is effective to treat intractable diseases, development of nanocarriers is indispensable for effective gene delivery system [8-9]. For example, in the case of cancer treatment, tumor suppressor genes and suicide genes show efficient therapeutic effects against cancers [10-13]. However, expression of these therapeutic genes in normal cells has risk of serious adverse effects [14-15]. Therefore, cancer-selective gene delivery is necessary technology to control gene expression and side effects. Thus, a number of nanocarriers have been investigated for safe and efficient gene delivery.

Multiple functions of nanocarriers arise from a variety of materials including lipids, polymers, dendrimers, peptides, and other substances [16-17]. Material design directly affects the ability of nanocarriers. In particular, thousands of polymers have been investigated due to highly defined molecular design and simple manufacturing preparation which could be advantageous in clinical supply. Previously, polyethyleneimine (PEI), poly(L-lysine) (PLL), chitosan, and their derivatives have demonstrated as nanocarriers for gene delivery with high gene expression by forming

stable polyplex with DNA [18-19]. On the other hand, biocompatible polymers such as polyethylene glycol (PEG) are commonly bound to nanocarriers due to increase stability of polymeric nanocarriers in blood stream by controlling undesired interaction with biogenic substances [20-22]. Moreover, chemical modification to polymeric nanocarriers such as ligands and other functional groups contribute to gene delivery efficiency.

Probably, one of the most important applications of gene nanocarriers will be cancer treatment. In a solid tumor tissue, tight junction of endothelium in tumor neovasculature is incomplete so that huge substances such as proteins or nano-particles can be leaked from the blood vessels (**Figure 1.2**). Immature lymph duct cannot excrete the accumulated nano-particles from the tumor tissue. Thus, nano-particles can be accumulated in solid tumor tissue through this effect if the nano-particle can be circulated stably in blood stream. This effect is known as the enhanced permeability and retention (EPR) effect and this is one of the most versatile and effective way for tumor specific drug accumulation [23-24]. Through this effect, effectiveness of treatment and reduction of adverse effect can be improved. In this context, nanocarriers which form nano-size complex with genetic medicine are essential in tumor gene delivery. However, such carriers should have following two important features to exhibit high therapeutic efficiency; 1) high stability of carrier/genetic medicine polyplex in blood circulation, 2) high specificity to tumor cells of the polyplex.

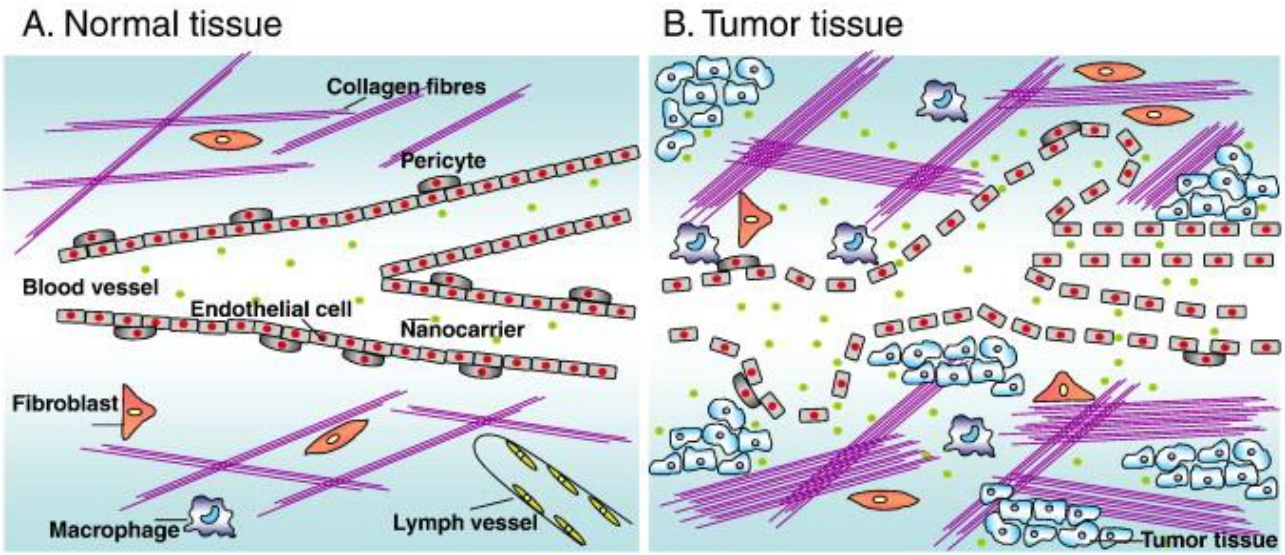

Figure 1.2. Differences between normal and tumor tissues. Tumor tissue composed of incomplete neovasculature and immature lymph duct that explain nano-particle accumulation by enhanced permeability and retention (EPR) effect. Reproduced with permission from [24] Copyright © 2010 Elsevier B.V. All rights reserved.

1.2. Current design of polymeric nanocarrier

Various improvements in gene-nanocarriers have been made with molecular design according to the results from *in vitro* and *in vivo* application. Intravenous administration will be the most versatile way to gene delivery system in systemic application [25-26]. However, nanocarrier has to overcome extra- and intracellular barriers *in vivo* gene delivery (**Figure 1.3**) [27-28].

At first, nanocarrier has to render the delivered genetic medicine a resistance against nuclease, because DNA molecule is quickly degraded by blood nucleases. For this point, polycation is generally used as gene nanocarrier to make tight complex with DNA to suppress the access of nucleases. However, the positive charge promotes undesired interaction with blood components to prohibit the stable blood circulation. Therefore, any measure has to be taken to reduce this interaction. Also, unexpected immune responses should be avoided.

In addition to such systemic barriers, intracellular barriers also exist. A DNA molecule has poor permeability against plasma membrane. Polycationic nanocarrier partially overcomes this issue, but the polyplex between nanocarrier and DNA is generally taken up with endocytosis. In this process, a DNA/carrier complex is wrapped with endosome and is transported to lysosome in which the DNA is degraded. Thus, nanocarrier also has to escape from the endosome before reaching to lysosome. These hurdles can be overcome at least partially with an appropriate design of carrier.

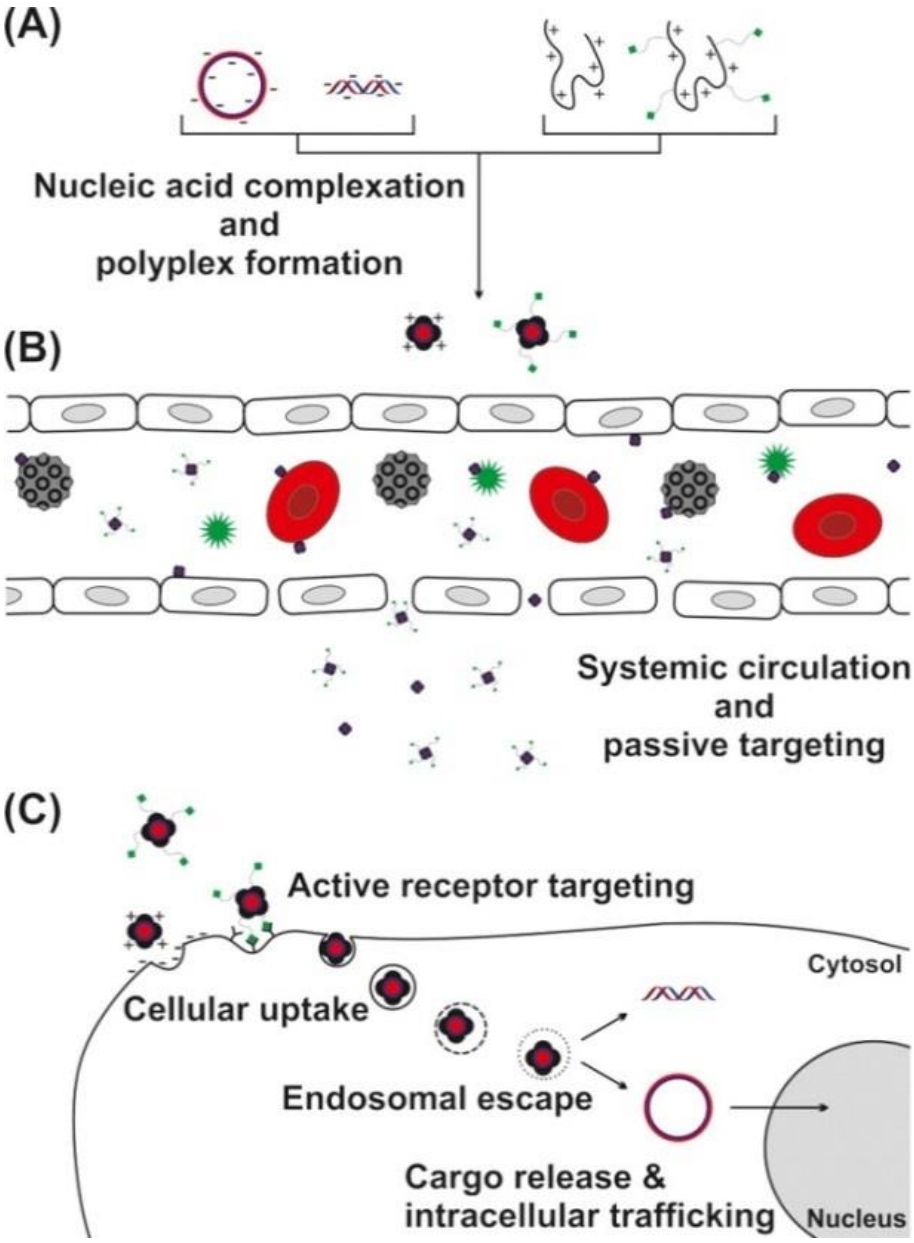

Figure 1.3. Extracellular and intracellular barriers in gene delivery system of polymeric nanocarrier. (A) Formation of stable polyplex of DNA/polymer complex. (B) Advance through bloodstream with avoiding systemic clearance and accumulation in a tumor tissue. (C) Cellular obstacles to gene expression. Reproduced from with permission from [27] Copyright © 2015, American Chemical Society.

The progress of polymer science provides highly refined synthesis of copolymers and enables polymers to form highly organized structure with plasmid DNA (pDNA). Kataoka and colleagues designed block type PEG-polycation copolymers such as PEG-b-poly(L-lysine) or PEG-b-poly{*N*-[*N*-(2-aminoethyl)-2-aminoethyl]aspart-amide} (PEG-PAsp(DET)). These copolymers formed polyplex micelles with pDNA through an electrostatic interaction (**Figure 1.4**) [29-31]. The core/shell assembly of the polyplex micelle provided biocompatibility with PEG-shielding layer to suppress interaction with blood components or to protect pDNA degradation by nucleases. Highly self-assembled nanoparticels have adjustable size by regulating preparation condition and degree of polymerization [32-33]. Size of nanocarriers significantly affects tissue penetration. Moreover cancer-target segments are able to be modified on polymers for realizing cancer-specific gene delivery. These precision polymers have improved efficiency of tumor-selective gene delivery by the combination of several segments and functions.

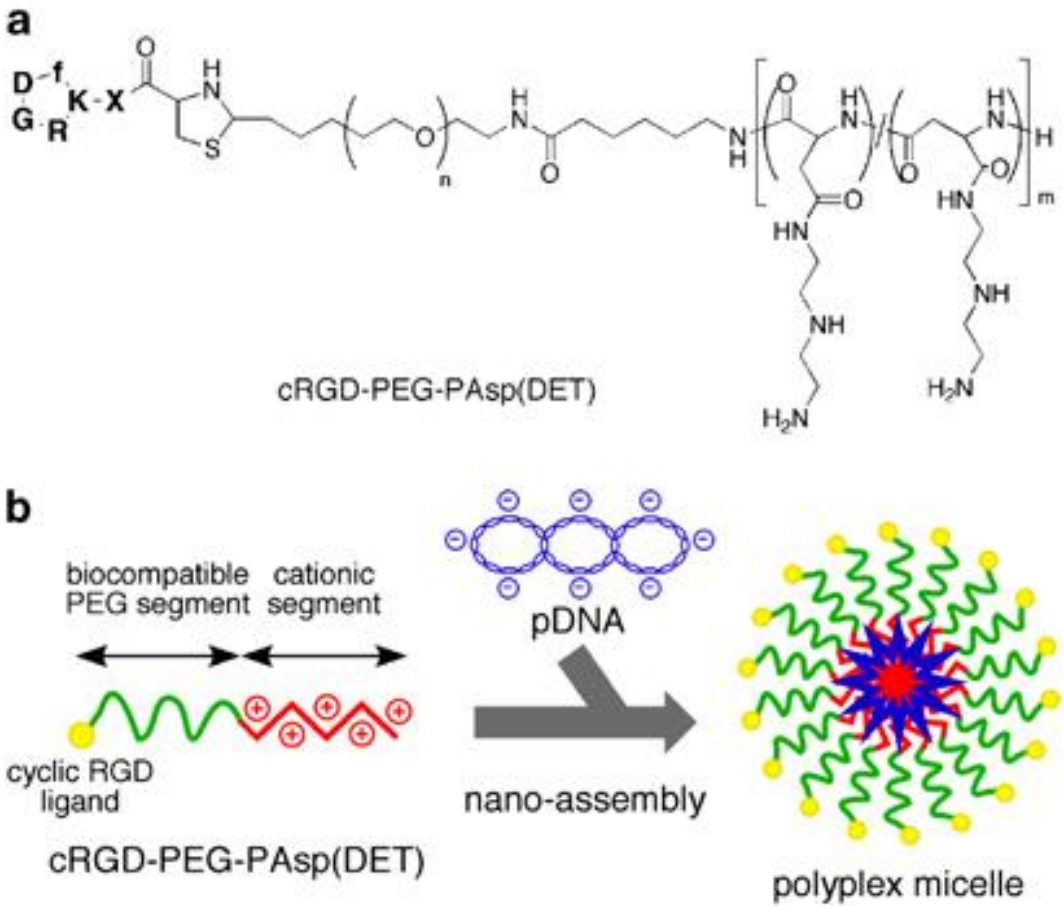

Figure 1.4. (a) Chemical structure of an example of polymers, cRGD-PEG-PAsp(DET) block copolymer. (b) Illustration of core/shell assembly of polyplex micelles formation through an electrostatic interaction. Reproduced from with permission from [30] Copyright © 2011, Rights Managed by Nature Publishing Group.

Wagner and colleagues reported various low molecular weight and precise sequence-defined polymers composed of different functional artificial amino acid utilizing solid-phase synthesis (**Figure 1.5**) [34-36]. Beside a polymer backbone component, some functional side chains can be incorporated in polymeric nanocarriers. For example, succinoyl-tetraethylene pentamine (Stp) and succinoyl-pentaethylene hexamine (Sph) were used as domains for increasing endosomal escape and DNA binding instead of high molecular weight PEI which is a gold standard of transfection reagents due to inherent endosome-escaping characteristics and high gene expression efficiency. Such restructuring of polymers in minimal and essential domain maximizes gene delivery efficiency and furthermore decreases undesirable effects like cytotoxicity.

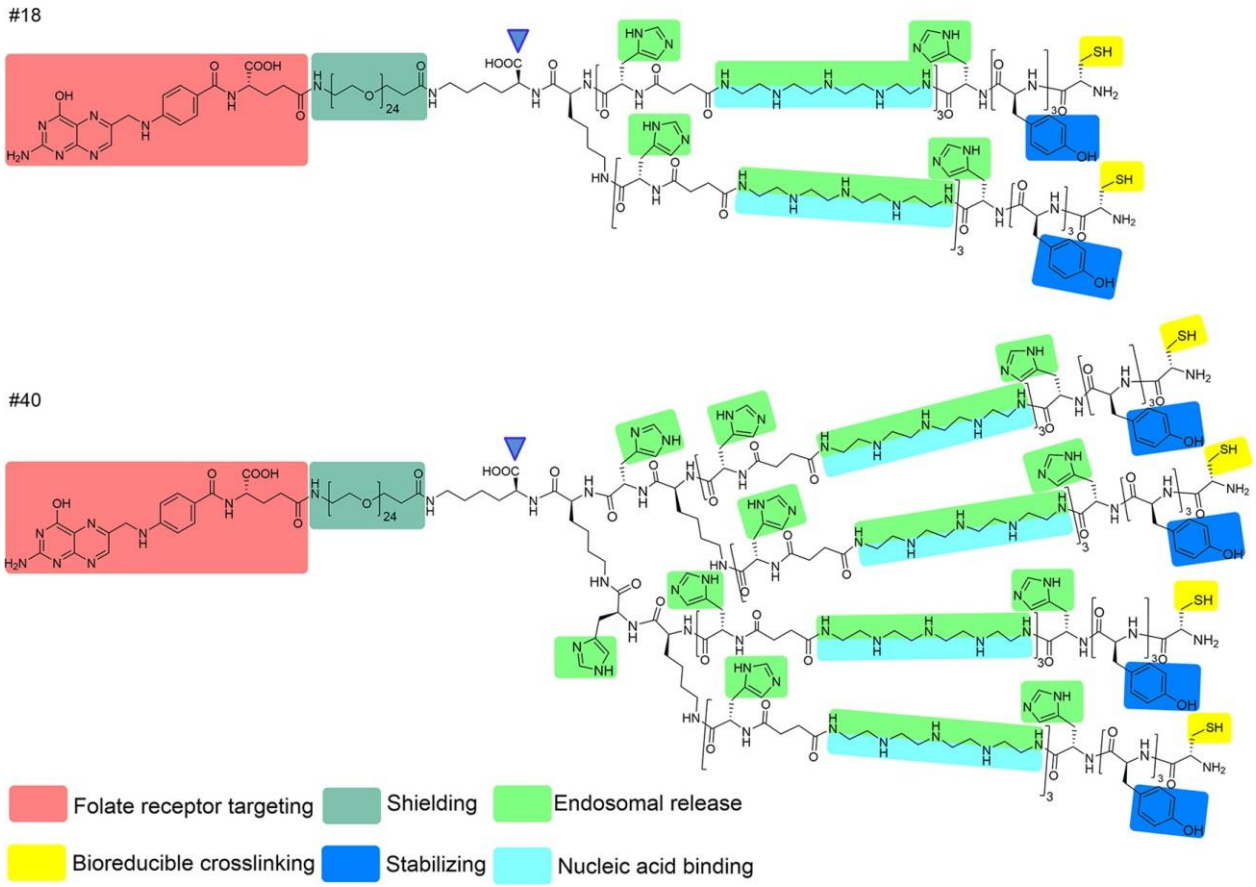

Figure 1.5. Sequence-defined cationic oligomers with two-arm (#18) and four-arm (#40) by solid-phase assisted synthesis. The multiple functions highlighted in color achieved effective transfection of pDNA *in vitro* experiment [34].

On the other hand, Harashima and colleagues coated polyplex with liposome and referred as multifunctional envelope-type nano device (MEND) (**Figure 1.6**) [37-38]. MEND consists of a DNA and polycation core and covered with lipid envelope equipped with multiple functions including cancer-targeting ligands, pH-sensitive fusogenic peptides for endosomal escape, and membrane penetration domain peptides. They call this strategy as "programmed packing" in order to overcome many obstacles of *in vivo* gene delivery and realize safe and efficient gene delivery by optimizing each function and material of MEND.

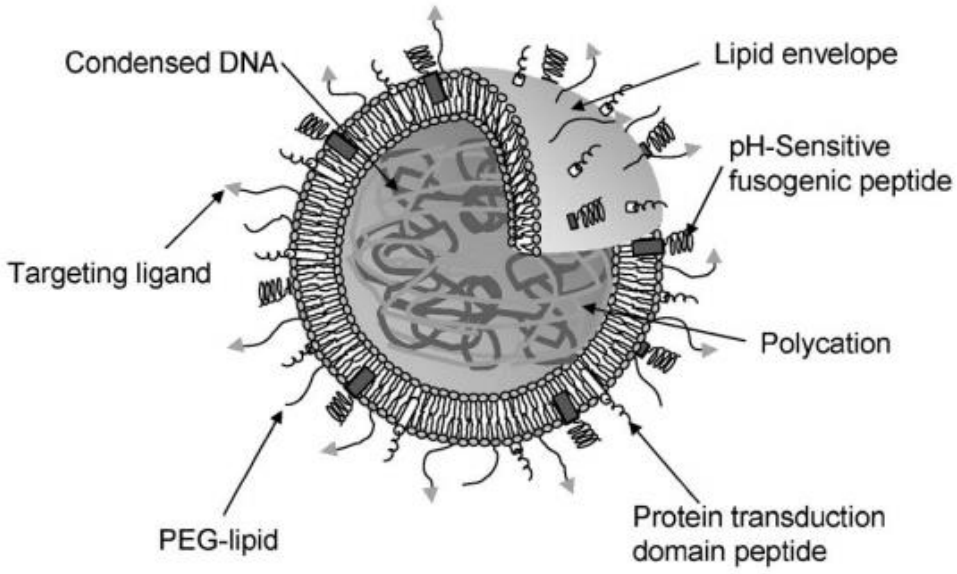

Figure 1.6. Schematic representation of a multifunctional envelope-type nano device (MEND). MEND particles consist of core of condnsed DNA and polycation, coated with a lipid envelope. Surface of MEND includes functinal devices such as targetig ligand, PEG, pH sensitive fusogenic peptide, and protein transduction domain peptide to improve *in vivo* DNA delivery efficiency [39].

Previous studies have shown that optimized nanocarriers accomplish cancer-selective gene delivery. And then material design and multiple functionlization have enhanced the delivery efficiency of DNA. Moreover, if nanocarriers suppress undesirable gene expression in non-targeted cells, such nanocarriers can expand the scope of usable therapeutic genes even having strong pharmacological activity such like suicide genes, because such system can ignore the undesired expression of the therapeutic genes in non-target cells. Next generation of nanocarriers requires such self-diagnostic ability to distinguish cellular condition.

1.3. Cancer cell-responsive transgene regulation system

If nanocarrier activates expression of the delivered gene in response to cancer specific factors, real cancer cell-specific system will be able to be designed. The author group has proposed such cancer-specific gene expression system as a novel gene delivery concept referred as “Drug or Gene Delivery System to Responding to Cellular Signals (D-RECS)”. In order to realize various disease cell-specificity, various signal proteins including protein kinase A (PKA) [40-41], caspacse-3 [42-43], Rho-associated kinase [44-45], and protein kinase Cα (PKCα) [46-47] can be used as a marker to distinguish target disease cells. In particular, PKCα is an important target of cancer-specific gene expression because PKCα serves essential roles for cellular processes in cancer development and is known to be abnormally activated in many types of malignant cancer cells [48-49]. In addition, PKCα has strong correlation with malignant transformation and cancer stem cell like activity [50-52]. On the other hand, activity of PKCα in normal cells and tissues is maintained sufficiently low [46]. Previous discovery of PKCα-specific substrate enabled D-RECS system as highly specific system against malignant cancer cells [53-54].

In D-RECS system, peptide-graft type polymer has proved the concept of PKCα-responsive gene expression (**Figure 1.7**). This polymer forms polyplex with pDNA through an electrostatic interaction and the polyplex was dissociated specifically in cancer cells responding to the phosphorylation reaction by PKCα [46-47]. Recently the author group has proposed a linear polyethyleneimine (LPEI)-substrate peptide conjugate as an optimized D-RECS polymer for tumor-specific nanocarrier. This polymer backbone possesses inherent endosome-escaping characteristics of PEI (**Figure 1.8a**) [55-56]. Thus, this LPEI-peptide conjugate demonstrated more than 100 folds enhancement of gene

expression in cancer cells comparing with that in normal cells in *in vitro* and *in vivo* experiments (**Figure 1.8b**). This result demonstrates the importance of polymer backbone in D-RECS polymer to secure sufficient PKCα-responsiveness.

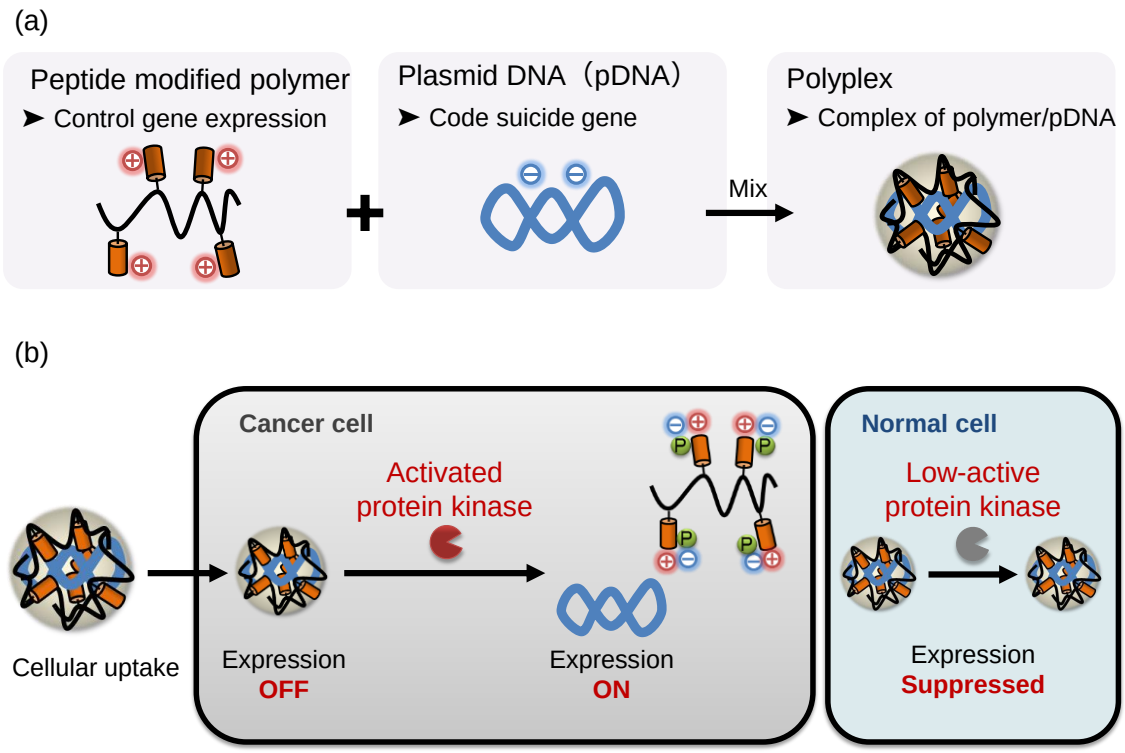

Figure 1.7. Scheme of the cancer cell-selective gene delivery system responding to activity of PKCα which is abnormally activated in various cancer cells. (a) The peptide-polymer conjugate forms polyplex with pDNA through an electrostatic interaction. (b) Transcription of the pDNA is suppressed by the formation of polyplex. After the phosphorylation reaction with PKCα in cancer cells, the pDNA is released from polyplex because of the decrease in net cationic charge, leading to transgene expression [55].

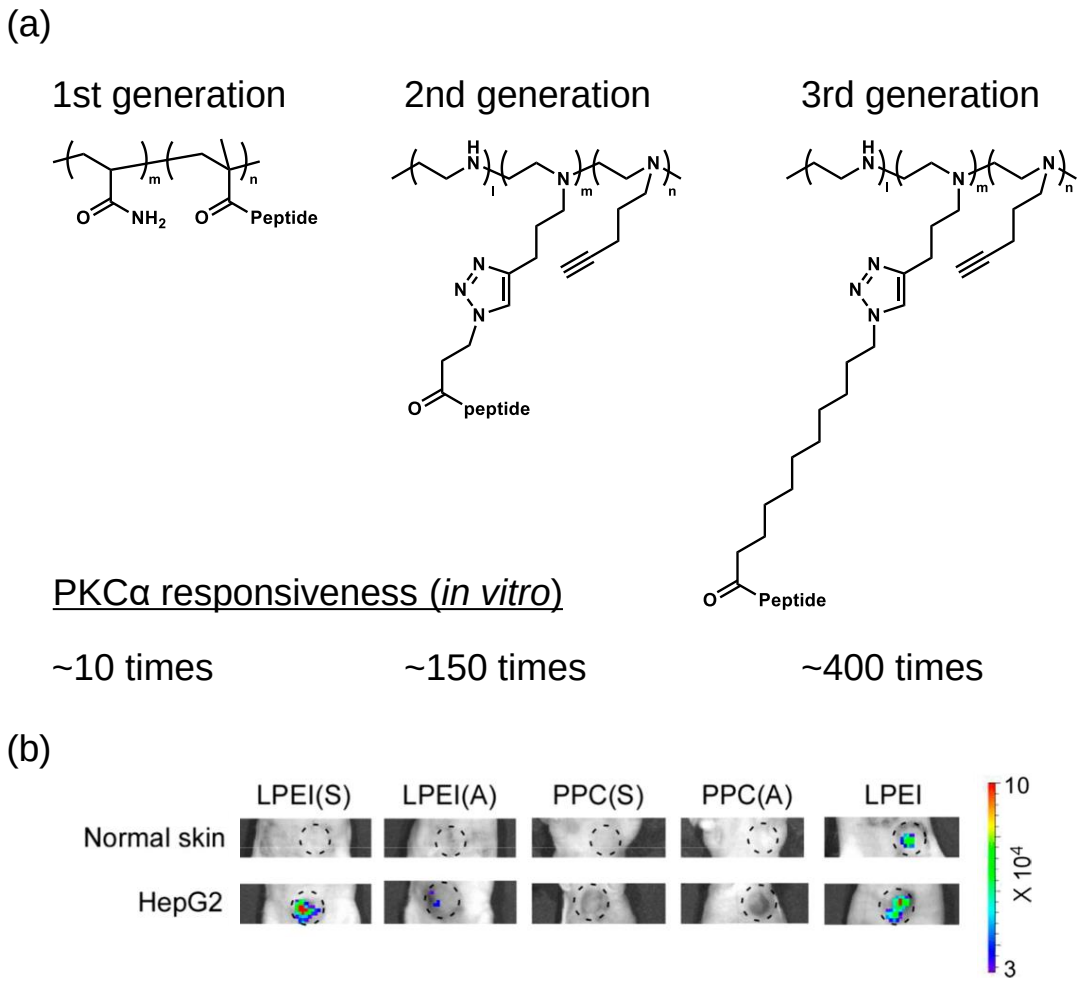

Figure 1.8. (a) Chemical structure of peptide-polymer conjugates classified in three main types and PKCα responsiveness as defined in gene expression ratio between PKCα-responsive polymer and non-responsive polymer in cancer cells with high activity of PKCα. (b) *In vivo* transgene expression in HepG2 tumor or normal tissue using 2nd generation polymer (LPEI(S)), 1st generation polymer (PPC(S), their non-responsive polymer (LPEI(A) and PPC(A)), and general gene transfer reagent (LPEI) [55].

1.4. Overview of this thesis

Demonstration of the PKCα-responsive gene expression and principle design of peptide-polymer conjugate in past studies encourage us to expand D-RECS system into systemic delivery. However, previous developed polymers were not applicable for systemic administration like intravenous injection. In fact, LPEI-peptide conjugate showed poor stability of polyplex in blood [55]. The polyplex quickly aggregated in blood stream. Additionally, multiple synthetic route of the LPEI-peptide conjugate is another disadvantage for practical use requiring of reproducible mass production because the peptide modification to LPEI needs click chemistry as orthogonally reaction [55-56]. In the view of practical use, previous LPEI-peptide conjugate polymers still have obstacles beside the instability of the polyplex under physiological conditions and the complicated synthetic process. In the previous D-RECS system, polyplex has to be freshly prepared for each experiment because the polyplex agglomeration cannot be avoided during lyophilization. Thus, preservation stability in long storage, simple preparation of polymer and sufficient physiological stability of polyplex are the problems that have to be solved for the development of practical D-RECS system [55]. In this thesis, the author studied the methodologies to improve colloidal stability of polyplex in storage and blood, as well as simple design of polymer with practical synthetic route. Physiological stability of polyplex is one of the essential factors to apply D-RECS system to *in vivo* gene delivery. Intravenous injection is the first step to deliver genetic medicine into target cells and control gene expression in both cancer cells and normal cells. Simple polymer design is also an advantageous factor in D-RECS system for considering its practical use.

Thus, two strategies are demonstrated in this thesis. One is the use of serum albumin for polyplex stabilization and another one is the use of branched

polyethyeleneimine (BPEI) for simple preparation. Additionally a structural factor affecting signal responsiveness in PEI-peptide conjugate was also investigated.

In chapter 2, a new technique to stabilize polyplex with serum albumin is introduced. Stearoyl groups were modified on LPEI backbone as a specific ligand for serum albumin. The author found that ternary complex composed of pDNA, LPEI, and serum albumin gained excellent stability under physiological saline condition with keeping the original diameter and prevented aggregation with red blood cells. The ternary complex has comparable transfection ability to original LPEI while the cytotoxicity is significantly lower than LPEI. Stearoyl modification achieved these desirable properties for intravenous injection with minimum stearoyl ligands incorporation.

In chapter 3, BPEI-based gene carriers which respond to cancer-specific activation of PKCα was designed. The carriers were synthesized straightforward by using amide bond formation between a peptide terminal carboxyl group and a primary amine group of BPEI with one pot synthesis. *In vitro* performance of these carriers showed a clear-cut response against PKCα to release pDNA for gene expression.

In chapter 4, effect of chemical property and length of linker between peptide and polymer backbone was investigated. The peptide-LPEI conjugates were synthesized with various length of the linker, controlled by using solid-phase peptide synthesis. The carriers showed the stability against anionic exchange of pDNA with heparin and enhanced *in vitro* gene expression responding to PKCα. Linker length enables peptide-polymer conjugates to assist PKCα responsiveness.

In chapter 5, the author summarizes the conclusion of this thesis.

1.5. References

[1] Gene Therapy Clinical Trials Worldwide. http://www.abedia.com/wiley/index.html (accessed Jan. 2017).

[2] M. Ferrari, *Nat. Rev. Cancer*, **5**, 161 (2005).

[3] O. Salata, *J. Nanobiotechnology*, **2**, 3 (2004).

[4] M. K. Teli, S. Mutalik, G. K. Rajanikant, *Curr. Pharm. Des*., **16**, 1882 (2010).

[5] B. Y. Kim, J. T. Rutka, W. C. Chan, *N. Engl. J. Med*., **363**, 2434 (2010).

[6] H. Cabral, K. Miyata, A. Kishimura, *Adv. Drug Deliv. Rev*., **74**, 35 (2014).

[7] V. P. Torchilin, *AAPS J*., **9**, E128 (2007).

[8] H. Yin, R. L. Kanasty, A. A. Eltoukhy, A. J. Vegas, J. R. Dorkin, D. G. Anderson, *Nat. Rev. Genet*., **15**, 541 (2014).

[9] I. Ojea-Jiménez, O. Tort, J. Lorenzo, V. F. Puntes, *Biomed. Mater*., **5**, 054106 (2012).

[10] S. Duarte, G. Carle, H. Faneca, M. C. de Lima, V. Pierrefite-Carle, *Cancer Lett*., **324**, 160 (2012).

[11] K. Yazawa, W. E. Fisher, F. C. Brunicardi, *World J. Surg*., **26**, 783 (2002).

[12] J. S. Bertram, *Mol. Aspects. Med*., **21**, 167 (2000).

[13] J. A. Roth, R. J. Cristiano, *J. Natl. Cancer Inst*., **89**, 21 (1997).

[14] A. G. Zeimet, C. Marth, *Lancet. Oncol*., **4**, 415 (2003).

[15] M. M. van der Eb, S. J. Cramer, Y. Vergouwe, F. H. Schagen, J. H. van Krieken, A. J. van der Eb, I. H. Borel Rinkes, C. J. van de Velde, R. C. Hoeben, *Gene Ther*., **5**, 451 (1998).

[16] M. Rawat, D. Singh, S. Saraf, S. Saraf, *Biol. Pharm. Bull*., **29**, 1790 (2006).

[17] K. Cho, X. Wang, S. Nie, Z. G. Chen, D. M. Shin, *Clin. Cancer Res*., **14**, 1310 (2008).

[18] D. W. Pack, A. S. Hoffman, S. Pun, P. S. Stayton, *Nat. Rev. Drug Discov*., **4**, 581 (2005).

[19] D. He, E. Wagner, *Macromol. Biosci*., **15**, 600 (2015).

[20] L. E. van Vlerken, T. K. Vyas, M. M. Amiji, *Pharm. Res*., **24**, 1405 (2007).

[21] R. Gref, M. Lück, P. Quellec, M. Marchand, E. Dellacherie, S. Harnisch, T. Blunk, R. H. Müller, *Colloids Surf. B: Biointerfaces*, **18**, 301 (2000).

[22] S. Hak, E. Helgesen, H. H. Hektoen, E. M. Huuse, P. A. Jarzyna, W. J. Mulder, O. Haraldseth, L. Davies Cde, *ACS Nano*, **6**, 5648 (2012).

[23] D. Peer, J. M. Karp, S. Hong, O. C. Farokhzad, R. Margalit, R. Langer, *Nat. Nanotechnol*., **2**, 751 (2007).

[24] F. Danhier, O. Feron, V. Préat, *J. Control. Release*, **148**, 135 (2010).

[25] M. Wacker, *Int. J. Pharm*., **457**, 50 (2013).

[26] M. Foldvari, D. W. Chen, N. Nafissi, D. Calderon, L. Narsineni, A. Rafiee, *J. Control. Release*, **240**, 165 (2016).

[27] U. Lächelt, E. Wagner, *Chem. Rev*., **115**, 11043 (2015).

[28] T. Wang, J. R. Upponi, V. P. Torchilin, *Int. J. Pharm*., **427**, 3 (2012).

[29] K. Osada, R. J. Christie, K. Kataoka, *R. Soc. Interface*., **6**, S325 (2009).

[30] H. Kagaya, M. Oba, Y. Miura, H. Koyama, T. Ishii T. Shimada, T. Takato, K. Kataoka, T. Miyata, *Gene Ther*., **19**, 61 (2012).

[31] K. Miyata, N. Nishiyama, K. Kataoka, *Chem. Soc. Rev*., **41**, 2562 (2012).

[32] A. Kishimura, *Polym. J*., **45**, 892 (2013).

[33] H. Cabral, Y. Matsumoto, K. Mizuno, Q. Chen, M. Murakami, M. Kimura, Y. Terada, M. R. Kano, K. Miyazono, M. Uesaka, N. Nishiyama, K. Kataoka, *Nat. Nanotechnol*., **6**, 815 (2011).

[34] D. He, K. Müller, A. Krhac Levacic, P. Kos, U. Lächelt, E. Wagner, *Bioconjug. Chem*., **27**, 647 (2016).

[35] W. Zhang, W. Rödl, D. He, M. Döblinger, U. Lächelt, E. Wagner, *J. Gene Med*., **17**, 161 (2015).

[36] P. M. Klein, K. Müller, C. Gutmann, P. Kos, A. Krhac Levacic, D. Edinger, M. Höhn, J. C. Leroux, M. A. Gauthier, E. Wagner, *J. Control. Release*, **205**, 109 (2015).

[37] K. Kogure, H. Akita, Y. Yamada, H. Harashima, *Adv. Drug Deliv. Rev*., **60**, 559 (2008).

[38] H. Hatakeyama, H. Akita, K. Kogure, M. Oishi, Y. Nagasaki, Y. Kihira, M. Ueno, K. Kobayashi, H. Kikuchi, H. Harashima, *Gene Ther*., **14**, 68 (2007).

[39] H. Hatakeyama, H. Akita, K. Kogure, H. Harashima, *Yakugaku Zasshi*, **127**, 1549 (2007).

[40] J. Oishi, K. Kawamura, J. H. Kang, K. Kodama, T. Sonoda, M. Murata, T. Niidome, Y. Katayama, *J. Control. Release*, **110**, 431 (2006).

[41] A. Tsuchiya, Y. Naritomi, S. Kushio, J. H. Kang, M. Murata, M. Hashizume, T. Mori, T. Niidome, Y. Katayama, *J. Biomed. Mater. Res. A*., **100**, 1136 (2012).

[42] Y. T. Sato, K. Kawamura, T. Niidome, Y. Katayama, *J. Control. Release*, **143**, 344 (2010).

[43] K. Kawamura, M. Kuramoto, T. Mori, R. Toita, J. Oishi, Y. Sato, J. H. Kang, D. Asai, T. Niidome, Y. Katayama, *J. Biomater. Sci. Polym. Ed*., **20**, 967 (2009).

[44] J. H. Kang, Y. Jiang, R. Toita, J. Oishi, K. Kawamura, A. Han, T. Mori, T. Niidome, M. Ishida, K. Tatematsu, K. Tanizawa, Y. Katayama, *Biochimie*., **89**, 39 (2007).

[45] A. Tsuchiya, J. H. Kang, D. Asai, T. Mori, T. Niidome, Y. Katayama, *J. Control. Release*, **155**, 40 (2011).

[46] J. H. Kang, D. Asai, J. H. Kim, T. Mori, R. Toita, T. Tomiyama, Y. Asami, J. Oishi, Y. T. Sato, T. Niidome, B. Jun, H. Nakashima, Y. Katayama, *J. Am. Chem. Soc*., **130**, 14906 (2008).

[47] R. Toita, J. H. Kang, J. H. Kim, T. Tomiyama, T. Mori, T. Niidome, B. Jun, Y. Katayama, *J. Control. Release*, **139**, 133 (2009).

[48] J. Koivunen, V. Aaltonen, J. Peltonen, *Cancer Lett*., **235**, 1 (2006).

[49] R. Mandil, E. Ashkenazi, M. Blass, I. Kronfeld, G. Kazimirsky, G. Rosenthal, F. Umansky, P. S. Lorenzo, P. M. Blumberg, C. Brodie, *Cancer Res*., **61**, 4612 (2001).

[50] W. L. Tam, H. Lu, J. Buikhuisen, B. S. Soh, E. Lim, F. Reinhardt, Z. J. Wu, J. A. Krall, B. Bierie, W. Guo, X. Chen, X. S. Liu, M. Brown, B. Lim, R. A. Weinberg, *Cancer Cell*., **24**, 347 (2013).

[51] Y. Chen, G. Yu, D. Yu, M. Zhu. *J. Exp. Clin. Cancer Res*., **29**, 104 (2010).

[52] C. W. Kim, D. Asai, J. H. Kang, A. Kishimura, T. Mori, Y. Katayama, *Tumor Biol*., **37**, 1901 (2016).

[53] J. H. Kang, D. Asai, S. Yamada, R. Toita, J. Oishi, T. Mori, T. Niidome, Y. Katayama, *Proteomics*., **8**, 2006 (2008).

[54] J. H. Kang, R. Toita, T. Tomiyama, J. Oishi, D. Asai, T. Mori, T. Niidome, Y. Katayama, *Bioorg. Med. Chem. Lett*., **19**, 6082 (2009).

[55] R. Toita, J. H. Kang, T. Tomiyama, C. W. Kim, S. Shiosaki, T. Niidome, T. Mori, Y. Katayama, *J. Am. Chem. Soc*., **134**, 15410 (2012).

[56] C. W. Kim, R. Toita, J. H. Kang, K. Li, E. K. Lee, G. X. Zhao, D. Funamoto, T. Nobori, Y. Nakamura, T. Mori, T. Niidome, Y. Katayama, *J. Control. Release*, **170**, 469 (2013).

2. Introduction of a specific ligand for serum albumin onto polyethyleneimine to stabilize polyplex by reversal coating with serum albumin

2.1. Introduction

Stability of nanocarrier/DNA polyplex in the blood environment is one of the most important factors for *in vivo* gene delivery. In the field of gene therapy, a wide variety of gene carriers have been designed for the goal of safe and efficient gene delivery into diseased cells to treat many diseases including cancer that are currently incurable [1-2]. Nonviral gene carriers have advantages over viral gene carriers, such as low immunogenicity and the feasibility of mass production through chemical processes [3-4]. Polyethylenimine (PEI) derivatives are one of the most successful nonviral gene carriers used in *in vitro* transfection. The polyplex that is formed by simply mixing PEI derivative and plasmid DNA (pDNA) shows efficient gene expression because of the inherent endosome-escaping characteristics of PEI backbone (**Figure 2.1**) [5-6]. However, systemic administration of positively charged polyplexes to delivery genes to target cells remains challenging because of the instability of polyplexes in biological fluids caused by undesirable interactions with blood components [7-9]. To overcome the issue, surface modification of polyplexes with polyethylene glycol (PEG) [10-12] or by anionic polysaccharides [13-15] is representative of the techniques reported in the literature. PEG-modified PEI forms a neutral and hydrophilic PEG layer on the surface of polyplexes that reduces interactions with the negatively charged erythrocytes, leading to significant improvement in the blood half-life of polyplexes (**Figure 2.3a**) [16-17]. Surface modification of positively charged polyplexes by anionic polysaccharides can be achieved by simply mixing the positively charged pDNA/PEI polyplex with anionic polysaccharides. The resulting ternary complexes showed marked improvement in

blood circulation (**Figure 2.3b**) [15].

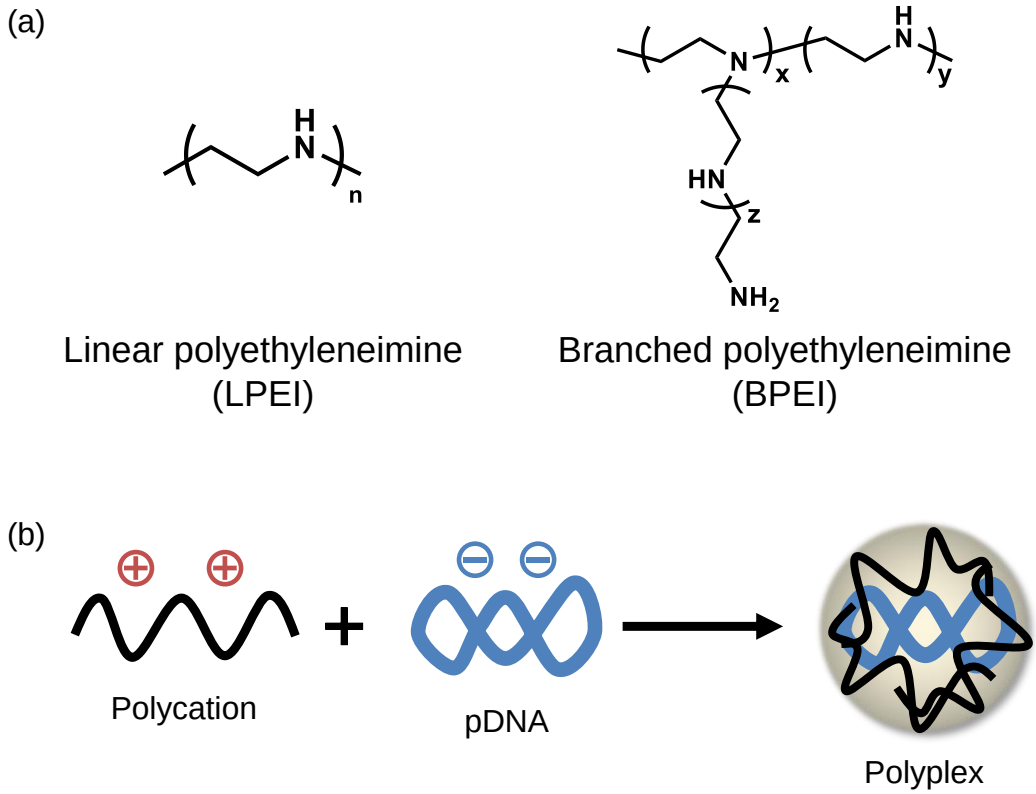

Figure 2.1. (a) Chemical structure of Linear and branched polyethyleneimine (LPEI and BPEI). (b) A scheme of polyplex formation through an electrostatic interaction between cationic polymer and anionic pDNA.

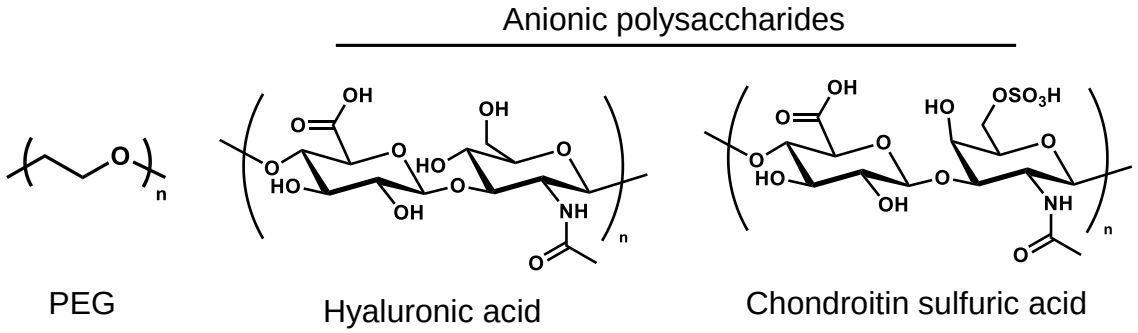

Figure 2.2. Chemical structure of polymers for *in vivo* gene delivery.

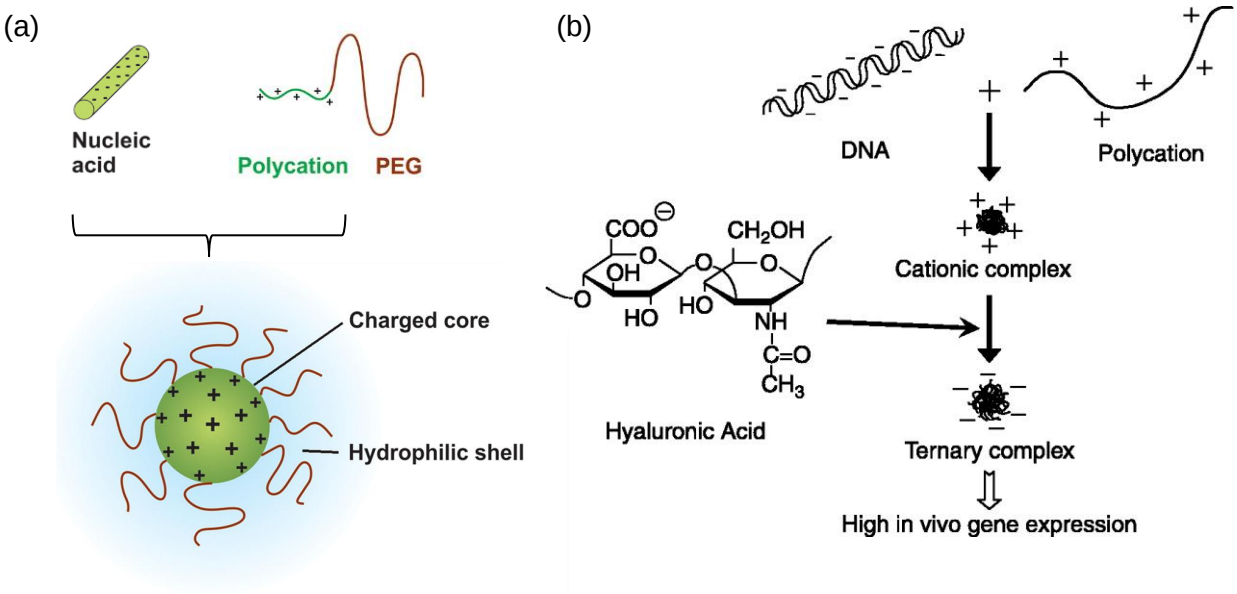

Figure 2.3. Shielding of polyplexes. (a) The core/shell assembly of shielded polyplex by hydrophobic PEG layer. Modified from [12]. (b) Formation of DNA/PEI/ hyaluronic acid ternary complex for *in vivo* gene delivery [13].

Previously the author group investigated simple PEGylation in D-RECS polymer (peptide-polymer conjugates) to stabilize its polyplex [18-19]. PEGylation actually prohibited aggregation of the polyplexes composed of peptide-polymer conjugates and pDNA. The content of PEG affected stability of polyplex and optimized content of PEG stabilized polyplexes and protected the aggregation induced by sodium chloride and bovine serum albumin (BSA). However, the PEG modification attenuated the gene suppression of D-RECS polymers which is important property in D-RECS system to reduce adverse effect. In addition, excess modification of PEG cancelled protection activity of the polymers against DNA degradation with nuclease so that pDNA was degraded under 20% serum condition. These results suggested that incorporation of PEG chains in D-RECS polymers rather weaken polyplexes and permits nucleases to pDNA under physiological conditions [19]. In addition, PEG modification in nanocarriers generally decreased cell uptake of the polyplex [18]. To overcome these undesired effects of PEG modification, the author group also developed another PEGylation technology in which PEG chains detach from the polyplex in response to the acidic extracellular conditions of tumor tissue. The detachment of PEG with slightly acidic condition enhanced the cellular uptake of the polyplex and relived the gene suppression in D-RECS system [18].

2.2. A ternary complex composed of pDNA, polymer and serum albumin

Recently, serum albumin has attracted attention in the field of drug delivery. Serum albumin is a negatively charged blood protein that has a long circulation half-life and plays a biological role in carrying fatty acids in the blood. Because the hydrophobic pockets within serum albumin that normally accommodate fatty acids are known to accommodate a variety of drugs, serum albumin has been used as a drug carrier (**Figure 2.4**) [20-21]. In this context, serum albumin has been used for surface modification of nanoparticles to improve blood circulation and accumulation within tumors [23-24]. Utilizing the anionic charge of serum albumin, surface modification of positively charged polyplexes is achieved via electrostatic interaction by simply mixing serum albumin and polyplexes (**Figure 2.5**) [25-26]. However, the resulting ternary complex is not very stable because the moderate anionic charge density of serum albumin results in a relatively weak electrostatic interaction. To strengthen the surface modification of polyplexes with serum albumin, several groups have reported covalent conjugation of PEI with serum albumin [27]. However, there is a concern about denaturation of serum albumin during the covalent conjugation step [28].

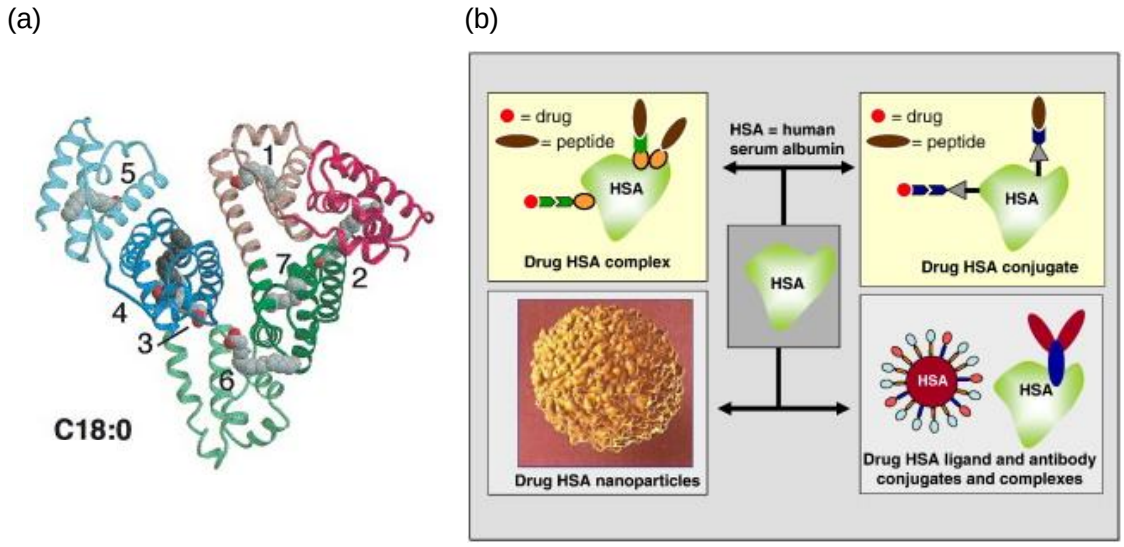

Figure 2.4. (a) Structures of a human serum albumin and hydrophobic pockets binding with fatty acids. The protein secondary structure is composed of the three domains (I, red; II, green; III, blue) Three domains have the A and B sub-domains (depicted in dark and light shades, respectively). (b) The application of serum albumin for drug carrier: conjugates or nanoparticles binding with drug, peptide or antibody. Modified from [21] and [22].

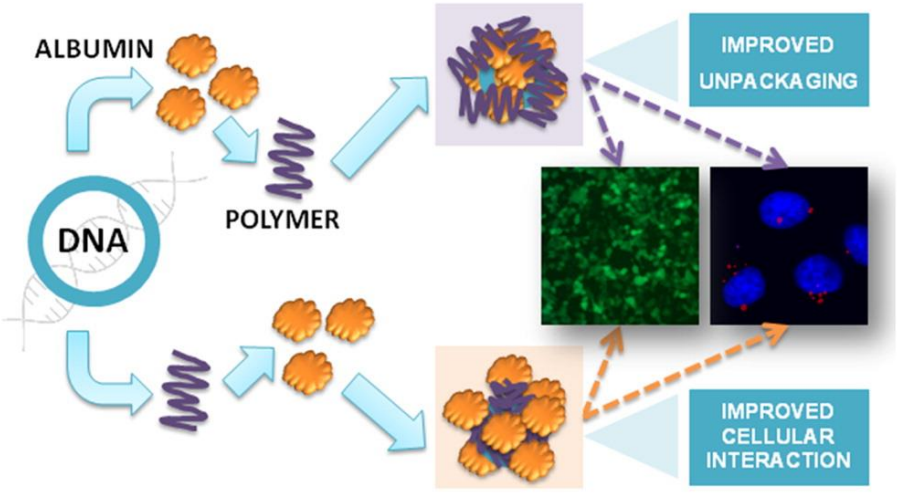

Figure 2.5. Schematic representation of ternary complex preparation and influence on transfection efficiency. Ternary complexes composed of pDNA, LPEI and bovine serum albumin through an electrostatic interaction [24].

Here, the author proposes an alternative strategy to enhance the stability of polyplexes with serum albumin. Thus, a hydrophobic ligand for serum albumin was modified on PEI. The polyplex between a ligand-modified PEI and pDNA will form stable complex with serum albumin via a specific interaction of the ligand with serum albumin's hydrophobic pockets as well as an electrostatic interaction (**Figure 2.6a**). The author chose stearic acid as a ligand for serum albumin and designed the ligand-modified PEI as shown in **Figure 2.6b**. In this chapter, the author attempted to develop basis of novel technologies to enhance stability of polyplexes using natural carrier, serum albumin.

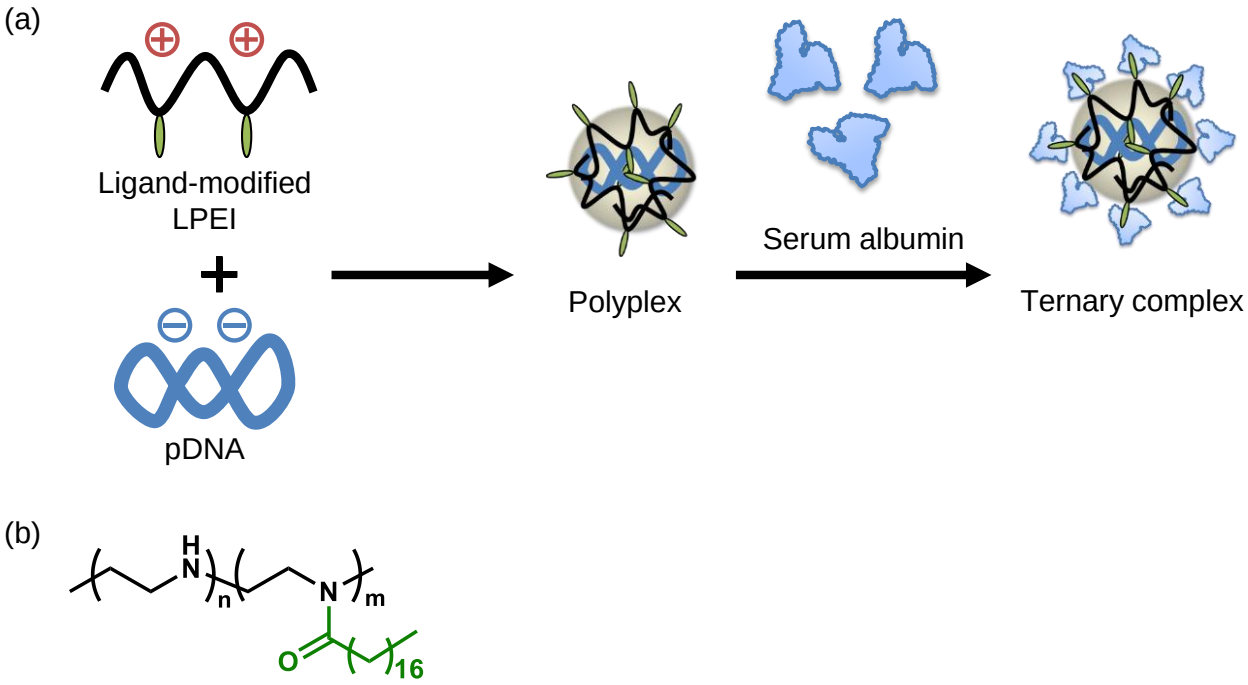

Figure 2.6. Schematic representation of the preparation of polyplex and ternary complex (a). Chemical structure of ligand-modified LPEI (b).

2.3. Materials and methods

2.3.1. Materials

Linear polyethylenimine (LPEI, 25 kDa) was purchased from Polysciences, Inc. (Warrington, PA, USA). Bovine serum albumin (BSA) fatty acid free, stearic acid, and TritonX-100 were purchased from Sigma Aldrich (Tokyo, Japan). (1-Cyano-2-ethoxy-2-oxoethylideneaminooxy) dimethylamino(morpholino)carbenium hexafluorophosphate (COMU) and diisopropylethylamine (DIPEA) were purchased from Watanabe Chemical (Hiroshima, Japan). Dimethyl sulfoxide (DMSO), ethidium bromide (EtBr), Roswell Park Memorial Institute (RPMI) 1640 medium, and D-luciferin potassium salt were purchased from Wako Pure Chemical Industries (Tokyo, Japan). YOYO-1 iodide, and Opti-MEM were purchased from Invitrogen Life Technologies (Carlsbad, CA, USA). 4-(2-hydroxyethyl)-1-piperazineethanesulfonic acid (HEPES) was purchased from Dojindo (Kumamoto, Japan). pCMV-luc2 (7.0 kbp) containing a firefly luciferase cDNA fragment driven by a CMV promoter was prepared as follows. The firefly luciferase cDNA fragment was obtained from pGL4.10[luc2] vector (Promega, WI, USA) by HindIII and XbaI. The fragment was inserted into the pcDMA3 vector (Invitrogen Life Technologies). The resulting pDNA was amplified in the Escherichia coli strain DH5α, isolated, and purified using a QIAGEN Plasmid Mega Kit (Qiagen, CA, USA).

2.3.2. Synthesis of stearate-conjugated LPEI

A total of 50 mg of LPEI (LPEI units: 1.16 mmol) was dissolved in 2.5-mL of DMSO. To this solution, 2-mL of DMSO solution including stearic acid (3.3 mg, 11.6 μmol) and COMU (250 mg, 580 μmol) was added, and then 0.5-mL of DIPEA in 0.5

mL DMSO solution was added drop-wise. Then the resulting mixture was stirred overnight at 70ºC. LPEI was collected by reprecipitation using cold diethyl ether. The obtained polymer was dialyzed against aqueous solution (15 mM $NaHCO_3$ (pH 8-9)) for 1 day and then deionized water for 2 days (SpectraPore 6, MWCO = 3,500). After lyophilization, the stearoyl group content in the polymers was determined by ^{1}H NMR spectrum. ^{1}H NMR (300 MHz, MeOD, δ): 0.88 (t, C*H*$_3$- of stearoyl), 1.27 (s, $CH_3C_{14}H_{28}$- of stearoyl), 1.59 (s, -C*H*$_2$CH$_2$CO- of stearoyl), 2.41 (d, -CH$_2$C*H*$_2$CO- of stearoyl), 2.72 (s, -C*H*$_2$C*H*$_2$NH- of LPEI units), 3.45 (s, -C*H*$_2$C*H*$_2$NCO- of LPEI units).

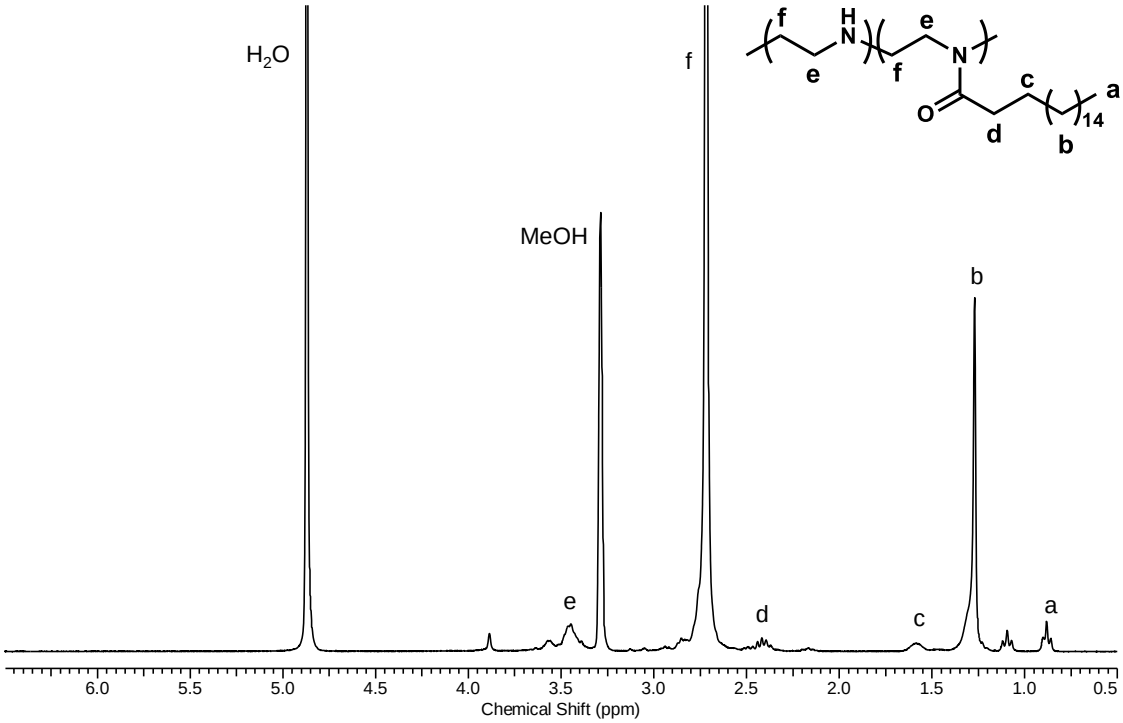

Figure 2.7. ^{1}H NMR spectra of ST(3.7) in MeOD.

2.3.3. Preparation of serum albumin-coated polyplex

Polyplexes were prepared by mixing equal volumes of 0.1 mg/mL pDNA (pDNA) solution and various concentrations of each polymer solution, then the mixture was incubated for 20 min at room temperature. The mixing ratio is expressed as the molar ratio of the amine groups in the polymer to the phosphate group of pDNA (N/P ratio). After polyplex formation, 10 mg/mL bovine serum albumin (BSA) solution was added, and then incubated for 10 min at room temperature. The polyplex solution was freeze dried if necessary and dissolved in deionized water. Aqueous solution of polyplex was diluted with buffer (HEPES (pH 7.4) or phosphate buffered saline (PBS)) to a desired concentration.

2.3.4. Agarose gel electrophoresis assay

To prepare polyplexes at various N/P ratios, pDNA (0.3 μg) and polymers were incubates at room temperature for 20 min in 10 mM HEPES buffer (pH 7.4). The polyplexes were analyzed by 1% agarose gel electrophoresis in 1× TAE buffer (100 V, 30 min). After electrophoresis, agarose gels were stained by 1× SYBR Gold staining solution for 20 min (Invitrogen Life Technologies).

2.3.5. Ethidium bromide exclusion assay

The relative binding affinity of polymer to condense pDNA was assessed by a standard EtBr fluorescence quenching [29-30]. Before polyplex formation, 0.1 mg/mL pDNA solution was stained with half volume of 50 μg/mL EtBr solution for 10 min at room temperature. The pDNA solution was added by polymer solution at various N/P ratios and incubated at room temperature for 20 min. The solution was diluted by 10

mM HEPES buffer (pH 7.4). Fluorescence measurements of each sample were performed at 25ºC using a multilabel counter ARVO (Wallac Incorporated, Turku, Finland). Excitation and emission wavelengths were 530 nm and 590 nm respectively. The relative fluorescence intensity (RFI) was determined by using the following equation: RFI = $(F_{obs}-F_e)/(F_0-F_e) \times 100\%$, where F_{obs}, F_e and F_0 are the fluorescence intensities of the polyplex at each N/P ratio, background (EtBr only), and free pDNA without polymer, respectively. Data are expressed as mean ± standard error of the mean (SEM) (n = 3).

2.3.6. Diameter and ζ-potential of polyplexes

Diameter and ζ-potential of the polyplexes were measured using a Zetasizer Nano ZS (Malvern Instruments, Worcestershire, UK) at 25ºC. Lyophilized samples were reconstituted in 10 mM HEPES buffer (pH 7.4) with the same pDNA concentration. The final concentrations of pDNA for diameter and ζ-potential measurements were 20 and 5 μg/mL, respectively. Data are expressed as mean ±SEM (n = 3).

2.3.7. Colloidal stability of polyplexes

The colloidal stability of the polyplexes against PBS was evaluated by monitoring the size increase using the Zetasizer Nano ZS at 25ºC. The aqueous solution of the polyplex was diluted with PBS to reach a final concentration of pDNA of 20 μg/mL.

2.3.8. *In vitro* erythrocyte aggregation

An *In vitro* erythrocyte aggregation assay was performed following methods available in literature [31]. Briefly, erythrocytes were collected from blood of ddy mouse (Kyudo Co. Ltd., Saga, Japan) by centrifugation at 3,000 ×g for 5 min at 4ºC. The cells were washed three times with ice-cold Ringer's solution and were resuspended with Ringer's solution. A 250-uL of cell suspension was placed in a 24-well plate (2×10^6 cells/well), then mixed with 50 μL polyplex solution (including pDNA 1.0 μg). The mixture was then incubated for 1 h at 37ºC. Animal studies were performed in accordance with the Guidelines for Animal Experiments of Kyushu University.

2.3.9. Cell Culture

CT-26 cells were cultured in RPMI 1640 containing 10% fetal bovine serum (FBS), 100 U/mL penicillin, 100 μg/mL streptomycin and 0.25 μg/mL amphotericin B (all from Gibco Life Technologies, Grand Island, NY, USA) under a humidified atmosphere containing 5% CO_2 and 95% air at 37 ^oC.

2.3.10. *In vitro* transfection study

CT-26 cells were then seeded on a 24-well plate (40,000 cells/well) in RPMI 1640 containing 10% FBS and incubated at 37ºC for 24 h. Polyplexes at an N/P ratio of 10 were prepared with pDNA (1 μg) and polymer for 20 min at room temperature. The medium was replaced with 500 μL of Opti-MEM containing polyplexes. After incubation for 4 h, the medium was changed to RPMI 1640 containing 10% FBS followed by a further incubation for 20 h. After washing the cells with Dulbecco's phosphate buffered saline (DPBS), the cells were lysed with 150 μL of lysis buffer (20

mM Tris-HCl containing 0.05% TritonX-100 and 2 mM EDTA (pH 7.4)) for 20 min. 10 μL of the lysate was mixed with 40 μL of Luciferase Assay Reagent (Promega) and then measured with a GloMax 20/20 Luminometer (Promega). Protein concentration was measured with Bio-Rad Protein Assay Dye Reagent (Bio-Rad, Hercules, CA). The result was presented as relative luminescence units (RLU)/mg total protein. Data are expressed as mean ± SEM (n = 3).

2.3.11. Fluorescence cytometry

pDNA was labeled with YOYO-1 (0.1 mg/mL pDNA and 16 μM YOYO-1 iodide in 1× TAE buffer). To prepare the polyplex, YOYO-1 labeled pDNA solution was mixed with polymer solution. After incubation for 20 min at room temperature, the polyplex solution was diluted with Opti-MEM. The final concentration of the plasmid DNA was 2 μg/mL (1 μg/well). CT-26 cells were seeded on a 24-well plate (40,000 cells/well) in 500 μL RPMI 1640 containing 10% FBS and incubated at 37ºC for 24 h. After washing the cells with DPBS, the polyplex solution was added into each well and incubated for 4 h. After incubation, the solution was removed and the cells were washed with DPBS. Efficiency of cellular uptake was analyzed using a Tali Image-Based Cytometer (Invitrogen Life Technologies Carlsbad, CA, USA).

2.3.12. Cytotoxicity of polyplexes

Cell viability was assessed using a Cell Counting Kit-8 (CCK-8, Dojindo, Kumamoto, Japan). CT-26 cells (8,000 cells) were seeded into a 96-well plate in 100 μL of RPMI 1640 and cultured for 24 h at 37°C. The medium in each well was replaced with 100-μL of Opti-MEM containing polyplexes at an N/P ratio = 10 with pDNA (0.2 μg/well). After incubation for 4 h, the medium was replaced with 100 μL of

RPMI 1640 containing 10 μL of the CCK-8 solution. After incubation for 2 h, each well was measured by reading the absorbance at 450 nm. The cell viability (%) was calculated by normalizing the absorbance of the treated cells to that of the untreated control cells, which were incubated with Opti-MEM. Data are expressed as mean ± SEM (n = 3).

2.4. Results and discussion

2.4.1. Synthesis of stearoyl-modified LPEI

Hydrophobic pockets of serum albumin bind hydrophobic molecules. Fatty acids are intrinsic typical hydrophobic molecules. Generally longer saturated fatty acids have higher binding affinity [32]. Stearic acid has been reported to have the highest binding affinity against serum albumins (K_a = 6.89 x 10^8 M^{-1}) among the reported fatty acids [32]. Thus, the author selected stearic acid as a ligand for serum albumin and prepared stearoyl-modified LPEIs (ST-PEIs) (**Scheme 2.1**). COMU was employed as a coupling agent between stearic acid and LPEI because COMU enables *N*-acylation of secondary amine groups [33]. The average degree of polymerization of parent LPEI used here was 580. The content of the stearoyl group in the synthesized ST-PEI was determined by ^{1}H NMR. Parameters of ST-PEI and the parent LPEI are summarized in **Table 2.1**. The author prepared three ST-PEIs with different stearoyl contents; 2, 22, and 46 stearoyl groups per LPEI chain, respectively.

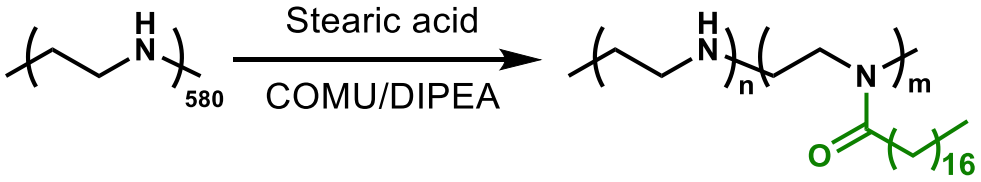

Scheme 2.1. Synthetic strategy for stearoyl-modified LPEI (ST-PEI).

Table 2.1. Characteristics of synthesized polymers.

Samples	Stearate contant[a] /mol%	Stearate no. /polymer	M_w[b] /10^4 g/mol	Count Rate[c] /kcps
LPEI	0	0	2.5	166
ST(0.4)	0.4	2	2.6	1026
ST(3.7)	3.7	22	3.1	2286
ST(7.8)	7.8	46	3.7	2413

[a] Determined by ^{1}H NMR spectrum. [b] Calculated from stearate contents and M_w of the parent LPEI (degree of polymerization; 580). [c] The theoretical count rate of polymers with zero attenuator.

2.4.2. Polyplex formation of stearoyl-modified LPEI (ST-PEI)

The author confirmed polyplex formation of the ST-PEI with pDNA by the gel retardation assay. The polyplexes were prepared by mixing pDNA and each ST-PEI at various N/P ratios in deionized water, and then the resulting polyplexes were mixed in 10 mM HEPES (pH 7.4). As shown in **Figure 2.8**, all the polymers completed the polyplex formation at the N/P ratio of 4 to 6 irrespective of the stearoyl content of the polymers.

The author examined polyplex formation of the ST-PEIs with pDNA by the ethidium bromide exclusion assay. **Figure 2.9** illustrates decrease in the fluorescence intensity of ethidium bromide (EtBr) with the formation of polyplex in various N/P ratios. Relative fluorescence intensity (RFI) indicates relative fluorescence intensity comparing with the fluorescence intensity of EtBr bound to free DNA. Decrease of RFI indicates the extent of DNA compaction because EtBr dissociate with compaction of DNA strand. Polyplex of ST(0.4) is similar in pDNA condensation to LPEI. In contrast, ST(3.7) showed the RFI decrease at a slow rate compared the other polymers. This loosing of polyplexes was reported to modify stearoyl ligands to branched polyethyleneimine (BPEI) due to reduced charge density of free amine groups and the steric hindrance of long fatty acids [34-36]. However, ST(7.8) had same pDNA condensation capacity compared to LPEI and ST(0.4). This indicates that hydrophobic interaction of stearoyl groups contributes to the formation of tight polyplex in this system. This result was discussed later along with the colloidal stability in section 2.4.4. Anyway, appropriate content of stearoyl group did not show prohibition of DNA compaction. N/P dependency of RFI(%) in PEI(0.4) was almost the same to that in original PEI. Thus, ST(0.4) was mainly used for following experiment. Also N/P=10 was chosen as sufficient value for the complete formation of fully compacted polyplex.

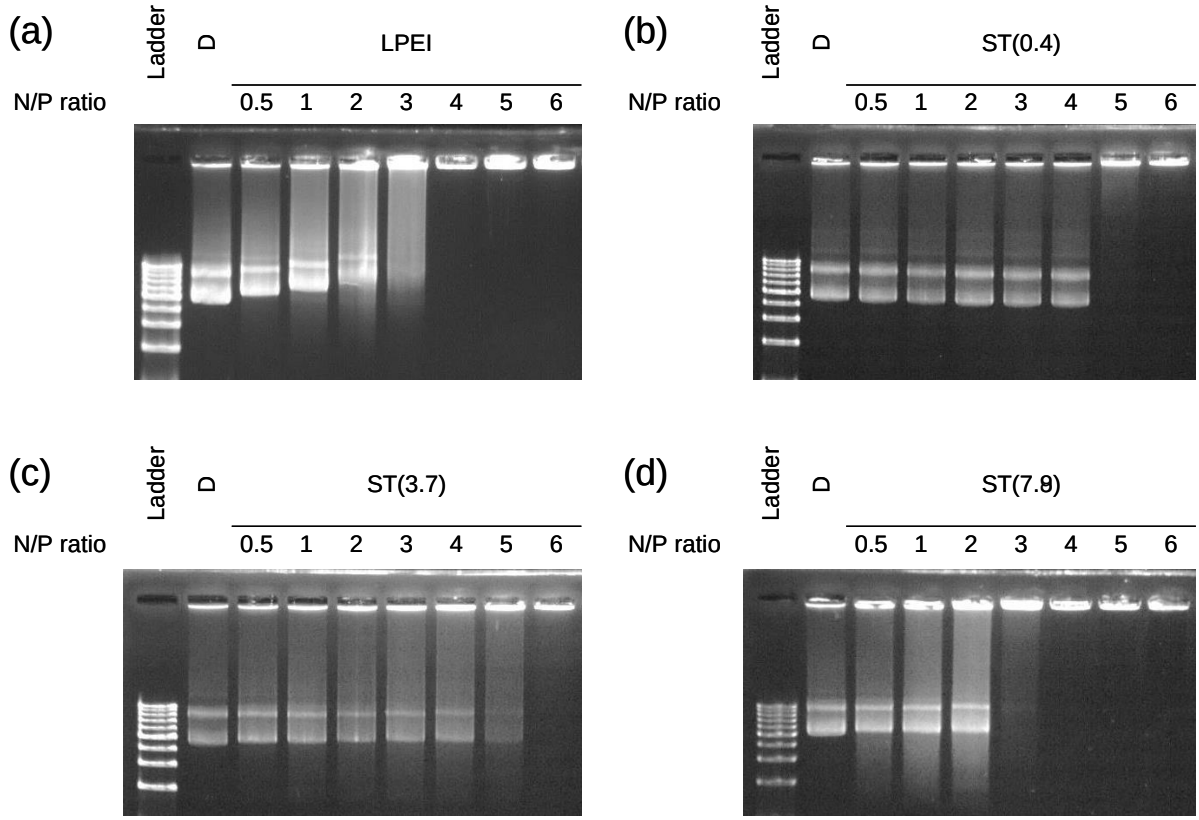

Figure 2.8 Polyplex formation evaluated by gel electrophoresis of LPEI (a), ST(0.4) (b), ST(3.7) (c), ST(7.8) (d). D indicates pDNA alone.

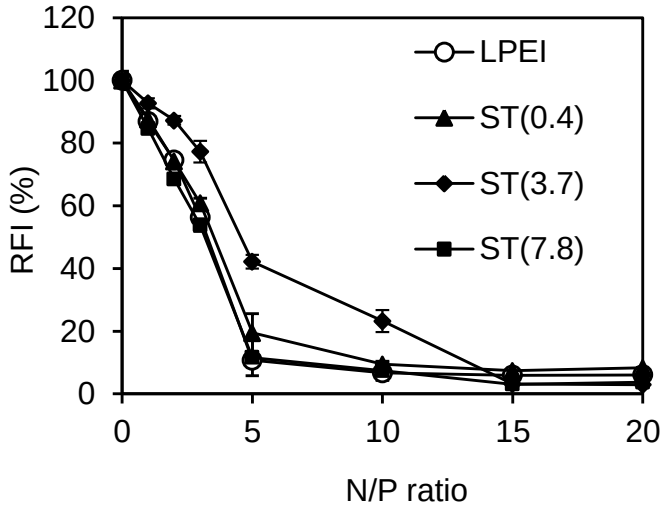

Figure 2.9. Polyplex formation evaluated by ethidium bromide exclusion assay. Data are expressed as means ± SEMs (n = 3).

2.4.3. Preparation of ternary complex

The polyplex was prepared by mixing pDNA and each ST-PEI at N/P = 10 in deionized water, then the resulting polyplex was mixed with 10 mg/mL BSA in 10 mM HEPES (pH 7.4) to prepare ternary complex. As shown in **Figure 2.10**, the polyplexes have diameters of 145 - 155 nm with positive surface charges (20 - 30 mV). After mixing the polyplexes with BSA, size increase and surface charge reversal were observed irrespective of the stearoyl content of ST-PEI, indicating successful formation of the ternary complexes. However, the contribution of the stearoyl group of ST-PEI to the binding with BSA to generate the ternary complexes was not clear because the ternary complexation was also observed for the parent LPEI, indicating that electrostatic interaction is sufficient for the ternary complexation under the conditions examined solution condition (10 mM HEPES (pH 7.4)).

Next, the author examined effect of lyophilization on the stability of the ternary complex. As shown in **Figure 2.10**, the reconstituted ternary complex of each ST-PEI has almost same diameter and ζ-potential value with the initial ternary complex. In contrast, the polyplexes of ST-PEI or parent LPEI formed macroscopic aggregate without BSA addition (**Figure 2.11**), indicating that BSA works as a cryoprotectant. Macroscopic aggregate of polyplexes had the low solubility in buffer although lyophilized powder of ternary complexes had the high solubility. So count ratio of polyplexes in dynamic light scattering measurement showed significantly lower value than it of ternary complex. Tolerance of the ternary complex to the lyophilization enables long-term storage in dry form and simple preparation of ternary complexes before systemic administration.

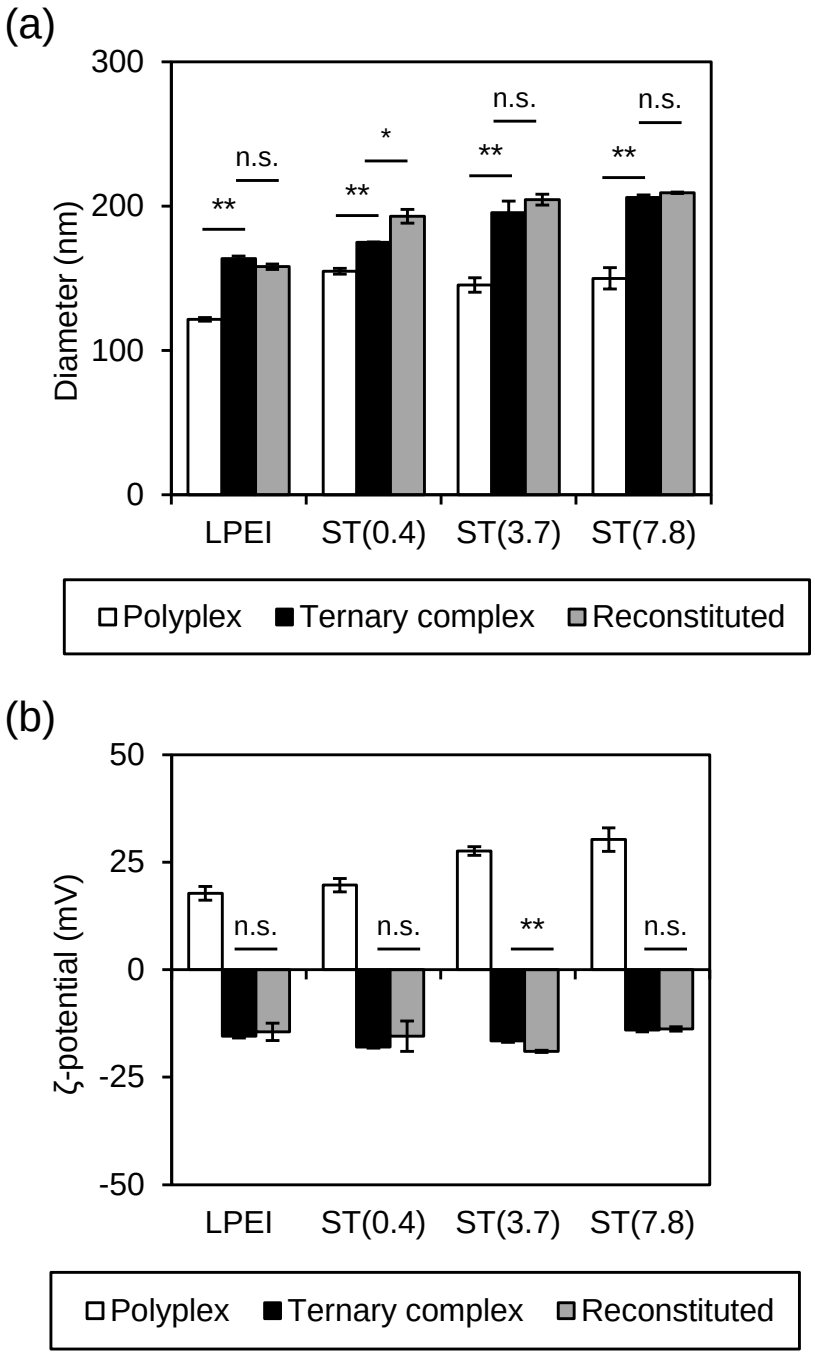

Figure 2.10. Diameter (a) and ζ-potential (b) of polyplex and ternary complex in 10 mM HEPES buffer (pH 7.4). Polyplex was prepared at N/P ratio = 10, then complexed with BSA. Data are expressed as means ± SEMs (n = 3, n.s.: not significant, *$p < 0.05$, **$p < 0.01$).

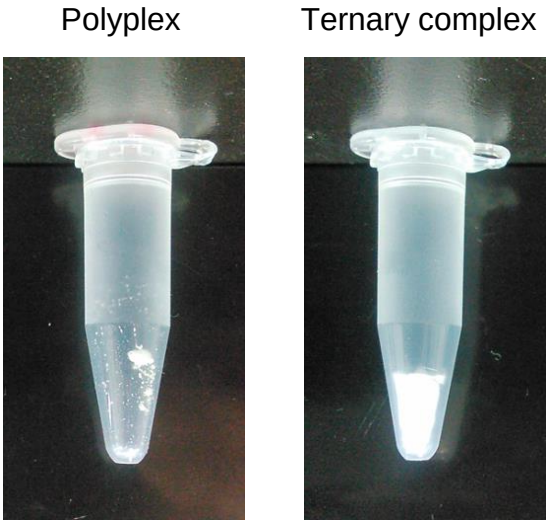

Figure 2.11. Samples of freeze-dried polyplex and ternary complex of ST(0.4) (The other polymers showed same samples). Polyplex was prepared at N/P ratio = 10, then complexed with BSA.

2.4.4. Colloidal stability of ternary complex under physiological conditions

To reduce the contribution of the electrostatic interaction to the ternary complexation, the ternary complex was prepared in PBS, which contains a physiological concentration of saline (ca. 140 mM NaCl). In the case of polyplexes other than ST(7.8) (**Figure 2.12a**), the particle size gradually increased with time through aggregation, and the aggregation speed of ST(0.4) and ST(3.7) became fast compared to LPEI. In contrast, in the case of the ternary complex of ST-PEI (**Figure 2.12b**), the aggregation was completely suppressed even for ST(0.4), which contained only two stearoyl groups per chain. The author further found that the particle size of the ternary complex of ST(0.4) remained constant even after a week of incubation. However, suppression of the aggregation was not observed for the ternary complex of LPEI. These results showed that the stearoyl group of ST-PEI is essential to the colloidal stability of the ternary complex in PBS. By the way, the author focused on colloidal stability of ST(7.8). Polyplex of ST(7.8) did not aggregate in the absence of BSA and had high colloidal stability under physiological conditions (**Figure 2.12a**). Hydrophobic modifications have been studied to form complex strongly through a hydrophobic interaction [37-39]. Cholesteric modification improved the colloidal stability of polyplexes [40]

To obtain evidence that BSA is bound with ST-PEI via the stearoyl group in the ternary complex, the author used a stearic acid-bound BSA in which BSA's binding pockets were already filled with stearic acid. BSA has several binding pockets, two of which have stronger binding affinity towards fatty acids [41]. Stearic acid-bound BSA with various ratios (stearic acid/BSA = 1 to 4) was prepared according to a previously described procedure [42]. The stearic acid-bound BSA was then mixed with the ST(0.4) polyplex to prepare the ternary complex. As shown in **Figure 2.12c**, stearic

acid-bound BSA with a mixing ratio above 2 did not suppress the aggregation of the polyplex. These results are the evidence that BSA bound to the polyplex via the stearoyl group of ST-PEI to form the ternary complex.

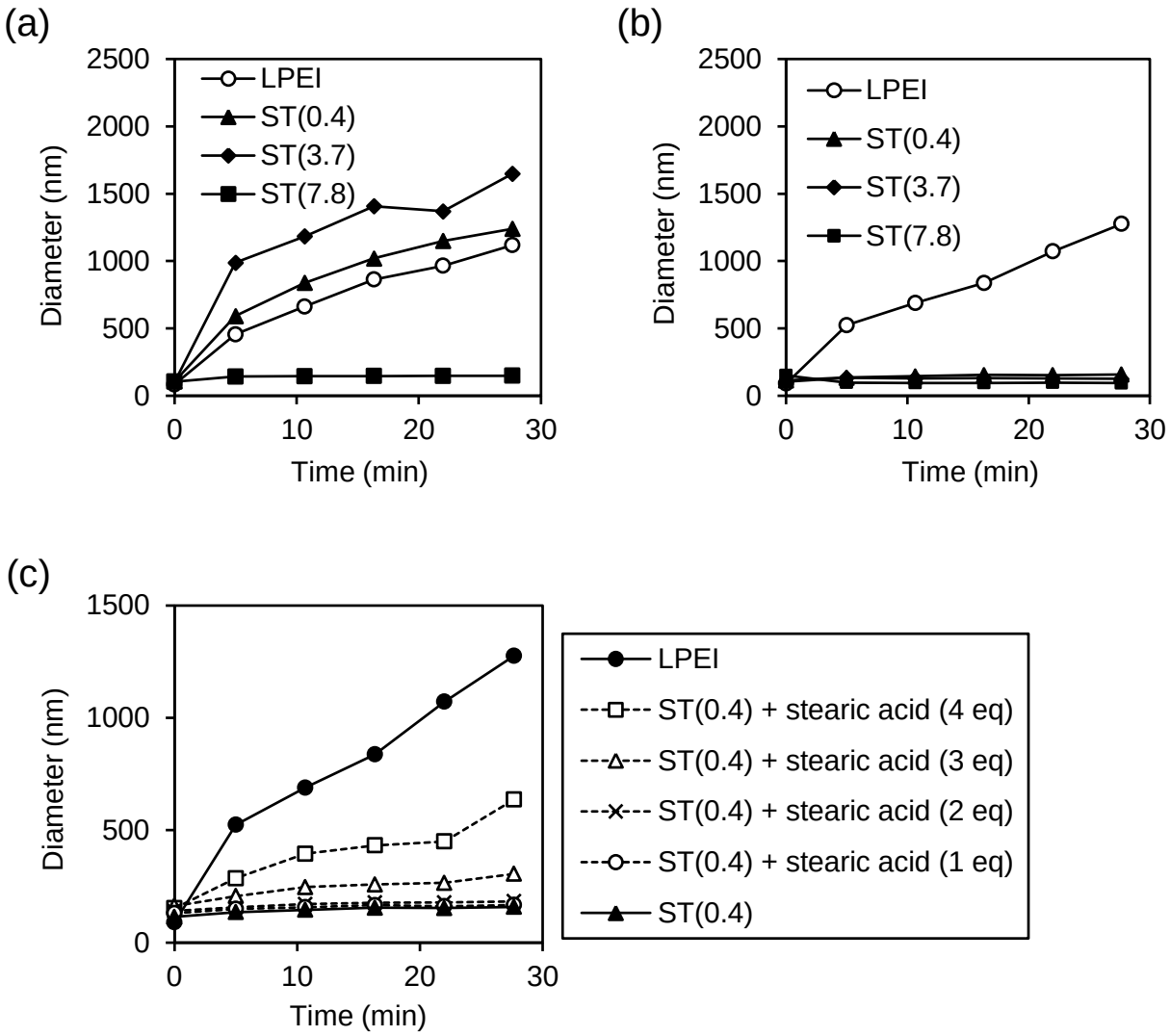

Figure 2.12. Effect of physiological salt condition on the colloidal stability of polyplex (a) and ternary complex (b). (c) Effect of stearic acid-bound BSA on the colloidal stability of ternary complex.

2.4.5. Effects on interaction between ternary complex and erythrocytes

The author examined the induction of erythrocyte aggregation with the ternary complex. It has been reported that intravenous injection of polyplexes of LPEI/pDNA into mice results in clot formation in the capillary blood vessels of the lung [43-44]. This clot was composed of polyplex and erythrocyte [43-44]. Such clot formation must be avoided for gene carriers under systemic administration [43-44]. As shown in **Figure 2.13**, the LPEI ternary complex induced aggregation of erythrocytes, while that of ST(0.4) did not. This result is promising feature of ST-PEI for *in vivo* applications.

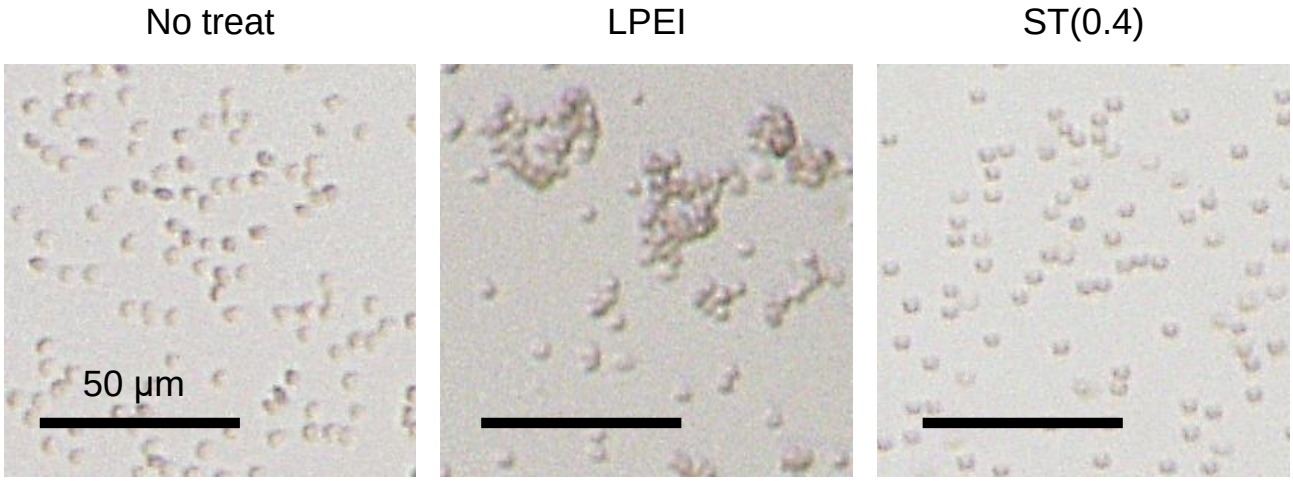

Figure 2.13. Aggregation of erythrocytes induced by ternary complex in Ringer's solution (pH 7.4).

2.4.6. Transgene expression of ternary complex *in vitro*

The transgene expression of luciferase-encoding pDNA was investigated by using LPEI or ST-LPEI in the presence or absence of BSA (**Figure 2.14**). Despite the negative surface charge observed in **Figure 2.10b**, the ternary complex showed almost equivalent gene expression to the parent polyplex. The gene expression of the ternary complexes decreased with increasing stearoyl group content, and ST(0.4) showed almost the same level of the gene expression as LPEI. Also the author confirmed effect of lyophilization on the gene expression of the ternary complex. As shown in **Figure 2.14**, the reconstituted ternary complex of each ST-PEI has same gene expression efficiency with the initial ternary complex. The cellular uptake of each ternary complex was quantified by fluorescence cytometry and found to be similar to that of the original polyplex (**Figure 2.15**)

The author examined the cytotoxicity of the polyplex towards CT-26 cells (**Figure 2.16**). The ternary complex showed a significant reduction in cytotoxicity. The cytotoxicity became higher with increasing stearoyl group content in ST-PEI. Thus, the lower gene expression with increasing stearoyl content may be explained by cytotoxicity. From the above obserbations, ST(0.4) is the best gene carrier, with low cytotoxicity and high gene expression.

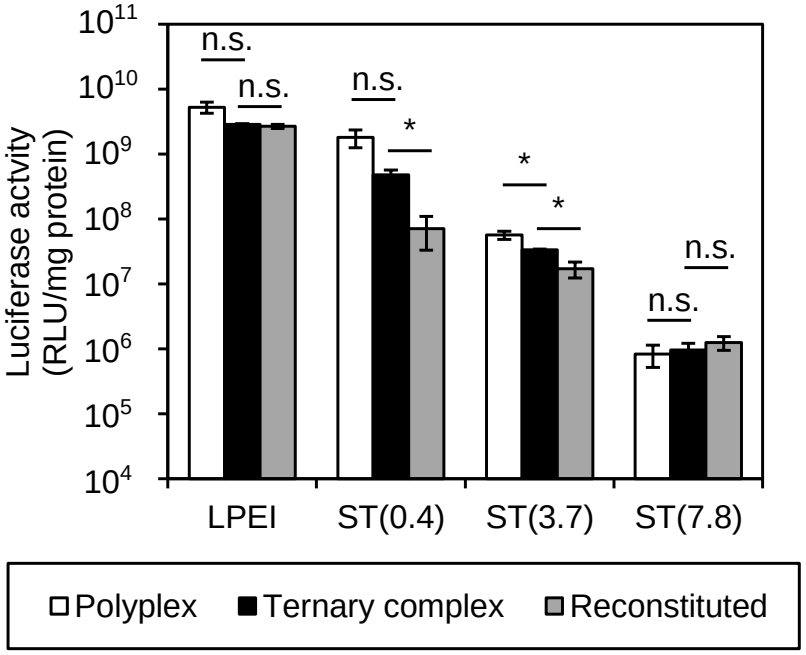

Figure 2.14. Transgene expression and cytotoxicity of polyplex and ternary complex evaluated by using CT-26 cells in OPTI-MEM. Data are expressed as means ± SEMs (n = 3, n.s.: not significant, *$p < 0.05$).

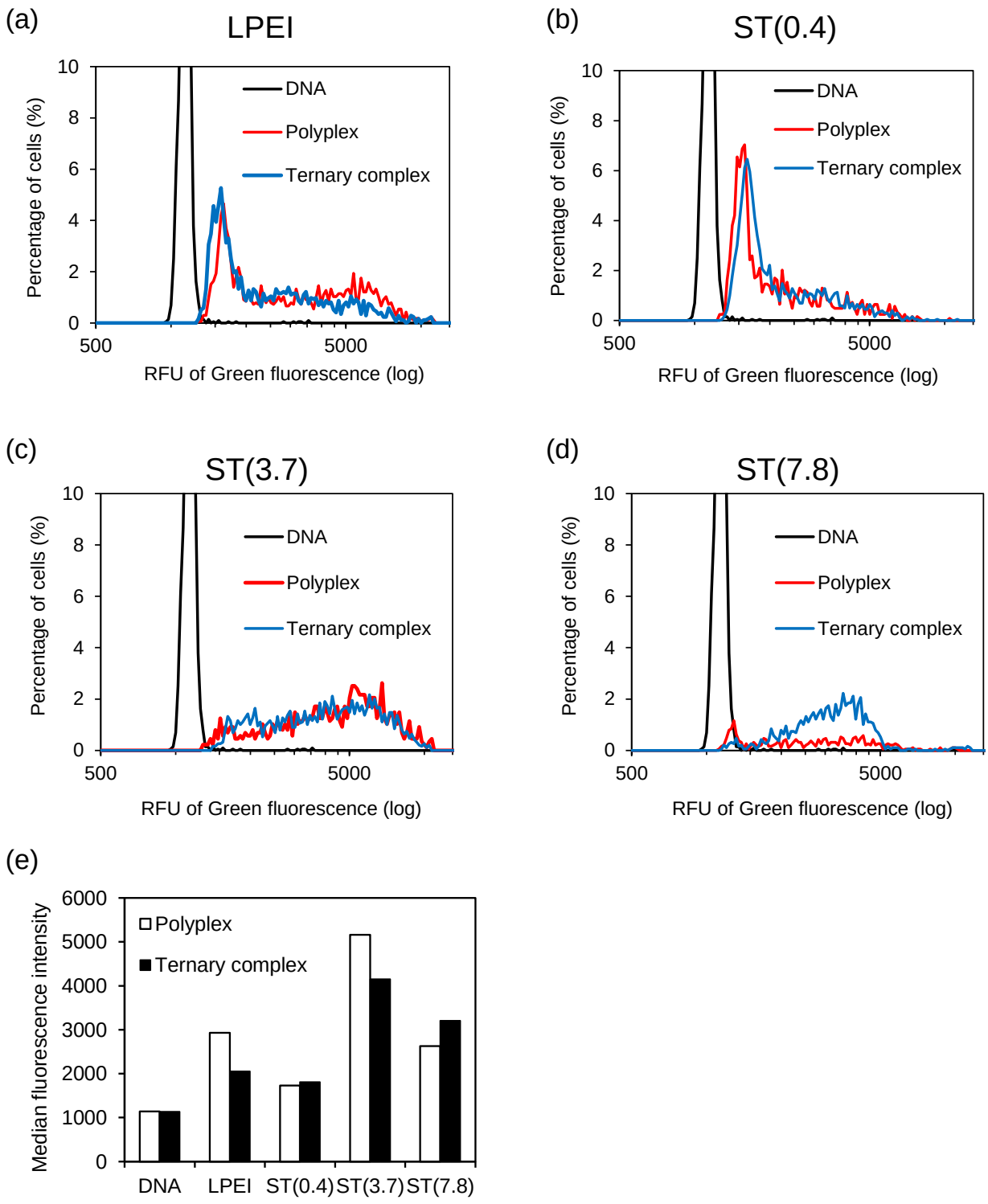

Figure 2.15. Cellular uptake of polyplex and ternary complex of LPEI (a), ST(0.4) (b), ST(3.7) (c), ST(7.8) (d) into CT-26 cells evaluated by fluorescence cytometry. (e) Calculated median fluorescence intensity from all cellular uptakes.

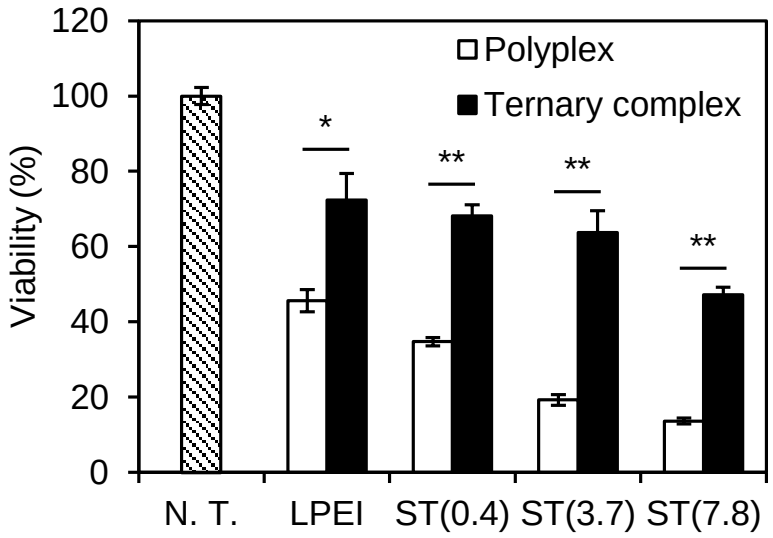

Figure 2.16. Cytotoxicity of polyplex and ternary complex evaluated by using CT-26 cells in OPTI-MEM. N.T. is non treated cells. Data are expressed as means ± SEMs (n = 3, *p < 0.05, ** p < 0.01).

2.5. Summary

Here, the author proposed a simple but effective technique to stabilize pDNA/PEI complex with serum albumin. The author used stearoyl-modified LPEI (ST-PEI) in which stearoyl group works as a specific ligand for the hydrophobic pockets of serum albumin. By mixing the pDNA/ST-PEI polyplex with serum albumin, a ternary complex was formed via specific interaction with the stearoyl ligand as well as an electrostatic interaction. Only two stearoyl groups per LPEI chain was enough to provide colloidal stability to the ternary complex under the physiological saline condition. Despite the surface anionic charge of the ternary complex, the cellular uptake and the gene expression was comparable to those of the parent polyplex. The ternary complex also significantly reduced the cytotoxicity of the parent polyplex. In addition, lyophilization procedure without inactivation permits ternary complexes to form small DNA/polymer complexes (<100 nm) at very low pDNA concentration and condense pDNA concentration for appropriate *in vivo* gene delivery [12, 13, 45].

2.6. References

[1] A. El-Aneed, *J. Control. Release,* **94**, 1 (2004).

[2] M. Foldvari, D. W. Chen, N. Nafissi, D. Calderon, L. Narsineni, A. Rafiee, *J. Control. Release,* **240**, 165 (2016).

[3] H. Yin, R. L. Kanasty, A. A. Eltoukhy, A. J. Vegas, J. R. Dorkin, D. G. Anderson, *Nat. Rev. Genet*., **15**, 541 (2014).

[4] Y. Zhang, A. Satterlee, L. Huang, *Mol. Ther*., **20**, 1298 (2012).

[5] A. Kichler, C. Leborgne, E. Coeytaux, O. Danos, *J. Gene Med*., **3**, 135 (2001).

[6] U. Lungwitz, M. Breunig, T. Blunk, A. Göpferich, *Eur. J. Pharm. Biopharm*., **60**, 247 (2005).

[7] R. Kircheis, L. Wightman, E. Wagner, *Adv. Drug Deliv. Rev*., **53**, 341 (2001).

[8] A. Aied, U. Greiser, A. Pandit, W. Wang, *Drug Discov. Today*, **18**, 1090 (2013).

[9] Y. Zhang, C. Wang, R. Hu, Z. Liu, W. Xue, *ACS. Biomater. Sci. Eng*., **1**, 139 (2015).

[10] R. Kircheis, L. Wightman, E. Wagner, *Adv. Drug Deliv. Rev*., **53**, 341 (2001).

[11] M. Kursa, G. F. Walker, V. Roessler, M. Ogris, W. Roedl, R. Kircheis, E. Wagner, *Bioconjug. Chem*., **14**, 222 (2003).

[12] U. Lächelt, E. Wagner, *Chem. Rev*., **115**, 11043 (2015).

[13] T. Ito, N. Iida-Tanaka, Y. Koyama, *J. Drug Target*., **16**, 276 (2008).

[14] T. Ito, C. Yoshihara, K. Hamada, Y. Koyama, *Biomaterials*, **31**, 2912 (2010).

[15] Y. He, G. Cheng, L. Xie, Y. Nie, B. He, Z. Gu, *Biomaterials*, **34**, 1235 (2013).

[16] M. Neu, O. Germershaus, M. Behe, T. Kissel, *J. Control. Release*, **124**, 69 (2007).

[17] T. Merdan, K. Kunath, H. Petersen, U. Bakowsky, K. H. Voigt, J. Kopecek, T. Kissel, *Bioconjug. Chem*., **16**, 785 (2005).

[18] S. Kushio, A. Tsuchiya, Y. Nakamura, T. Nobori, C. W. Kim, G. X. Zhao, T. Funamoto, E. K. Lee, K. Lee, T. Niidome, T. Mori, Y Katayama, *Biomed. Eng*., **25**, 1340005 (2013).

[19] A. Tsuchiya, Y. Naritomi, S. Kushio, J. H. Kang, M. Murata, M. Hashizume, T. Mori, T. Niidome, Y. Katayama, *J. Biomed. Mater. Res. Part A*, **100**, 1136 (2012).

[20] F. Kratz, *J. Control. Release*, **132**, 171 (2008).

[21] A. A. Bhattacharya T. Grüne, S. Curry, *J. Mol. Biol*., **303**, 721 (2000).

[22] B. Elsadek, F. Kratz, *J. Control. Release*, **157**, 4 (2012).

[23] J. Yokoe, S. Sakuragi, K. Yamamoto, T. Teragaki, K. Ogawara, K. Higaki, N. Katayama, T. Kai, M. Sato, T. Kimura, *Int. J. Pharm*., **353**, 28 (2008).

[24] S. Son, S. Song, S. J. Lee, S. Min, A. A. Kim, J. Y. Yhee, M. S. Huh, I. C. Kwon, S. Y. Jeong, Y. Byun, S. H. Kim, K. Kim, *Biomaterials*, **34**, 9475 (2013).

[25] M. I. Syga, E. Nicolì, E. Kohler, V. P. Shastri, *Biomacromolecules*, **17**, 200 (2016).

[26] S. Simões, V. Slepushkin, P. Pires, R. Gaspar, M. C. Pedroso de Lima, N. Düzgüneş, *Biochim. Biophys. Acta*., **1463**, 459 (2000).

[27] J. L. Chen, S. W. Peng, W. H. Ko, C. J. Wu, T. W. Li, M. K. Yeh, C. H. Chiang, *J. Nanopart. Res*., **16**, 2593 (2014).

[28] H. M. Rawel, S. Rohn, H. P. Kruse, J. Kroll, *Food Chem*., **78**, 443 (2002).

[29] A. J. Geall, I. S. Blagbrough, *J. Pharm. Biomed. Anal*., **22**, 849 (2000).

[30] J. B. LePecq, C. Paoletti, *J. Mol. Biol*., **27**, 87 (1967).

[31] M. Ogris, S. Brunner, S. Schüller, R. Kircheis, E. Wagner, *Gene Ther*., **6**, 595 (1999).

[32] T. Peters, *All about Albumin*: Biochemistry, Genetics, and Medical Applications, Academic Press, San Diego (1995).

[33] A. El-Faham, F. Albericio, *J. Pept. Sci*., **16**, 6 (2010).

[34] Z. Liu, Z. Zhang, C. Zhou, Y. Jiao, *Prog. Polym. Sci*., **35**, 1144 (2010).

[35] A. Neamnark, O. Suwantong, R. K. Bahadur, C. Y. Hsu, P. Supaphol, H. Uludağ, *Mol. Pharm*., **6**, 1798 (2009).

[36] V. Incani, E. Tunis, B. A. Clements, C. Olson, C. Kucharski, A. Lavasanifar, H. Uludag, *J. Biomed. Mater. Res. A*., **81**, 493 (2007).

[37] H. Ayame, N. Morimoto, K. Akiyoshi, *Bioconjug. Chem*., **19**, 882 (2008).

[38] S. Toita, S. Sawada, K. akiyoshi, *J. Control. Release*, **155**, 54 (2011).

[39] K. Akiyoshi, A. Ueminami, S. Kurumada, Y. Nomura, *Macromolecules*, **33**, 6752 (2000).

[40] A. Tsuchiya, Fukuoka, Kyushu University, Ph. D. thesis (2011).

[41] G. V. Richieri, A. Anel, A. M. Kleinfeld, *Biochemistry*, **32**, 7574 (1993).

[42] C. J. Kubarych, M. M. Adams, E. V. Anslyn, *Org. Lett*., **12**, 4780 (2010).

[43] R. Kircheis, L. Wightman, A. Schreiber, B. Robitza, V. Rössler, M. Kursa, E. Wagner, *Gene Ther*., **8**, 28 (2001).

[44] P. Chollet, M. C. Favrot, A. Hurbin, J. L. Coll. *J. Gene Med*., **4**, 84 (2002).

[45] K. Miyata, Y. Kakizawa, N. Nishiyama, Y. Yamasaki, T. Watanabe, M. Kohara, K. Kataoka, *J. Control. Release*, **109**, 15 (2005).

3. Branched polyethylenimine-based PKCα-responsive gene carriers

3.1. Introduction

As discussed in chapter 1, cancer-specific gene delivery is important to avoid side effects especially when the suicide genes to destroy the transfected cells are employed [1-2]. Active and passive targeting strategies have been reported to avoid undesired distribution of therapeutic genes to the healthy tissue [3-5]. However, the non-specific distribution of the gene carriers to the healthy tissue is inevitable. This indicates that strategy to accelerate the accumulation of drugs in tumor is not enough to secure sufficient specificity. For solving this issue, pharmacological activity of genetic drug should be suppressed in non-target normal cells but has to be activated only in target tumor cells. To achieve this cancer cell-specific release of therapeutic genes, the authors have utilized the dysregulations of the intracellular signaling in cancer cells [6-9]. In malignant tumor cells, intracellular signal transduction should be abnormal comparing with that in normal cells. Thus, such abnormal signaling will be an ideal candidate to distinguish tumor cells. In this context, the author group has developed unique strategy of signal-responsive gene releasing system. Using this system, a therapeutic gene can be released only in tumor cells. The authors designed cationic peptide-grafted polymers as such signaling responsive gene carriers [10-12]. The grafted cationic peptides are substrates for protein kinase Cα (PKCα) which are specifically activated in the cancer cells [13]. The polymer forms polyplexes with plasmid DNA (pDNA) due to the cationic charge of the peptides. While after phosphorylation of the peptides, the polyplexes dissociate due to the reduced net cationic charge to release pDNA for the gene expression.

3.2. Branched polyethylenimine-peptide conjugate

Recently, the authors developed linear polyethylenimine (LPEI)-based signal-responsive polymers [14]. Due to the buffering capacity of the polyethylenimine main chain [15-16], the resulting polyplexes efficiently escape from the endosome and show a clear-cut response toward PKCα activity. In spite of the excellent signal-responsive ability of these polymers, the synthesis of the polymers requires multistep modification using click chemistry.

In this chapter, the author selected a branched polyethylenimine (BPEI) as a backbone of new gene carriers to modify PKCα-specific substrate peptides. Because BPEI contains many reactive primary amine groups on the end of the branched chains [17-19], the substrates peptides were readily modified to the primary amine groups. Then, the BPEI-peptide conjugates were applied to the PKCα-responsive gene expression system as depicted in **Figure 3.1**. When optimizing the peptide contents in the conjugate, the conjugates showed excellent response to PKCα activity.

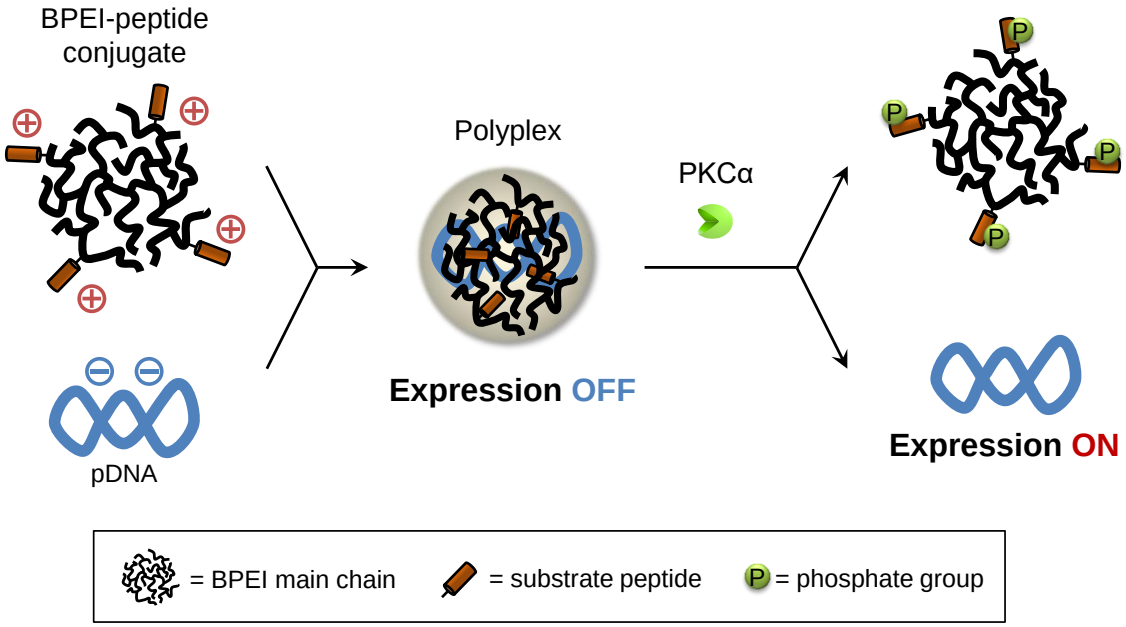

Figure 3.1. Polyplex formation of PKCα-responsive carrier and PKCα-responsive release of pDNA from the polyplex.

3.3. Materials and methods

3.3.1. Materials

Sieber Amide resin (amine density of 0.69 mmol/g) and all Fmoc-protected amino acids were obtained from Novabiochem, Merck (Hohenbrunn, Germany). 1-hydroxybenzotriazole hydrate (HOBt•H_2O), O-(benzotriazol-1-yl)-*N,N,N',N'*-tetramethyluronium hexafluorophosphate (HBTU), trifluoroacetic acid (TFA), diisopropylethylamine (DIPEA), 1-methyl-2-pyrrolidone (NMP) and dichloromethane (DCM) were purchased from Watanabe Chemical (Hiroshima, Japan). Pyridine, methanol, 2-(1H-7-azabenzotriazol-1-yl)-1,1,3,3-tetramethyl hexafluorophosphate (HATU), 1-hydroxy-7-azabenzotriazole (HOAt), dimethyl sulfoxide (DMSO), ethidium bromide (EtBr), Dulbecco's modified Eagle's medium (DMEM), and Roswell Park Memorial Institute (RPMI) 1640 were purchased from Wako Pure Chemical Industries (Tokyo, Japan). Triisopropylsilane and succinic anhydride were purchased from Tokyo Chemical Industry (Tokyo, Japan). BPEI (molecular weight 25,000) and TritonX-100 were purchased from Sigma Aldrich (St. Louis, MO, USA). YOYO-1 was purchased from Invitrogen Life Technologies (Carlsbad, CA, USA).

A plasmid DNA (pDNA); pCMV-luc2, containing a firefly luciferase cDNA fragment driven by a CMV promoter was prepared as follows. The firefly luciferase cDNA fragment was obtained from pGL4.10[luc2] vector (Promega, WI, USA) by *Hind*III and *Xba*I. This fragment was inserted into the pcDMA3 vector (Invitrogen, CA, USA). The resulting pDNA was amplified in the *Escherichia coli* strain DH5a, isolated, and purified using a QIAGEN Plasmid Mega Kit (Qiagen, CA, USA).

3.3.2. Synthesis of substrate peptide with protected side groups

The PKCα-specific substrate peptide with protected side groups (peptide-S; HOOC-$(CH_2)_2$-CO-FK(Boc)K(Boc)Q(Trt)G*S(tBu)*FAK(Boc)K(Boc)K(Boc)-NH_2) and its negative control peptide (peptide-A; HOOC-$(CH_2)_2$-CO-FK(Boc)K(Boc)Q(Trt)G S(tBu)F*A*K(Boc)K(Boc)K(Boc)-NH_2) were synthesized by standard Fmoc-chemistry using the Sieber Amide resin. After the coupling reaction and Fmoc-removal of the last amino acid; phenylalanine (F), the *N*-terminal site of the peptide was reacted with succinic anhydride dissolved in 0.9 M DIPEA/NMP. The peptide with protected side groups was cleaved from the resin by treating with 1% TFA/DCM. The solution including peptide was neutralized by adding 10% pyridine/methanol. The protected peptide was reprecipitated by using cold water, and then dried in vacuo. The purity of the peptide was confirmed by reverse-phase liquid chromatography after deprotection to be > 90%.

3.3.3. Synthesis of BPEI-peptide conjugate

BPEI (BPEI units; 0.23 mmol) was dissolved in 1 mL of DMSO. To this solution, 1 mL of DMSO solution including the protected substrate peptide of PKCα (peptide-S or peptide-A; 11.5-46 μmol), HATU (11.5-46 μmol), HOAt (11.5-46 μmol) and DIPEA (0.23 mmol) were added and the resulting mixture was stirred overnight at room temperature. After the reaction, the polymer was recovered by reprecipitation with cold diethyl ether and then dried in vacuo. The obtained polymer was deprotected with a mixture of TFA/triisopropylsilane/water (95/2.5/2.5) and washed with diethyl ether. The obtained polymer was dialyzed against aqueous solution of $NaHCO_3$ (15 mM, pH 8-9) for 2 days and then pure water for 2 days (SpectraPore 6, MWCO = 3,500). After lyophilization, the content of the peptide in the polymers was determined by ^{1}H NMR

spectrum. ^{1}H NMR (300 MHz, D_2O, δ): 1.18-1.26 (13H, m, K(γ), A(β)), 1.44 (10H, s, K(δ)), 1.61 (10H, m, K(β), 1.84-1.95 (2H, d, Q(β)), 2.21-3.11 (4H, m, NC*H*$_2$C*H*$_2$ of BPEI), 2.21 (2H, s, Q(γ)), 2.29-2.32 (4H, d, COC*H*$_2$C*H*$_2$CO), 2.54 (10H, s, K(ε)), 3.00 (4H, s, F(β)), 3.61 (2H, s, S(β)), 3.79 (2H, s, G(α)), 4.10-4.12 (8H, d, A(α), K(α), Q(α)), 4.24 (1H, s, S(α)), 4.45 (1H, s, F(α)), 4.69 (2H, s, H_2O), 7.09-7.16 (10H, d, F(C_6H_5)). Peptide contents were calculated using two peaks of 2.21-3.11 (4H, m, NC*H*$_2$C*H*$_2$ of BPEI) and 7.09-7.16 (10H, d, F(C_6H_5)).

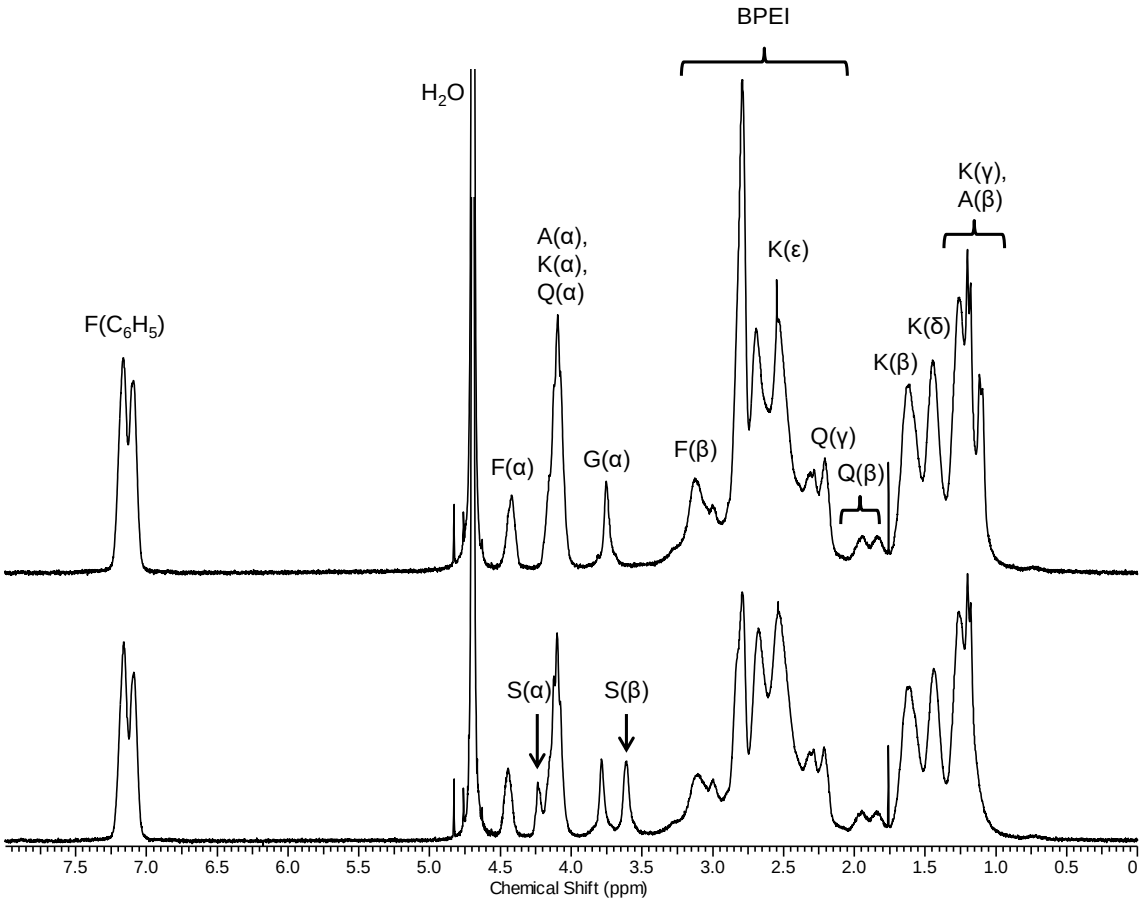

Figure 3.2. ^{1}H NMR spectra of BPEI-peptide-A conjugate (upper panel) and BPEI-peptide-S conjugate (lower panel) in D_2O.

3.3.4. Agarose gel electrophoresis assay

To prepare polyplexes at various N/P ratios, pDNA (0.3 μg) and polymers were incubates at room temperature for 15 min in 10 mM HEPES buffer (pH 7.4). The polyplexes were analyzed by 1% agarose gel electrophoresis at 100V for 30 min.

3.3.5. Ethidium bromide Exclusion Assay

Polymer/pDNA polyplexes were prepared at various N/P ratios with EtBr in 10 mM HEPES buffer (pH 7.4). To prepare the polyplex, the solutions were incubated at room temperature for 15 min. The final concentrations of pDNA and EtBr were 5.0 and 1.25 μg/mL, respectively. Fluorescence measurements of each sample were performed at 25 ^{o}C using a multilabel counter ARVO (Wallac Incorporated, Turku, Finland). Excitation and emission wavelengths were 530 nm and 590 nm respectively. The relative fluorescence intensity (RFI) was determined by using the following equation: $RFI = (F_{obs}-F_e)/(F_0-F_e) \times 100\%$, where F_{obs}, F_e and F_0 are the fluorescence intensities of the polyplex at each N/P ratio, background (EtBr only), and free pDNA without carrier, respectively. Data are expressed as mean ± standard error of the mean (SEM) (n = 3).

3.3.6. Diameter and ζ-potential of polyplexes

Diameter and ζ-potential of the polyplexes was measured using a Zetasizer Nano instrument (Malvern Instruments, Worcestershire, UK) at 25 °C. For the preparation of the solutions for diameter measurement, 15 μl of pDNA (0.05 mg/mL) solution and 15 μL of polymer solution were mixed, and then mixture was incubated for 15 min at room temperature. The final concentration was adjusted to 12.5 μg/ml by 10 mM HEPES buffer (pH 7.4). For the preparation of the solutions for ζ-potential measurement, the final concentration of pDNA was adjusted to 3.1 μg/ml by 10 mM HEPES buffer (pH 7.4). Data are expressed as mean SEM (n = 2 or 3).

3.3.7. Cell Culture

CT-26 cells were cultured in RPMI 1640. Huh-7 cells were cultured in DMEM medium. All medium containing 10% fetal bovine serum (FBS), 100 U/mL penicillin, 100 μg/mL streptomycin and 0.25 μg/mL amphotericin B (all from Gibco Life Technologies, Grand Island, NY, USA). All cells were cultured under a humidified atmosphere containing 5% CO_2 and 95% air at 37 ^{o}C.

3.3.8. Cellular uptake of polyplex

A 250-μL of 0.1 μg/μL pDNA was mixed with 5 μL of 10× TAE buffer and 200 μL of 10 μM YOYO-1 in TE buffer. The solution was mixed for at least 1 h at room temperature in the dark, and then stored at -20 ^{o}C. To prepare the polyplex, solutions of pDNA and BPEI, S-3 or A-3 were first mixed to adjust the N/P ratio of 5 in Opti-MEM (pH 7.4) and then incubated for 15 min (pDNA concentration was 0.033 μg/μL). 30 μL of this solution was mixed with 480 μL of Opti-MEM. CT-26 cells were seeded on a

24-well plate (20,000 cells/well) in RPMI 1640 containing 10% FBS and incubated at 37 ^{o}C for 24 h. After washing the cells with PBS, the polyplex solution was added into each well and incubated for 4 h. Efficiency of cellular uptake was analyzed using a Tali^{TM} Image-Based Cytometer (Invitrogen)

3.3.9. Confocal laser scanning microscopy (CLSM)

Huh-7 cells were plated at a density of 1 × 10^5 cells in 35-mm glass bottom dishes (Matsunami, Osaka, Japan) at 37 °C in 1 mL of DMEM containing 10 % FBS for 18 h. pDNA was labeled with tetramethylrhodamine (TAMRA) by using a Label-IT reagent (Mirus, WI, USA) (labeling efficiency; 1 TAMRA / 100 base pair). Polyplexes at the N/P ratio of 5 were prepared with TAMRA-labeled pDNA (2 μg) and polymer for 15 min at room temperature. The medium was replaced with Opti-MEM containing pDNA/polymer polyplexes. After incubation for 6 h, the medium was changed to DMEM containing 10 % FBS, and the cells were further incubated for 18 h. Polyplexes were observed by CLSM (ZEISS LSM 700, Carl Zeiss, Oberlochen, Germarny) equipped with a Plan-Apochromat 63×/1.40 Oil Ph3 M27 objective after staining acidic late endosomes and lysosomes with LysoTracker Green for 1 h and nuclei with Hoechst 33342 (Molecular Probes, Eugene, OR) for 15 min before each observation.

3.3.10. Transfection study

To prepare the polyplex, solutions of pDNA and polymers were first mixed to adjust the N/P ratio of 2.5, 5, 7.5 or 10 in Opti-MEM and then incubated for 15 min (pDNA concentration was 0.05 μg/μL). 20μL of this solution was mixed with 480 μL of Opti-MEM. CT-26 cells were then seeded on a 24-well plate (20,000 cells/well) in

RPMI 1640 containing 10% FBS and incubated at 37 ^{o}C for 24 h. Then the medium was replaced with the polyplex solutions. After incubation for 4 h, the medium was changed to RPMI 1640 containing 10% FBS followed by a further incubation for 20 h. After washing the cells with PBS, the cells were lysed with 200 μL of lysis buffer (20 mM Tris-HCl containing 0.05% TritonX-100 and 2 mM EDTA (pH 7.4)) for 20 min. 10 μL of the lysate were mixed with 40 μL of luciferase assay solution (Promega) and then measured with a MiniLumat LB 9506 (EG & G Berthold, Wildbad, Germany). The results are presented as relative luminescence units (RLU)/mg total protein. Data are expressed as mean SEM (n = 3).

3.3.11. Cytotoxicity of polyplex

Cell viability was assessed using a Cell Counting Kit-8 (CCK-8, Dojindo, Kumamoto, Japan). CT-26 cells (5,000 cells) were seeded into a 96-well plate in 100 μL of RPMI 1640 and cultured for 24 h at 37 °C. The medium in each well was replaced with 100-μL of Opti-MEM containing polyplexes at N/P ratio = 5 with pDNA (0.2 μg/well). After incubation for 4 h, the medium was changed to RPMI 1640 containing 10% FBS followed by a further incubation for 20 h. And then the medium was replaced with 100 μL of RPMI 1640 containing 10 μL of the CCK-8 solution. After incubation for 2 h, each well was measured by reading the absorbance at 450 nm. The cell viability (%) was calculated by normalizing the absorbance of the treated cells to that of the untreated control cells, which were incubated with Opti-MEM. Data are expressed as mean ± SEM (n = 3).

3.4. Results and discussion

3.4.1. Synthesis of BPEI-peptide conjugates

The BPEI-peptide conjugates were readily synthesized by modification of protected peptides on to the primary amine groups of BPEI followed by deprotection (**Scheme 3.1**). The content of the peptides in the polymers was determined by ^{1}H NMR. The characteristics of the polymers are summarized in **Table 3.1**. The author prepared both PKCα-responsive polymers (S-series polymers) and negative control polymers (A-series polymers) which are not phosphorylated by PKCα because their serine residue was replaced with alanine residue. To investigate the effect of the peptide contents on the performance as a cancer-specific gene carrier, the author prepared polymers with three kinds of peptide contents (3, 5, and 12 mol%). The polymers possess three kinds of cationic groups that are originated from peptide's lysine groups and BPEI's amino and imino groups. Because this system controls the stability of the polyplex by the charge shift of the peptide upon phosphorylation, the cationic charge of the BPEI core should minimize the contribution to the polyplex formation.

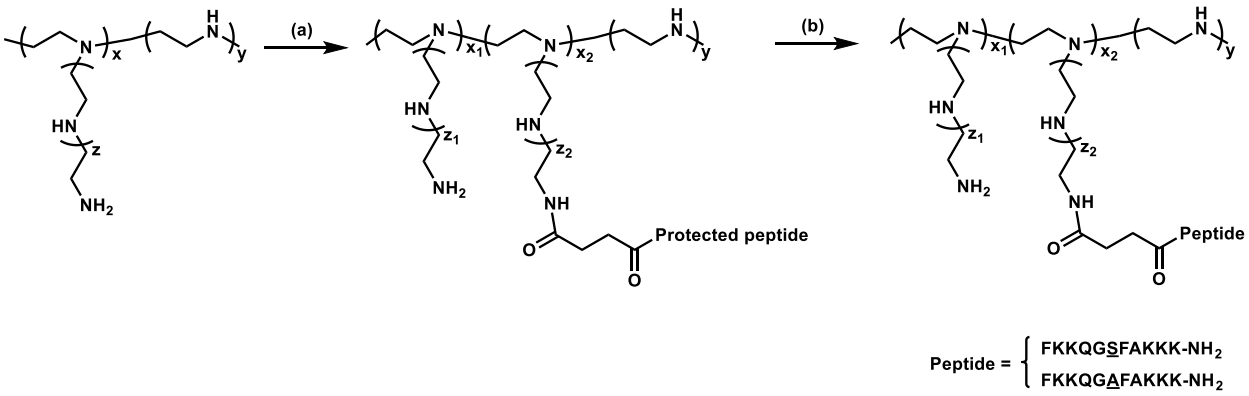

Scheme 3.1. Synthetic scheme for preparing BPEI-peptide conjugates. Reagents and conditions; (a) modification of peptide with HATU, HOAt and DIPEA in DMSO for 1 day at room temperature, (b) deprotection of protected group with TFA/triisopropylsilane/water for 2 hours at room temperature.

Table 3.1. Molecular parameters of gene carriers.

Polymer	Peptide content / mol%[a]	Number of peptide	Number of amine groups	
			Peptide	BPEI
PKCα-responsive polymers				
S-3	2.6	15	74	570
S-5	5.2	30	150	550
S-12	12	69	350	510
Negative control polymers				
A-3	2.9	17	84	560
A-5	5.2	31	150	550
A-11	11	63	310	520

a) Determined by ^{1}H-NMR spectrum.

3.4.2. Polyplex formation of BPEI-peptide conjugates

The author examined polyplex formation of the BPEI-peptide conjugates with pDNA by the gel retardation assay. As shown in **Figure 3.3**, all the polymers completed the polyplex formation at the N/P ratio of 1 to1.5, irrespective of the peptide content of the polymers.

The polyplex formation was also examined by the ethidium bromide exclusion assay. As shown in **Figure 3.4**, the critical N/P ratio where the RFI decrease is leveled off (critical N/P ratio) was varied with the difference of peptide content. The smallest critical N/P ratio was achieved by S-5 polymer which has the middle peptide content. This result indicates that the excess peptide content (~12 mol%) of the polymer inversely weakens the electrostatic interaction in the polyplex because crowding of the peptide chains on the BPEI surface will disturb the stoichiometric electrostatic interaction of the peptides with pDNA. The minimum RFI values after leveled off in S-3 and S-5 polymers are much smaller than those of previous gene carriers which have acrylamide or linear polyethylenimine main chains [10, 14]. The tighter pDNA condensation observed in the BPEI-peptide conjugates will be attributable to the appropriate density of the peptide chains on the BPEI core and geometry of the polymer backbone.

Figure 3.5a shows the average hydrodynamic diameter of the polyplexes of each polymer prepared at various N/P ratios. All the polymers gave large size aggregates (> 2 μm) at around N/P ratio of 3 because of the neutral surface charges of the polyplexes. The neutral surface changes of the polyplexes were confirmed by ζ-potential measurement (**Figure 3.5b**). This N/P ratio is in accordance with the critical N/P ratio where the RFI values are leveled off in the ethidium bromide exclusion assay (**Figure 3.4**).

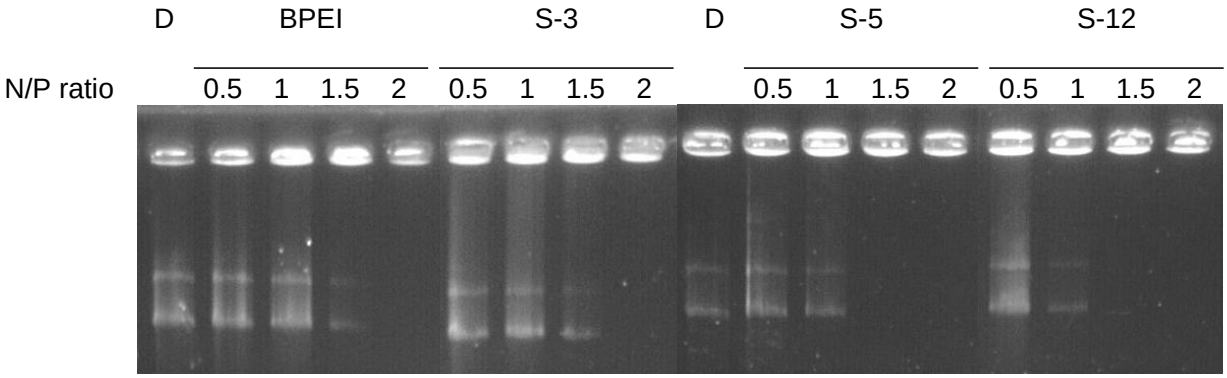

Figure 3.3. Polyplex formation evaluated by gel electrophoresis. D indicates pDNA alone.

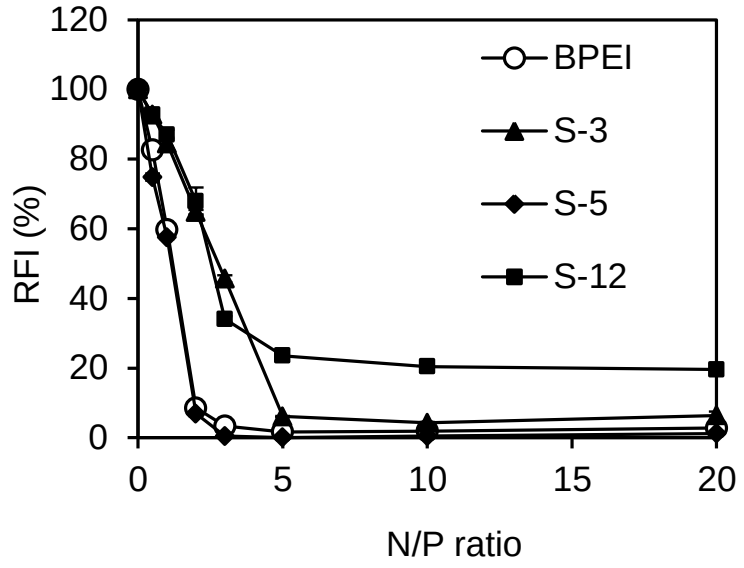

Figure 3.4. Polyplex formation evaluated by ethidium bromide exclusion assay. RFI stands for relative fluorescence intensity. Data are means ± SEM (n = 3).

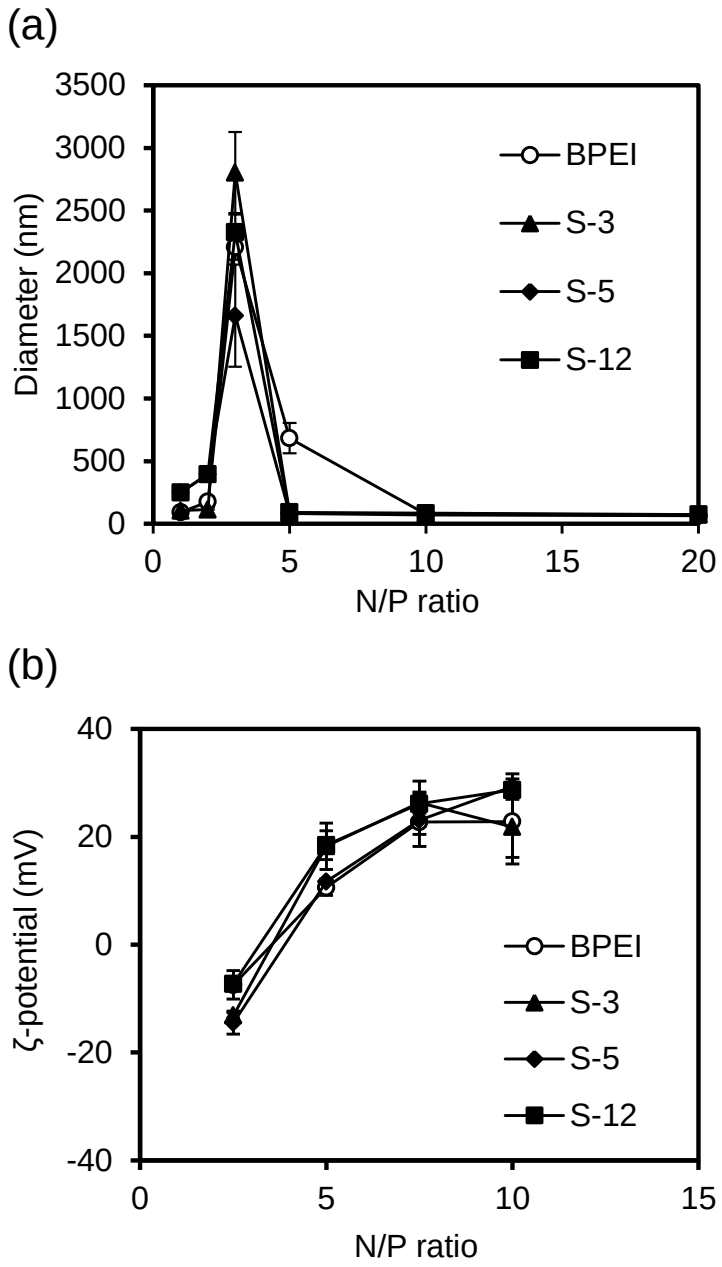

Figure 3.5. Hydrodynamic diameters (a) and ζ-potential (b) of polyplexes of each polymer at various N/P ratios. Data are expressed as means ± SEMs (n = 3).

3.4.3. Cellular uptake and cellular trafficking of polyplex

The cellular uptake of the polyplex was evaluated by using pDNA labeled with YOYO-1. As shown in **Figure 3.6**, the cellular uptake of the polyplex of S-3 was somewhat lower than that of the original BPEI probably because of the weaker condensation ability of S-3 than BPEI as revealed by the ethidium bromide exclusion assay (**Figure 3.4**).

Intracellular trafficking of the polyplexes in Huh-7 human hepatoma cell was monitored by CLSM. This cell line was reported to have relatively high PKCα activity [20]. pDNA was labeled with TAMRA and endosome/lysosome was stained with LysoTracker Green. In the case of the BPEI polyplex, red and yellow fluorescent dots were observed in cytoplasm, which result from polyplexes existing in the endosome and in the cytosol, respectively (**Figure 3.7a**). This result shows the quite high endosomal escaping ability of BPEI polyplex. The polyplexes of S-3 and S-10 also showed red spots resulting from the endosome-escaped polyplexes (**Figure 3.7b and c**). Thus, these polyplexes formed from the BPEI-peptide conjugates retain the endosomal escaping ability resulting from the BPEI core even after dense modification of the peptides.

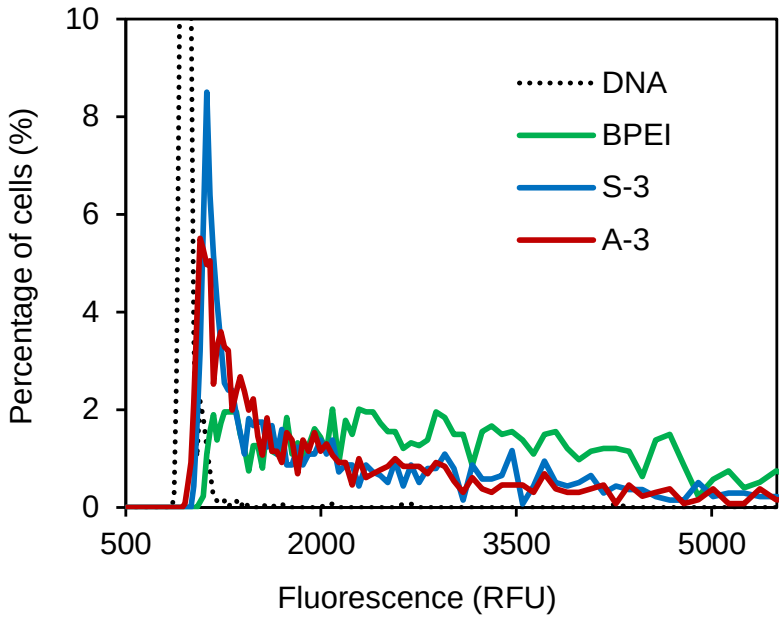

Figure 3.6. Cellular uptake of polyplexes of each polymer formed at N/P ratio of 5. RFU; relative fluorescence units.

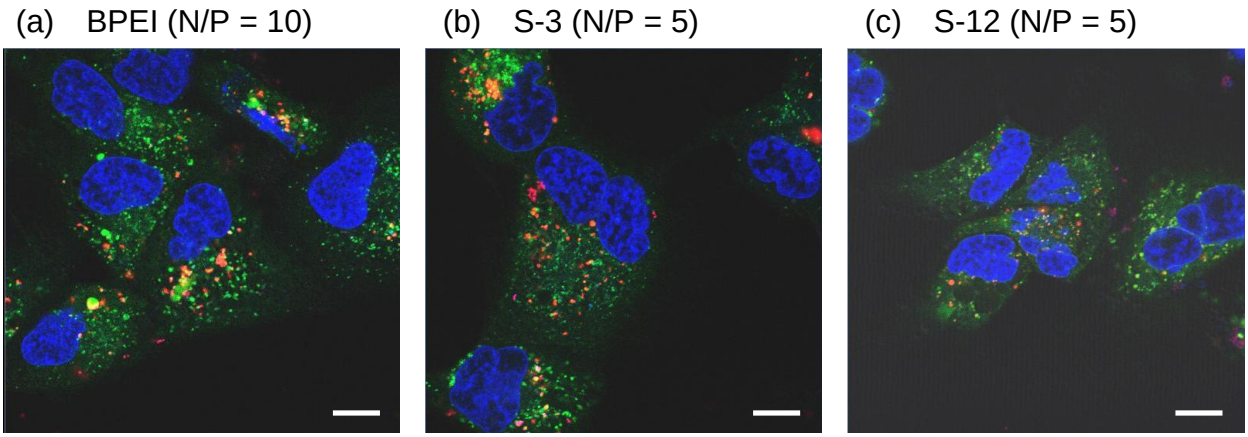

Figure 3.7. Intracellular trafficking of (a) BPEI (N/P = 10), (b) S-3 (N/P = 5), and (c) S-12 (N/P = 5) polyplexes was monitored by CLSM. Polyplexes were incubated in Huh-7 cells for 18 h in DMEM containing 10% FBS after 6 h incubation in OPTI-MEM. pDNA was labeled with TAMRA (red). Late endosomes/lysosomes and the nuclei were stained with LysoTracker Green (green) and Hoechst 33342 (blue), respectively. The scale bar represents 20 μm.

3.4.4. Regulation of transgene expression

The PKCα-responsive transgene activation was evaluated by using luciferase encoding pDNA in CT-26 mouse colon cancer cell. The author confirmed that this cell line has as high PKCα activity as those of other malignant cancer cell lines (B16 melanoma, U-87 MG, and HepG2) in which the authors succeed in PKCα-responsive gene expression previously using other types of peptide-polymer conjugates [10, 14]. The PKCα activity was evaluated based on the phosphorylation of the substrate peptide following previous procedures [13, 14]. The authors reported that the xenografted tumors prepared from these cell lines showed more than 5 times higher PKCα activity than the normal tissues [10].

As shown in **Figure 3.8**, in all three kinds of polyplexes, the S-series polymers showed the higher gene expression than those of the A-series polymers. This result showed that the polyplexes of the S-series polymers responded to PKCα to release pDNA for the gene expression. The ratio of the gene expression in the S-series and the A-series polymers (S/A ratio) can be an index of PKCα responsiveness of the polyplexes. 3- and 5-mol% polymers showed higher S/A ratios than the 10-mol% polymers. The highest S/A ratio was obtained in the 3-mol% polymers at the N/P ratio of 10, where more than 100 times higher gene expression was observed in S-3 than A-3. The clear-cut response in the 3- and 5-mol% polymers indicates that after escaping from the endosome, the polyplexes are tolerant toward the exchange reaction with cytosolic macromolecules until the phosphorylation by PKCα. However, once the peptide is phosphorylated, the polyplexes efficiently release pDNA for gene expression.

The lower response of the 10-mol% polymers toward PKCα will be explained by the weak condensation ability which was revealed by the ethidium bromide exclusion

assay (**Figure 3.4**). The weak condensation will result in the dissociation of the polyplex without the phosphorylation of the peptides. When the author compared the gene expression of the negative control polymers, A-11 was the highest at most of the N/P ratios in spite of its weakest condensation ability of pDNA. This result indicates that the polyplex of A-11 is enough tight to deliver pDNA into cells and the buffering capacity of the BPEI backbone of A-11 was not lost even in the high modification ratio of the peptide. This may not surprising because the peptide is modified onto the primary amine groups of the BPEI backbone which contribute less to the buffering capacity than secondary amine groups. Moreover, the author examined the cytotoxicity of the polyplex on CT-26 cells. As shown in **Figure 3.9**, all the polymers showed similar cytotoxicity irrespective of the peptide content of the polymers.

Notably, the successful gene regulation of the S-series polymers shows that the charge shifting of the peptides upon the phosphorylation controls the polyplexes stability even in the presence of the highly cationic BPEI core. This can be explained by the core-shell-like segregated structure between the BPEI core and the peptide shell in the polymers, in which the contribution of the cationic BPEI core on the interaction with pDNA can be minimized.

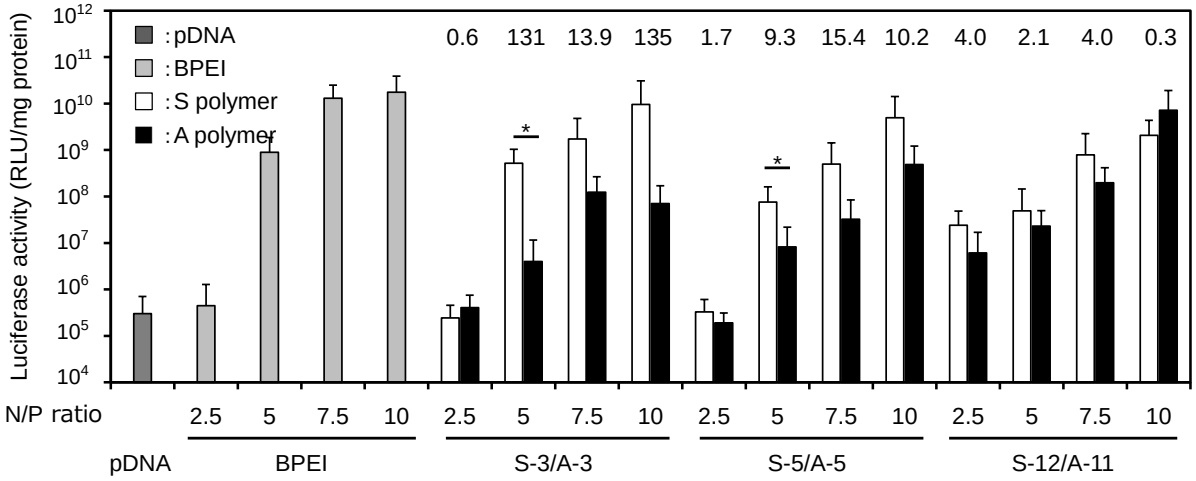

Figure 3.8. Transfection of polyplexes into CT-26 cells at various N/P ratios. Each value described above bar graph is the ratio of luciferase activities of S-series polymer and A-series polymer. Data are expressed as means ± SEM (n = 3, * $p < 0.05$).

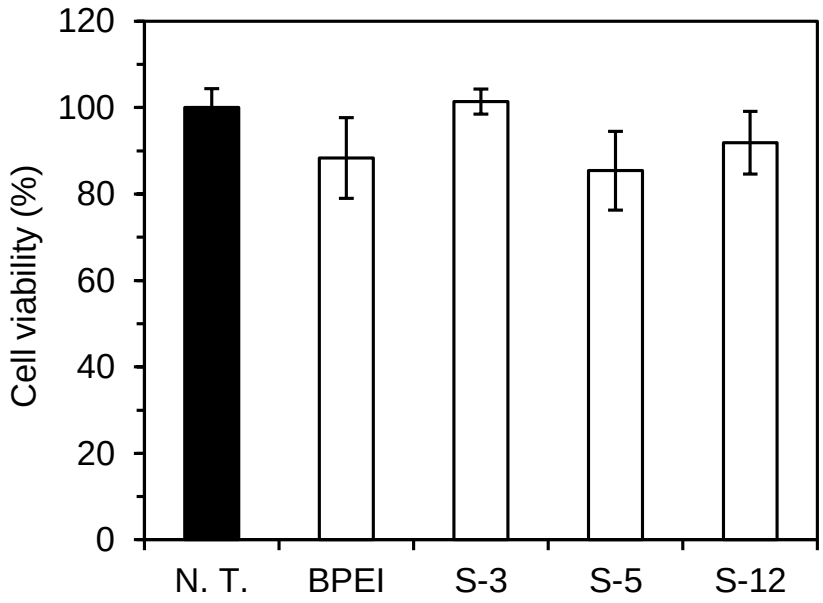

Figure 3.9. Cytotoxicity of polyplex into CT-26 cells at various N/P ratio = 5. N.T. is non treated cells. Data are expressed as means ± SEM (n = 3).

3.5. Summary

Here the author designed cancer-specific gene carriers, which are substrate peptide-modified BPEI. The carriers tightly condensed pDNA and effectively migrated to the cytosol from the endosome due to the buffering effect of the BPEI core. The carriers showed clear-cut response to intracellular PKCα of cancer cells to express pDNA. The simple design and straightforward synthesis of the present BPEI-based carriers will be generally applicable to any kinds of protein kinases which are specifically activated in disease cells.

3.6. References

[1] B. Sangro, C. Qian, V. Schmitz, J. Prieto, *Ann. N. Y. Acad. Sci*., **963**, 6 (2002).

[2] H. Faneca, A. Faustino, M. C. Pedroso de Lima, *J. Control. Release*, **126**, 175 (2008).

[3] Y. W. Cho, J. D. Kim, K. Park, *J. Pharm. Pharmacol*., **55**, 721 (2003).

[4] H. Hatakeyama, H. Akita, H. Harashima, *Adv. Drug Deliv. Rev*., **63**, 152 (2011).

[5] J. H. Kang, R. Toita, Y. Katayama, *Biotechnol. Adv*., **28**, 757 (2010).

[6] P. Cohen Eur, *J. Biochem*., **268**, 5001 (2001).

[7] J. Koivunen, V. Aaltonen, J. Peltonen, *Cancer Lett*., **235**, 1 (2006).

[8] P. C. Gordge, M. J. Hulme, R. A. Clegg, W. R. Miller, *Eur. J. Cancer*, **32**, 2120 (1996).

[9] K. Kawamura, J. Oishi, S. Sakakihara, T. Niidome, Y. Katayama, *J. Drug Target*., **14**, 456 (2006).

[10] J. H. Kang, D. Asai, J. H. Kim, T. Mori, R. Toita, T. Tomiyama, Y. Asami, J. Oishi, Y. T. Sato, T. Niidome, B. Jun, H. Nakashima, Y. Katayama, *J. Am. Chem. Soc*., **130**, 14906 (2008).

[11] T. Tomiyama, J. H. Kang, R. Toita, T. Niidome, Y. Katayama, *Cancer Sci*., **100**, 1532 (2009) .

[12] R. Toita, J. H. Kang, J. H. Kim, T. Tomiyama, T. Mori, T. Niidome, B. Jun, Y. Katayama, *J. Control. Release*, **139**, 133 (2009).

[13] J. H. Kang, D. Asai, S. Yamada, R. Toita, J. Oishi, T. Mori, T. Niidome, Y. Katayama, *Proteomics*., **8**, 2006 (2008).

[14] R. Toita, J. H. Kang, T. Tomiyama, C. W. Kim, S. Shiosaki, T. Niidome, T. Mori, Y. Katayama, *J. Am. Chem. Soc*., **134**, 15410 (2012).

[15] O. Boussif, F. Lezoualc'h, M. A. Zanta, M. D. Mergny, D. Scherman, B. Demeneix, J. P. Behr, *Proc. Natl. Acad. Sci. USA*, **92**, 7297 (1995).

[16] M. Meyer, A. Philipp, R. Oskuee, C. Schmidt, E. Wagner, *J. Am. Chem. Soc*., **130**, 3272 (2008).

[17] W. T. Godbey, K. K. Wu and A. G. Mikos, *J. Control. Release*, **60**, 149 (1999).

[18] S. Choosakoonkriang, B. A. Lobo, G. S. Koe, J. G. Koe, C. R. Middaugh, *J. Pharm. Sci*., **92**, 1710 (2003).

[19] A. El-Aneed, *J. Control. Release*, **94**, 1 (2004).

[20] J. H. Kang, D. Asai, R. Toita, H. Kitazaki, Y. Katayama, *Carcinogenesis*, **30**, 1927 (2009).

4. Effect of linker length for cancer-selective gene expression in peptide grafted polymers

4.1. Introduction

The author has developed PKCα-responsive polymeric gene carriers for tumor specific gene therapy [1-2]. In this concept, PKCα responsiveness is one of the most important factors to obtain sufficient therapeutic effect where fully suppression of the therapeutic gene in normal cells and the gene activation is high enough in tumor cells. In this context, the author group has investigated the structural factors affecting the signal responsiveness in D-RECS peptide grafted polymers.

In the previous studies, it is clarified that peptide content and molecular weight of the polymer backbone (polymer length) are the key factors to secure PKCα responsiveness in LPEI-type conjugate [5]. For example, 6-10 mol% of peptide content and polyethyleneimine with molecular weight of 25,000 gave the optimal signal responsiveness so that more than 100 folds amplification of gene expression was realized in response to PKCα [5]. This means 30-60 peptide side chains exist in a LPEI chain. Moreover, incorporation of hydrophobic long alkyl chain between peptide and polymer backbone enhanced the PKCα responsiveness to 390 times comparing with PKCα non-responsive conjugate due to the stabilization of the polyplex and improvement of cell uptake with the hydrophobic interaction between the incorporated alkyl chains [6]. Dramatic shrinkage of malignant glioblastoma was observed when suicide gene, caspase-8 encoding plasmid, was used in LPEI-peptide conjugate system using xenograft model mice. Therefore, further stabilization of the polyplex and enhancement of the signal responsiveness will contribute to the development of practical gene regulation delivery *in vivo*.

4.2. Linker length of peptide-polymer conjugate

In the previous study, peptide content, molecular weight of polymer backbone, and hydrophobic interaction were examined to increase PKCα responsiveness [5-6]. In this chapter, an effect of linker length of peptide side chain on the ability of gene regulation in response to PKCα was examined as another structural factor. Because pDNA used for D-RECS system is quite rigid and huge molecule with 500 nm in its radius, 10^4 folds shrinkage should be required to be packed in polyplex with 100 nm in size [7-8]. The author hypothesized if linker elongation contributes to stabilization of the polyplex by tangling the linker to pDNA strand to keep pDNA compacted state (**Figure 4.1**). Thus, some peptide-polymer conjugates with various length of the linker moieties were designed and investigated the effect of linker on PKCα responsiveness.

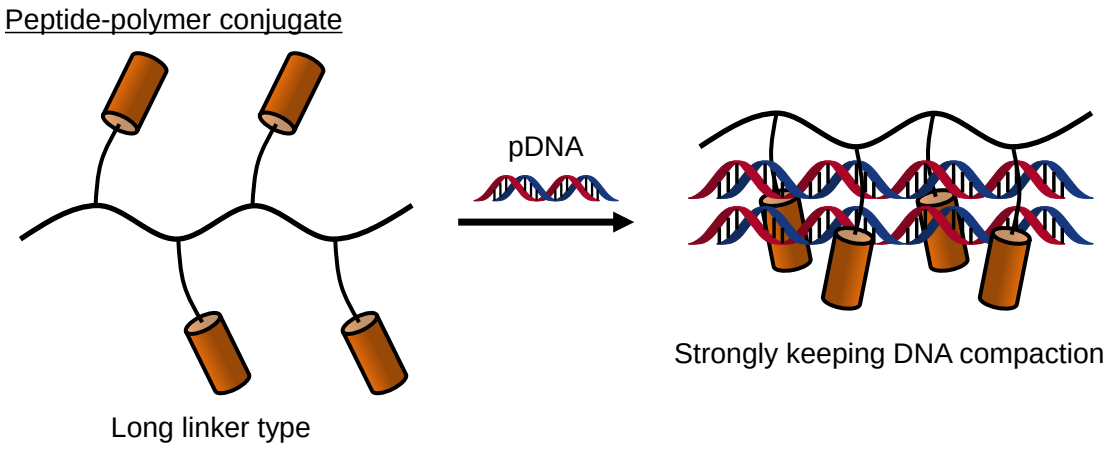

Figure 4.1. Strategy of linker length. Long linker of peptide-polymer conjugates assists to get tangled with pDNA strongly.

4.3. Materials and methods

4.3.1. Materials

Linear polyethylenimine (LPEI, 25 kDa) was purchased from Polysciences, Inc. (Warrington, PA, USA). Sieber Amide resin (amine density of 0.69 mmol/g) and all Fmoc-protected amino acids were obtained from Novabiochem, Merck (Hohenbrunn, Germany). Fmoc-8-amino-3,6-dioxaoctanoic acid (Fmoc-mini-PEG^{TM}) was purchased from Peptide Institute, Inc. (Osaka, Japan). (1-Cyano-2-ethoxy-2-oxoethylideneaminooxy) dimethylamino(morpholino)carbenium hexafluorophosphate (COMU), dimethyl sulfoxide (DMSO), trifluoroacetic acid (TFA), diisopropylethylamine (DIPEA), 1-methyl-2-pyrrolidone (NMP) and dichloromethane (DCM) were purchased from Watanabe Chemical (Hiroshima, Japan). Pyridine, methanol, dimethyl sulfoxide (DMSO), ethidium bromide (EtBr), heparin sodium, D-luciferin potassium salt, and Roswell Park Memorial Institute (RPMI) 1640 were purchased from Wako Pure Chemical Industries (Tokyo, Japan). Triisopropylsilane and succinic anhydride were purchased from Tokyo Chemical Industry (Tokyo, Japan). 4-(2-hydroxyethyl)-1-piperazineethanesulfonic acid (HEPES) was purchased from Dojindo (Kumamoto, Japan). Opti-MEM and Quant-iT PicoGreen dsDNA Reagent were purchased from Invitrogen Life Technologies (Carlsbad, CA, USA). pCMV-luc2 (7.0 kbp) containing a firefly luciferase cDNA fragment driven by a CMV promoter was prepared as follows. The firefly luciferase cDNA fragment was obtained from pGL4.10[luc2] vector (Promega, WI, USA) by HindIII and XbaI. The fragment was inserted into the pcDMA3 vector (Invitrogen Life Technologies). The resulting pDNA was amplified in the Escherichia coli strain DH5α, isolated, and purified using a QIAGEN Plasmid Mega Kit (Qiagen, CA, USA).

4.3.2. Synthesis of substrate peptide with protected side groups

The PKCα-specific substrate peptide with protected side groups (peptide-S; HOOC-$(CH_2)_2$-CO-X_y-FK(Boc)K(Boc)Q(Trt)G*S(tBu)*FAK(Boc)K(Boc)K(Boc)-NH_2) and its negative control peptide (peptide-A; HOOC-$(CH_2)_2$-X_y-CO-FK(Boc)K(Boc) Q(Trt)G*A*FAK(Boc)K(Boc)K(Boc)-NH_2) for 3 different linkers (y = 0, 2, 4) so that 6 kinds were designed. The peptides were synthesized by standard Fmoc-chemistry, using the Sieber Amide resin (0.3 mmol), 20% piperidine/DMF for deprotection of Fmoc group, DIPEA as a base, and COMU as coupling reagents (0.9 mmol). Presence of free amines was checked by the standard Kaiser (ninhydrin) test and the amount of loading amino acids was evaluated by Fmoc test (ε_{301} = 7800 $L \cdot mol^{-1} \cdot cm^{-1}$) one by one. Fmoc-mini-PEG^{TM} was used for the linker (X; -NH-$(CH_2CH_2O)_2$-CH_2-CO-). After the coupling reaction and Fmoc-removal of the last amino acid, the N-terminal site of the peptide was reacted with 1 mmol succinic anhydride dissolved in 10% DIPEA/DMF. The peptide with protected side groups cleaved from the resin by treating with 1% TFA/DCM. The solution including peptide was neutralized by adding 10% pyridine/methanol. The protected peptide was reprecipitated and washed by using cold water, and then dried in vacuo. The purity of the peptide was confirmed by reverse-phase liquid chromatography and MALDI-TOF-MS after deprotection to be > 90%.

4.3.3. Synthesis of LPEI-peptide conjugate

LPEI (10 mg, 0.23 mmol) was dissolved in 0.8 mL of DMSO. To this solution, 0.5 mL of DMSO solution including the protected substrate peptide (17.3 μmol, 7.5 mol%) and COMU (0.12 mmol) was added and then 50% DIPEA/DMSO (0.4 mL) was dropped. The resulting mixture was stirred overnight at 70ºC. After the reaction,

the polymer was recovered by reprecipitation using cold diethyl ether and then dried. The obtained precipitate was deprotected with a mixture of 2 mL TFA/triisopropylsilane/water (95/2.5/2.5) for 2 hour at room temperature. The deprotected polymer was obtained by reprecipitation using cold diethyl ether and dialyzed against aqueous solution of $NaHCO_3$ (pH 8-9) for 1 day and then pure water for 2 days (SpectraPore 6, MWCO = 3,500). After lyophilization, the content of the peptide and stearate in the polymer was determined by ^{1}H NMR spectrum. ^{1}H NMR of S-type (300 MHz, D_2O, δ): 1.26 (3H, d A(β)), 1.37 (10H, m, K(γ)), 1.60 (10H, d, K(δ)), 1.71 (10H, d, K(β)), 2.00 (2H, Q(β)), 2.48 (2H, s, Q(γ)), 2.54 (4H, d, COC*H*$_2$C*H*$_2$CO), 2.81-2.91 (4H, m, -C*H*$_2$C*H*$_2$NH- of LPEI units), 2.91 (-NH-(C*H*$_2$C*H*$_2$O)$_2$- of Linker(X)), 3.07 (4H, s, F(β)) 3.39 (10H, d, K(ε)), 3.55-3.64 (4H, m, -C*H*$_2$C*H*$_2$NCO- of LPEI units), 3.81 (4H, m, S(β) and G(α)), 3.99 (-C*H*$_2$CO- of Linker(X)), 4.19 (8H, q, A(α), K(α), Q(α)), 4.31 (1H, t, S(α)), 4.57 (1H, q, F(α)), 4.75 (2H, s, H_2O), 7.21 (10H, t, F(C_6H_5)).

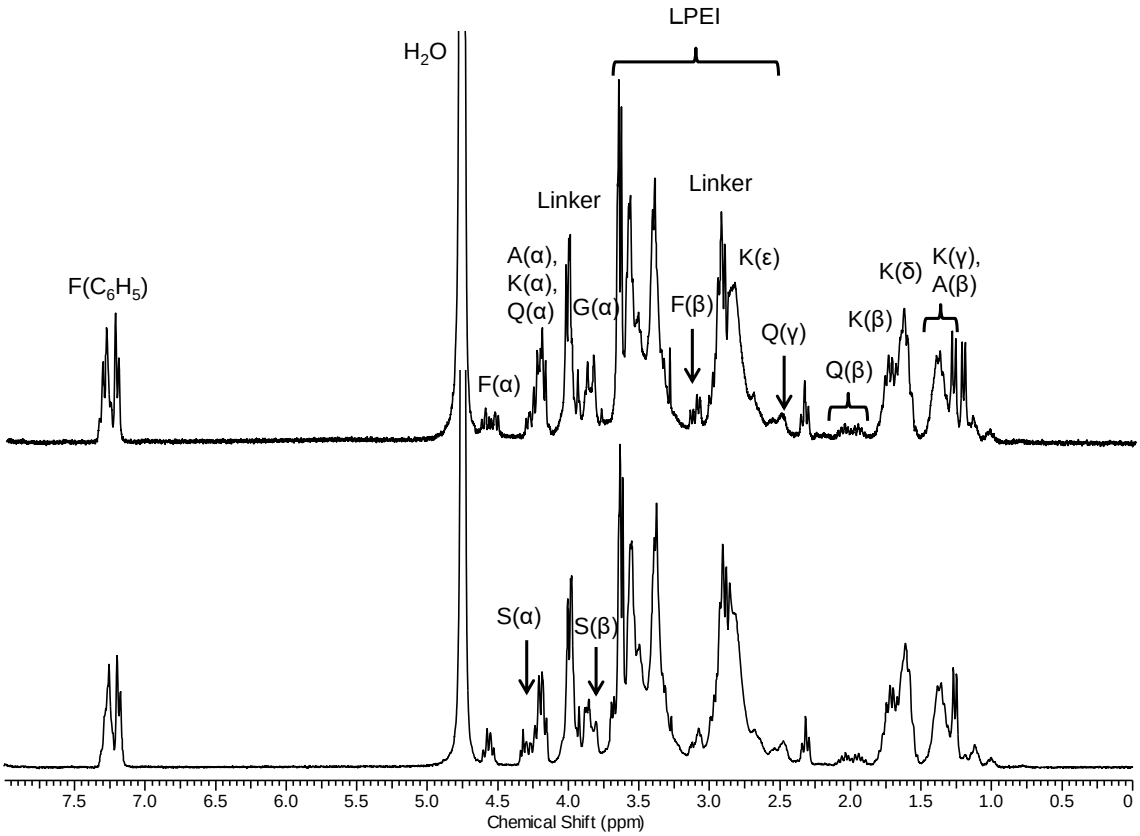

Figure 4.2. ^{1}H NMR spectra of LPEI-peptide-A conjugate (upper panel) and LPEI-peptide-S conjugate (lower panel) in D_2O.

4.3.4. Preparation of polyplex of LPEI-peptide conjugate and pDNA

Polyplexes were prepared by adding polymer solution to equal volume of 0.1 mg/mL pDNA solution, and allowed to incubate for 20 min at room temperature. The mixing ratio is expressed as the molar ratio of the amino group of polymer to the phosphate group of pDNA (N/P ratio). Each polyplex was diluted in aqueous buffers (10 mM HEPES buffer (pH 7.4)). Characterization of polyplex was performed by ethidium bromide exclusion assay and dynamic light scattering.

4.3.5. Ethidium bromide exclusion assay

The relative binding affinity of polymer to condense pDNA was assessed by a standard EtBr fluorescence quenching [9-10]. Before polyplex formation, 0.1 mg/mL pDNA solution was stained with half volume of 50 μg/mL EtBr solution for 10 min at room temperature. The pDNA solution was added by polymer solution at various N/P ratios and incubated at room temperature for 20 min. The solution was diluted by 10 mM HEPES buffer (pH 7.4). Fluorescence measurements of each sample were performed at 25ºC using a multilabel counter ARVO (Wallac Incorporated, Turku, Finland). Excitation and emission wavelengths were 530 nm and 590 nm respectively. The relative fluorescence intensity (RFI) was determined by using the following equation: $RFI = (F_{obs}-F_e)/(F_0-F_e) \times 100\%$, where F_{obs}, F_e and F_0 are the fluorescence intensities of the polyplex at each N/P ratio, background (EtBr only), and free pDNA without polymer, respectively. Data were expressed as mean ± standard error of the mean (SEM) (n = 3).

4.3.6. Diameter and ζ-potential of polyplexes

Diameter and ζ-potential of the polyplexes were measured using a Zetasizer Nano ZS (Malvern Instruments, Worcestershire, UK) at 25ºC. The final concentration of pDNA for diameter and ζ-potential measurement was 20 and 5 μg/mL, respectively. Freeze-dried process followed up polyplex formation and then freeze-dried sample was redissolved in 10 mM HEPES buffer (pH 7.4).

4.3.7. Heparin-induced decomplexation assay.

Heparin-induced decomplexation assay was performed by PicoGreen quantification according to literature [11]. The fluorescence intensity of PicoGreen dye increases significantly upon binding double strand DNA, allowing the quantification that heparin releases DNA from polyplex. Polyplexes at the N/P ratio of 10 were prepared with pDNA (1 μg) and polymer for 20 min at room temperature. After polyplex formation, an equal volume of 2× PicoGreen and heparin (10 units, 0.2 units/μL) solution was added. The mixture was diluted in 10 mM HEPES buffer (pH 7.4), and then incubated for 16 h at 37°C. Fluorescence measurements of each sample were performed at 25ºC using the multilabel counter ARVO (Ex/Em = 485/535 nm). The decomplex degree was determined by using the following equation: Decomplex degree = $(F_{sample}-F_{blank})/(F_{DNA}-F_{blank})$, where F_{sample}, F_{DNA} and F_{blank} are the fluorescence intensities of the polyplex, free pDNA without polymer, and background (PicoGreen only), respectively.

4.3.8. Cell Culture

CT-26 cells were cultured in RPMI 1640 containing 10% fetal bovine serum (FBS), 100 U/mL penicillin, 100 μg/mL streptomycin and 0.25 μg/mL amphotericin B (all from Gibco Life Technologies, Grand Island, NY, USA) under a humidified atmosphere containing 5% CO_2 and 95% air at 37^{o}C.

4.3.9. Real time luciferase gene expression.

The real time luciferase gene expression of polyplexes was performed according to literature [12-13]. CT-26 cells (120,000 cells) were seeded into a 35 mm dish (Iwaki, Tokyo, Japan) in 2 mL of RPMI-1640 and cultured for 24 h at 37°C. The medium in dishes was replaced with 1-mL of Opti-MEM containing polyplexes at N/P ratio = 10 with pDNA (2 μg/dish). After incubation for 4 h, the medium was changed to fresh medium containing 10% FBS, 200 μM D-luciferin potassium salt, and 10 mM HEPES buffer (pH 7.4). The dishes were set in a luminometer (AB-2500 Kronos Dio, ATTO, Tokyo, Japan), and the bioluminescence was monitored every 20 min with an exposure time of 1 min.

4.3.10. *In vitro* transfection study

CT-26 cells were then seeded on a 24-well plate (40,000 cells/well) in RPMI 1640 containing 10% FBS and incubated at 37ºC for 24 h. Polyplexes at the N/P ratio of 10 were prepared with pDNA (1 μg) and polymer for 20 min at room temperature. The medium was replaced with 500 μL Opti-MEM containing polyplexes. After incubation for 4 h, the medium was changed to RPMI 1640 containing 10% FBS followed by a further incubation for 20 h. After washing the cells with Dulbecco's phosphate buffered saline (DPBS), the cells were lysed with 150 μL of lysis buffer (20 mM Tris-HCl containing 0.05% TritonX-100 and 2 mM EDTA (pH 7.4)) for 20 min. 10 μL of the lysate was mixed with 40 μL of Luciferase Assay Reagent (Promega) and then measured with a GloMax 20/20 Luminometer (Promega). Protein concentration was measured with Bio-Rad Protein Assay Dye Reagent (Bio-Rad, CA, USA). The result was presented as relative luminescence units (RLU)/mg total protein. Data were expressed as mean ± SEM (n = 3).

4.4. Results and discussion

4.4.1. Synthesis of LPEI-peptide conjugates with long linker

Linker was incorporate at amino terminus of the PKCα substrate peptide using Fmoc chemistry (**Figure 4.2**). Fmoc-miniPEG^{TM} was used as a linker unit due to the easiness for the preparation. Because Fmoc-miniPEG^{TM} is hydrophilic and includes two ethylene glycol units, it is easy to prepare various length of linker, and also effect of linker length can be evaluated without any hydrophobic interaction. Thus, three kinds of peptides with 0, 2 and 4 Fmoc-miniPEG^{TM} units as linkers were synthesized (**Table 4.1**). The longest linker was 48 Å which is much longer than previously investigated hydrophobic linker (20 Å). Synthesized protected peptide was introduced into imino nitrogen of LPEI without deprotection in 6-10 mol% (**Scheme 4.1**). For the introduction of peptide via amide bonding, ordinary condensation reagents are usually not successful. Thus, COMU, which has high ability for condensation reaction, was used and the peptide could be incorporated with 70% of conversion. For the evaluation of PKCα responsiveness on gene regulation, PKCα responsive (S-series) and non-responsive (A-series) polymers were prepared in each linker lengths as shown in chapter 3. Thus, S- and A-series polymers for 3 different linkers so that 6 kinds of polymers were synthesized (**Table 4.2**).

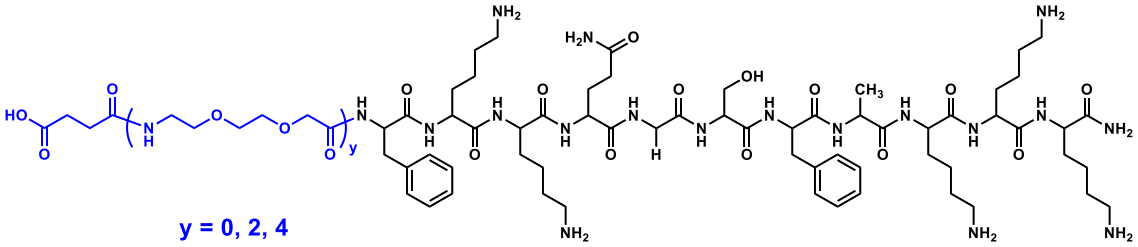

Figure 4.2. Liker modification on PKCα-specific substrate peptides.

Table 4.1. Peptide sequence and linker length of prepared polymers.

Peptide sequence[a]	y, linker no.	Mw/ g/mol	Linker length[b] / Å
PKCα-specific substrate peptides			
HOOC-$(CH_2)_2$-CO-FKKQG**S**FAKKK-NH_2	0	1395.7	4
HOOC-$(CH_2)_2$-CO-**X**$_2$-FKKQG**S**FAKKK-NH_2	2	1686.0	26
HOOC-$(CH_2)_2$-CO-**X**$_4$-FKKQG**S**FAKKK-NH_2	4	1976.3	48
Negative control peptides			
HOOC-$(CH_2)_2$-CO-FKKQG**A**FAKKK-NH_2	0	1379.7	4
HOOC-$(CH_2)_2$-CO-**X**$_2$-FKKQG**A**FAKKK-NH_2	2	1670.0	26
HOOC-$(CH_2)_2$-CO-**X**$_4$-FKKQG**A**FAKKK-NH_2	4	1960.3	48

[a] Define linker as X (-NH-$(C_2H_4O)_2$-CH_2O-). [b] Calculated by molecule editor software.

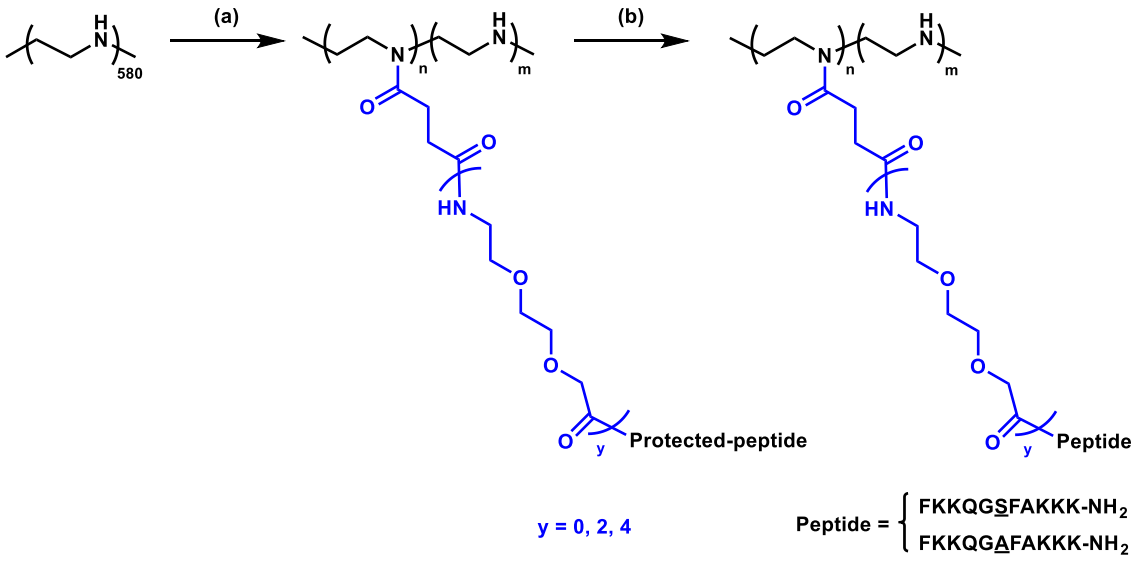

Scheme 4.1. Modification of the peptide into polymer backbone. Reagents and conditions; (a) modification of peptide with COMU and DIPEA in DMSO overnight at 70ºC, (b) deprotection of protected group with TFA/triisopropylsilane/water for 2 hours at room temperature.

Table 4.2. Molecular parameters of gene carriers.

Polymer	y, linker no.	Peptide content[a] / mol%	Number of peptide	M_w[b] / 10^4 g/mol
PKCα-responsive polymers				
S(X0)	0	5.3	31	6.8
S(X2)	2	4.9	29	7.3
S(X4)	4	5.5	32	8.7
Negative control polymers				
A(X0)	0	7.0	41	8.0
A(X2)	2	5.8	34	8.0
A(X4)	4	6.5	38	9.9

[a] Determined by ^{1}H-NMR spectrum. [b] Calculated from peptide contents and Mw of the parent LPEI (degree of polymerization; 580).

4.4.2. Polyplex formation of LPEI-peptide conjugates

As shown in chapter 3, DNA condensation ability of newly synthesized LPEI-peptide conjugates was evaluated by ethidium bromide (EtBr) exclusion assay. After EtBr was added to pDNA solution and incubated to intercalate the EtBr to DNA strand, polyplex was formed with each LPEI-peptide conjugate. In this assay, EtBr is excluded from DNA with the compaction of the DNA strand in the polyplex formation. Thus, decrease of the EtBr fluorescence intensity can be used as index of the DNA compaction. As shown in **Figure 4.3**, fluorescence intensity decreased with formation of the polyplex and reached to minimum value at N/P of 5 in all the polymers. All the obtained curves were nearly the same regardless of the linker length so that DNA compaction ability in other word binding ability of the polymer to pDNA was similar in all the polymers. Obtained DNA compaction ability was also similar to that of LPEI itself. These results indicated that there are no steric effects of the peptide and linker against the suppression of DNA compaction. Physical characteristics of the polyplexes such as size and ζ-potential are listed in **Table 4.3**. All the obtained polymers formed polyplex with pDNA with similar size and ζ-potential at around 110 nm and +20 mV, respectively (**Table 4.3**). These results demonstrated that linker length did not show any obvious effect on physicochemical characteristics in polyplex formation.

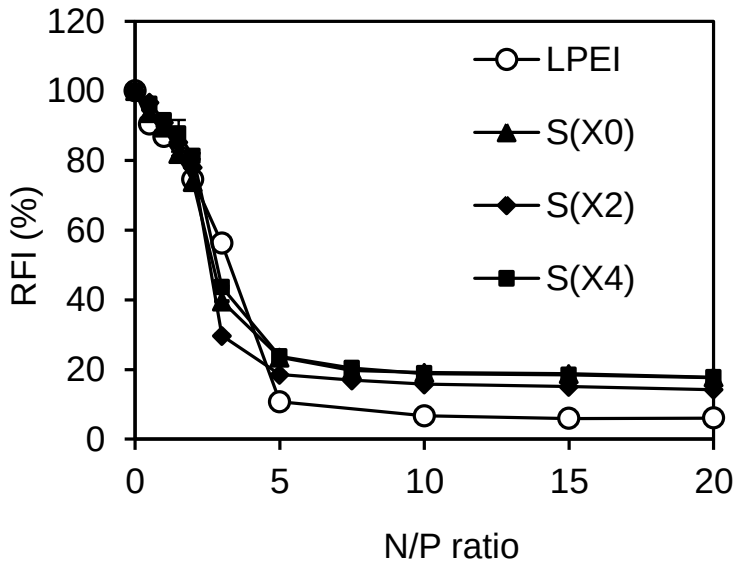

Figure 4.3. Polyplex formation evaluated by ethidium bromide exclusion assay in LPEI and peptide grafted LPEI with different linker length. RFI stands for relative fluorescence intensity. Data are means ± SEM (n = 3).

Table 4.3. Hydrodynamic radius and ζ-potential of polyplex between obtained polymers and pDNA.

Polymer	Diameter (nm)	PdI[a]	Count Rate (kcps)	ζ-potential (mV)
S(X0)	115	0.14	9834	24.3
S(X2)	116	0.12	7373	24.9
S(X4)	119	0.11	9160	18.0
A(X0)	118	0.13	10247	21.2
A(X2)	121	0.10	8031	22.1
A(X4)	121	0.14	9141	17.6

[a] PdI; Polydispersity index.

Then, stability of the polyplex was evaluated with exchanging efficiency of polyanion to pDNA in the polyplex. Thus, heparin as a polyanion 2 unis/mL was added to each polyplex and incubated at 37℃ for 16 hours, then released pDNA was quantified by PicoGreen as a detection reagent of DNA. As shown in **Figure 4.4**, dissociated pDNA decreased with increasing linker length. S(X4) suppressed pDNA releasing with heparin by 20% comparing with S(X0). This suppression of polyanion exchanging is probably due to the enhanced entanglement of the peptide with longer linker and also polymer backbone to pDNA. This increased entanglement may resist to the exchange of heparin and pDNA. In S(X0) which has no linker moiety in side chain, peptide and polymer chain cannot fully tangle with pDNA due to the steric hindrance if sufficient peptides bind to the pDNA through an electrostatic interaction. Thus, pDNA released by exchanging with heparin was easier in S(X0) than that in S(X4).

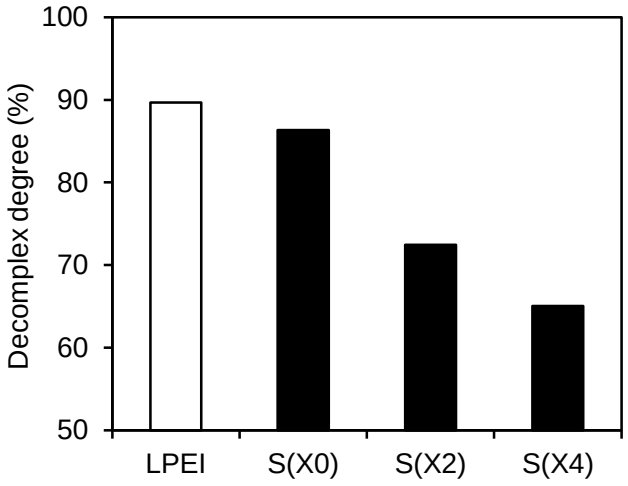

Figure 4.4. Effect of linker length on polymer-DNA complexation strength evaluated by heparin-induced polyplex decomplexation.

4.4.3. Regulation of transgene expression

Time dependent gene expression from the polyplex in CT-26 cells was monitored by real time luminescence counter. Thus, after the polyplex between luciferase encoding pDNA and peptide-polymer conjugate was formed, the polyplex was transfected in CT-26 cells. Then luminescence was monitored for 48 hours after the transfection. **Figure 4.5** indicates larger expression level was observed in S-series polymers than in A-series-polymers in all the case. Thus, obtained polymers demonstrated PKCα responsiveness. To investigate the effect of the linker length on PKCα responsiveness, S(X0) and S(X4) showed suppressed gene expression compared to S(X2). This result indicates the low cellular uptake or suppression of gene expression. Therefore, the author confirmed gene expression in a quantitative way.

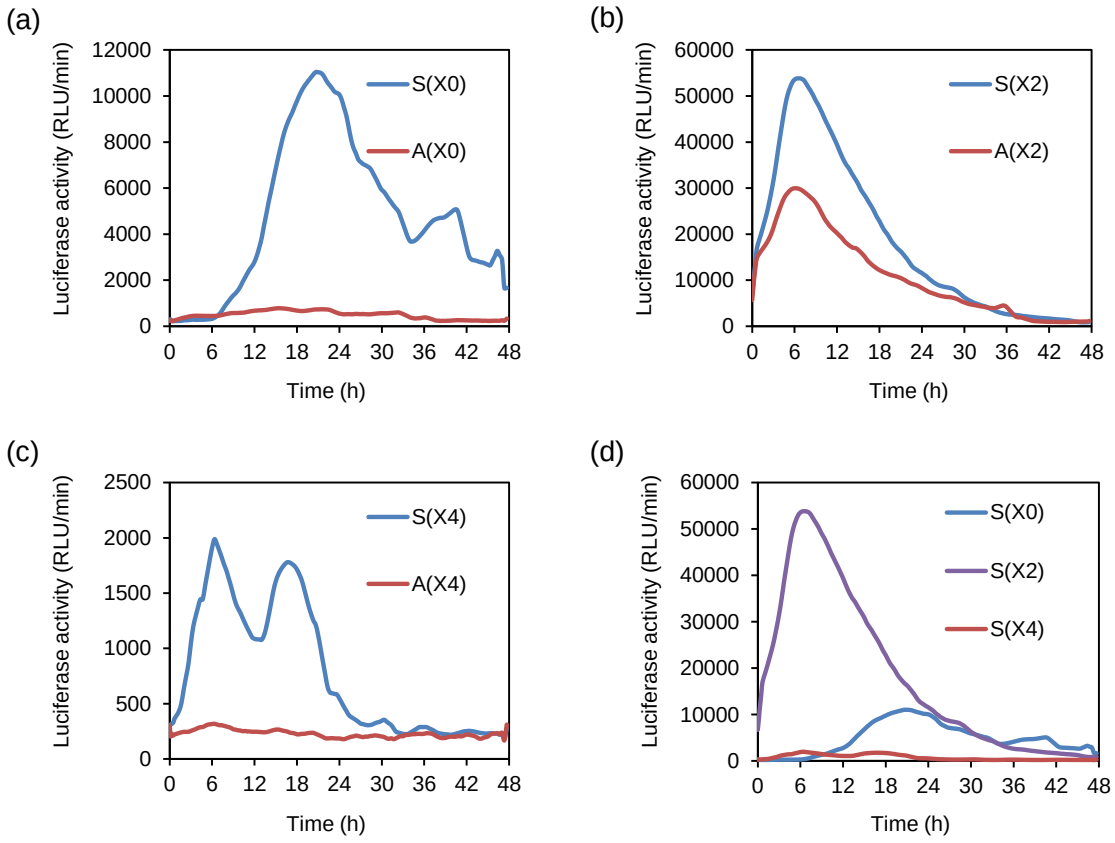

Figure 4.5. Time dependent expression of luciferase of polyplexes in CT-26 cells.

PKCα responsiveness in each polymer was evaluated with luciferase encoding pDNA in CT-26 cells which has high activity of PKCα (**Figure 4.6**). When expression ratio between S-polymer and A-polymer was compared between S(X2) and S(X4), S(X2) shows much lower S/A expression level which is lower than 1 than that in S(X4), although expression level was higher than S(X4). S(X4) which has the longest linker showed quite high S/A ratio (10-17 folds) while expression level declined to one fifth than that in S(X2). This indicates that longer linker enhances the suppression of transgene with strong entanglement which contributes to the stability of the polyplex. However, this suppression can be still canceled with phosphorylation of the peptide. On the other hand, S(X0) without extra-linker showed the lowest expression level probably due to the lower cellular uptake, but S/A ratio was nearly 1 indicating no obvious PKCα responsiveness. This may be caused by the weak suppression ability of the transgene.

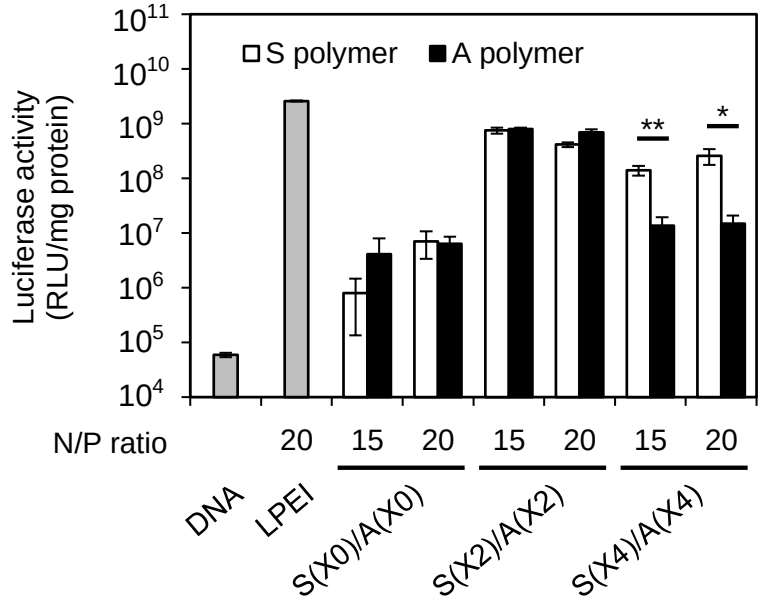

Figure 4.6. Result of *in vitro* transfection in various polyplex into CT-26 cells. Data are expressed as means ± SEM (n = 3, * $p < 0.05$, ** $p < 0.01$).

4.5. Summary

In this chapter, effect of linker moiety in D-RECS polymer on the PKCα responsive gene regulation was investigated. Peptide grafted LPEIs with different length if linker moiety were successfully synthesized by solid phase synthesis and Fmoc chemistry. Length of the linker between peptide and polymer chain affected to the PKCα responsiveness and optimization of the linker length increased 10 times in PKCα responsiveness. Combination of this hydrophilic linker with the previous BPEI-type polymer may be able to further improve the PKCα responsiveness.

4.6. References

[1] J. H. Kang, D. Asai, J. H. Kim, T. Mori, R. Toita, T. Tomiyama, Y. Asami, J. Oishi, Y. T. Sato, T. Niidome, B. Jun, H. Nakashima, Y. Katayama, *J. Am. Chem. Soc*., **130**, 14906 (2008).

[2] R. Toita, J. H. Kang, J. H. Kim, T. Tomiyama, T. Mori, T. Niidome, B. Jun, Y. Katayama, *J. Control. Release*, **139**, 133 (2009).

[3] J. H. Kang, D. Asai, S. Yamada, R. Toita, J. Oishi, T. Mori, T. Niidome, Y. Katayama, *Proteomics*., **8**, 2006 (2008).

[4] J. H. Kang, R. Toita, T. Tomiyama, J. Oishi, D. Asai, T. Mori, T. Niidome, Y. Katayama, *Bioorg. Med. Chem. Lett*., **19**, 6082 (2009).

[5] R. Toita, J. H. Kang, T. Tomiyama, C. W. Kim, S. Shiosaki, T. Niidome, T. Mori, Y. Katayama, *J. Am. Chem. Soc*., **134**, 15410 (2012).

[6] C. W. Kim, R. Toita, J. H. Kang, K. Li, E. K. Lee, G. X. Zhao, D. Funamoto, T. Nobori, Y. Nakamura, T. Mori, T. Niidome, Y. Katayama, *J. Control. Release*, **170**, 469 (2013).

[7] K. Yoshikawa, *Adv. Drug Deliv. Rev*., **52**, 235 (2001).

[8] K. Yoshikawa., M. Takahashi, V. V. Vasilevskaya, A. R. Khokhlov, *Phys. Rev. Lett*., **76**, 3029 (1996).

[9] A. J. Geall, I. S. Blagbrough, *J. Pharm. Biomed. Anal*., **22**, 849 (2000).

[10] J. B. LePecq, C. Paoletti, *J. Mol. Biol*., **27**, 87 (1967).

[11] A. F. Ghobadi, R. Letteri, S. S. Parelkar, Y. Zhao, D. Chan-Seng, T. Emrick, A. Jayaraman, *Biomacromolecules*, **17**, 546 (2016).

[12] M. Oba, K. Aoyagi, K. Miyata, Y. Matsumoto, K. Itaka, N. Nishiyama, Y. Yamasaki, H. Koyama, K. Kataoka, *Mol. Pharm.*, **5**, 1080 (2008).

[13] S. Takae, K. Miyata, M. Oba, T. Ishii, N. Nishiyama, K. Itaka, Y. Yamasaki, H. Koyama, K. Kataoka, *J. Am. Chem. Soc*., **130**, 6001 (2008).

5. Conclusion

5.1. Chapter summary

The availability of nanocarriers has potential in medical and pharmaceutical applications for treatment of intractable diseases. Previous researches reported cancer-selective gene delivery by nanocarriers with multiple functions. Therefore, the author developed cancer-specific gene expression system in order to control powerful therapeutic genes in cancer cells and in normal cells. Previously, the author group demonstrated cancer-specific gene expression responding to highly activated protein kinase Cα (PKCα) in cancer cells, referred to as "Drug or Gene Delivery System to Responding to Cellular Signals (D-RECS)". In this system, conjugate of PKCα-substrate peptide and polymer showed PKCα responsive gene expression in cancer cells and cancer tissues with high PKCα activity. As a next step, the author attempted to develop a new technique to stabilize polyplexes of pDNA/polymer complexes under physiological conditions and a new peptide-polymer conjugate with simple synthesis step. In addition, the author re-examined molecular architecture of peptide-polymer conjugates due to improve PKCα responsiveness and achieve a clear-cut gene expression system without undesirable side effects.

In chapter 2, the author reported a new technique to stabilize pDNA/linear polyethyleneimine (LPEI) complex using serum albumin. Stearoyl group was modified on LPEI as a specific ligand for serum albumin. Stearoyl modification enhanced the colloidal stability of ternary complex composed of stearoyl-modified LPEI, pDNA, and serum albumin even under physiological saline condition. In addition, the author found formation of ternary complex has advantages in preventing aggregation with red blood cells and transfection ability to LPEI while the cytotoxicity was significantly lower than LPEI. Structure formation of ternary complex achieved these desirable

properties for intravenous injection in spite of minimum stearoyl ligands.

In chapter 3, the author designed branched polyethyleneimine (BPEI)-based gene carriers which respond to cancer-specific activation of PKCα. Because BPEI contains many reactive primary amine groups on the end of the branched chain structure, the PKCα substrates peptides were readily modified to the primary amine groups by one step. The carriers showed tight DNA condensation and effective cellular uptakes due to the endosomal escaping ability of the BPEI core unit. *In vitro* performance of these carriers showed a clear-cut response to PKCα to release pDNA for gene expression. The simple design including BPEI core structure achieved the PKCα responsiveness and straightforward synthesis step.

In chapter 4, the author discussed the linker length of peptide-polymer conjugates and the effect on PKCα responsiveness. Linker segment was introduced to peptides using solid phase peptide synthesis and linker length was controlled by the number of repeated coupling reactions. Although linker did not affect polyplex formation, conjugates with linker showed resistance against the decomplexation. *In vivo* experiment, the carriers exhibited improvement in PKCα responsiveness. These results indicate the effect of linker length on cancer-selective gene delivery.

In this thesis, the author developed a new technique to stabilize polyplex, BPEI-based gene carriers with simple synthesis step, and linker modified gene carriers. These technologies are a first step to achieve systemic administration of nanocarriers and reduction in production cost.

5.2. Conclusion

This thesis provides a fresh perspective on previous design of peptide-polymer conjugates. Previous design focused on main chain of polymer, peptide, and hydrophobic linker in order to control cancer-selective gene expression responding to PKCα. Previous results showed the stabilization of polyplex composed of peptide-polymer conjugates and pDNA increases PKCα responsiveness due to suppression of undesirable PKCα non-responsive gene expression. However, there are many obstacles that need to be overcome to put cancer-selective gene expression system into practical use; the low physiological stability of polyplex, the complicated synthetic step, and missing piece of molecular design for the improved PKCα responsiveness. The author developed three gene carrier designs in order to solve these problems. Stearoyl modification formed a ternary complex via a specific interaction of the stearoyl group with serum albumin and gave the high colloidal stability under physiological conditions. This stable ternary complex may be expected to give applicable functions to systemic administration of nanocarriers. On the other hand, structural feature of BPEI achieved both simple synthesis step and PKCα responsiveness in cancer-selective gene expression system. Chemical structure of polymers has an advantage in easiness not only for the precise molecular design but also for the industrial production for practical use. In addition, linker length between peptide and polymer backbone was an important factor for suppression of polyanion exchanging of pDNA with heparin by entanglement of the peptide-polymer conjugates to pDNA. This entanglement enhanced PKCα responsiveness by the enhanced suppression of transgene. This linker design expands the structure freedom of peptide-polymer conjugate in order to improve PKCα responsiveness furthermore.

In a future, stearoyl groups should be incorporated in the PKCα responsive

peptide-modified BPEI to realize more practical carrier. Moreover, linker incorporation between peptide and BPEI will be an essential factor for cancer-selective gene expression. Also previous results showed hydrophobic long alkyl chain linker increased PKCα responsiveness due to the stabilization of the polyplex and increment of cellular uptake with the hydrophobic interaction between the alkyl chains [1-2]. In fact, too long alkyl chain decreases the water solubility of gene carrier. Thus, effective linker is combination of hydrophobic segments and hydrophilic segments. Such linker also should be incorporated between stearoyl group and BPEI backbone because the structure freedom of stearoyl groups could help interaction with serum albumin considering undesirable steric hindrance of the peptide chains.

In the view of synthesis step, two modifications of peptide and stearoyl group are not complicate. The many primary amine groups of the BPEI backbone are acceptable to amide bond formation with carboxyl groups of peptide and stearoyl group. Although the modification of stearoyl groups needs to be performed before the peptide incorporation because of steric hindrance of the peptide chains, reaction step is able to be synthesized continuously using a coupling reagent. The simple design and synthesis step of peptide- and stearoyl-modified BPEI will accelerate the clinical use of cancer-selective gene expression system.

5.3. Perspective

In this thesis, the author achieved the high physiological stability of polyplex, the simple synthetic process of peptide-polymer conjugate, and also elucidated the linker length affected to PKCα responsiveness. More practical peptide-polymer conjugates will be able to be designed by using these findings. In general, accumulation of polyplex in target tumor and evaluation of the therapeutic effect are the major categories to be investigated for the development of nanocarriers. Firstly, in systemic administration, small particles of polyplex (< 100 nm) accumulate in tumor tissues efficiently and show rather high gene expression compared to large particles (ca. 200 nm) [3-4]. Herein, it has been known that small polyplex can be obtained by using diluted pDNA condition [5-6]. However, concentration technique such as lyophilization will be required for *in vivo* application. In this thesis, the author elucidated that reversible coating of polyplex with serum albumin allowed lyophilization keeping its characteristics. Secondly, suicide gene has an advantage to demonstrate a powerful treatment effect [7-8]. In particular, caspase-8 showed suppression of tumor growth in previous studies [9]. However, such gene may cause severe adverse effect in non-target organs. PKCα responsive gene regulation carriers demonstrated in this thesis will solve this issue by suppressing undesired activation of the gene in normal organs. Together with all findings here, the peptide- and stearoyl-modified BPEI will be optimized nanocarriers for tumor selective gene therapy. It will form small ternary complex with pDNA and serum albumin, and will be able to suppress tumor growth through intravenous injection.

In the future, the author hopes that combination of various technologies advances systemic administration and cancer selective gene expression of PKCα-responsive gene carriers. In particular, it is necessary to design polymer, linker

and peptide, then to control size and surface property of nanocarriers for safe and efficient gene delivery.

5.4. References

[1] R. Toita, J. H. Kang, T. Tomiyama, C. W. Kim, S. Shiosaki, T. Niidome, T. Mori, Y. Katayama, *J. Am. Chem. Soc*., **134**, 15410 (2012).

[2] C. W. Kim, R. Toita, J. H. Kang, K. Li, E. K. Lee, G. X. Zhao, D. Funamoto, T. Nobori, Y. Nakamura, T. Mori, T. Niidome, Y. Katayama, *J. Control. Release*, **170**, 469 (2013).

[3] R. Kircheis, L. Wightman, A. Schreiber, B. Robitza, V. Rössler, M. Kursa, E. Wagner, *Gene Ther*., **8**, 28 (2001).

[4] P. Chollet, M. C. Favrot, A. Hurbin, J. L. Coll. *J. Gene Med*., **4**, 84 (2002).

[5] T. Ito, N. Iida-Tanaka, Y. Koyama, *J. Drug Target*., **16**, 276 (2008).

[6] K. Miyata, Y. Kakizawa, N. Nishiyama, Y. Yamasaki, T. Watanabe, M. Kohara, K. Kataoka, *J. Control. Release*, **109**, 15 (2005).

[7] S. Kumar, *Cell Death Differ*., **14**, 32 (2007).

[8] C. H. Homburg, M. de Haas, A. E. von dem Borne, A. J. Verhoeven, C. P. Reutelingsperger, D. Roos, *Blood*, **85**, 532 (1995).

[9] T. Tomiyama, R. Toita, J. H. Kang, D. Asai, S. Shiosaki, T. Mori, T. Niidome, Y. Katayama, *J. Control. Release*, **148**, 101 (2010).

Accomplishments

Publications

1) Y. Nakamura, C. W. Kim, A. Tsuchiya, S. Kushio, T. Nobori, K. Li, E. K. Lee, G. Xi Zhao, D. Funamoto, T. Niidome, T. Mori, Y. Katayama, Branched polyethylenimine-based PKCα-responsive gene carriers, *J. Biomater. Sci.-Polym. Ed.*, **24**, 1858 (2013).

2) D. Funamoto, D. Asai, C. W. Kim, Y. Nakamura, E. K. Lee, T. Nobori, T. Niidome, T. Mori, Y, Katayama, Tandemly repeated peptide for cancer-specific gene carrier prepared by native chemical ligation, *Chem. Lett*. **44**, 474 (2015).

3) K. Li, H. Sato, C.W. Kim, Y. Nakamura, G.X. Zhao, D. Funamoto, T. Nobori, A. Kishimura, T. Mori, Y. Katayama, Tumor accumulation of protein kinase-responsive gene carrier/DNA polyplex stabilized by alkanethiol for intravenous injection, *J. Biomater. Sci. Polym. Ed*., **26**, 657 (2015).

4) G. X. Zhao, H. Tanaka, C. W. Kim, K. Li, D. Funamoto, T. Nobori, Y. Nakamura, T. Niidome, A. Kishimura, T. Mori, Y. Katayama, Histidinylated poly-L-lysine-based vectors for cancer-specific gene expression via enhancing the endosomal escape, *J. Biomater. Sci. Polym. Ed*., **25**, 519 (2014).

5) T. Nobori, S. Shiosaki, T. Mori, R. Toita, C. W. Kim, Y. Nakamura, A. Kishimura, T. Niidome, Y. Katayama, A fluorescent polyion complex nanoparticle that incorporates an internal standard for quantitative analysis of protein kinase activity, *Bioconjugate Chem*., **25**, 869 (2014).

6) H. Sato, Y. Nakamura, E. Nakhaei, D. Funamoto, C. W. Kim, T. Yamamoto, A. Kishimura, T. Mori, Y. Katayama, A liposome reversibly coated with serum albumin, *Chem. Lett*., **43**, 1481 (2014).

7) S. Kushio, A. Tsuchiya, Y. Nakamura, T. Nobori, C. W. Kim, G. X. Zhao, T. Funamoto, E. K. Lee, K. Lee, T. Niidome, T. Mori, Y Katayama, Cancer-specific gene carriers responding to cancer microenvironment: acidosis and hyper-activated protein kinases, *Biomed. Eng*. **25**, 1340005 (2013)

8) S. Shiosaki, T. Nobori, T. Mori, R. Toita, Y. Nakamura, C. W. Kim, T. Yamamoto, T. Niidome, Y. Katayama, A protein kinase assay based on FRET between quantum dots and fluorescently-labeled peptides, *Chem. Commun*., **49**, 5592 (2013).

9) C. W. Kim, R. Toita, J. H. Kang, K. Li, E. K. Lee, G. X. Zhao, D. Funamoto, T. Nobori, Y. Nakamura, T. Mori, T. Niidome, Y. Katayama, Stabilization of cancer-specific gene carrier via hydrophobic interaction for a clear-cut response to cancer signaling, *J. Controlled Release*, **170,** 469 (2013).

Symposium and Awards

1) *The 136th Annual Meeting of the Pharmaceutical Society of Japan*, **Oral Presentation**, GS02-4, Kanagawa, Japan, March 2016.

2) *The Lecture Meeting of Seibu Branch, the Society of Fiber Science and Technology, Japan*, **Oral Presentation**, Kumamoto, Japan, January 2016, **Invited Lecture**.

3) *Pacifichem 2015*, *Poster Presentation*, 667, Hawaii, USA, December, 2015.

4) *The 31st Annual Meeting of the Japan Society Drug Delivery System*, **Oral Presentation**, 1-5-06、Tokyo, Japan July 2015, **Presentation Award**.

5) *The 52th Joint Meeting in Kyushu of Chemical Affiliates*, **Poster Presentation**, PF-4-0048, Fukuoka, Japan, June 2015, **Poster Award**.

6) *The Lecture Meeting in Kyushu of the Japanese Society for Biomaterials*, **Poster Presentation**, 23, Fukuoka, Japan, September 2014.

7) *The 15th IUMRS-International Conference in Asia*, **Poster Presentation**, B1-P26-018, Fukuoka, Japan, August, 2014.

8) *The 94th Annual Meeting of the Chemical Society of Japan*, **Oral Presentation**, 3G2-37, Nagoya Japan. March 2014.

9) *The 23th Biopolymers Science Symposium*, **Oral Presentation**, 10, Tokyo, Japan, July 2013.

10) *The 61th SPSJ Annual Meeting*, **Poster Presentation**, 1Pa123, Kyoto, Japan, May, 2013.

11) *The 49th Joint Meeting in Kyushu of Chemical Affiliates*, **Poster Presentation**, 5_6.082, Fukuoka, Japan, June, 2012.

12) *The 61th SPSJ Annual Meeting*, **Poster Presentation**, 1Pf146, Kanagawa, Japan, May, 2012.

Acknowledgements

I would like to acknowledge precious experience over the last six years and a great relationship in Katayama laboratory. I could not complete my doctoral thesis, if I did not meet people who have helped my study in Kyushu University.

Firstly, I am deeply grateful to Professor Yoshiki Katayama for his suggestive advice and close assistance during the research. His constant pointer guides my researcher's life so that my doctoral thesis is fulfilled.

I would like to thank my doctoral thesis committee members; Professor Masamichi Kamihira and Professor Masahiro Goto, for their invaluable advice and questions.

Moreover, special thanks to Associate Professor Takeshi Mori in working through many problems in my research. His valuable advice and helpful assistance give me the power of research accomplishment. I practice a lot of presentation and discussion in my research due to his daily care. My Doctor of Philosophy degree receives his knowledge and encouragement.

I would like to thank the advice of Associate Professor Akihiro Kishimura in polymer science. I express my gratitude to Professor Takuro Niidome (Kumamoto University) and his special technique in peptide synthesis 'pepti-do'. I also want to thank Associate Professor Tatshuhiro Yamamoto, Dr. Jeong-Hun Kang (National Cerebral and Cardiovascular Center), and Dr. Daisuke Asai (St. Marianna University School of Medicine) for their kind advice in various experiment.

I thank Professor Masahiro Goto and Professor Noriho Kamiya for assistance in CLSM study. I also thank this work was financially supported by a Grant-in-Aid for Scientific Research from the Ministry of Education, Culture, Sports, Science and Technology of Japan.

Special thanks to my D-RECS group members, Dr. Akira Tsuchiya (Kyushu University), Mr. Satoshi Kushio, Dr. Shujiro Shiosaki, Dr. Chan Woo Kim (Catholic University of Korea), Dr. Daiki Funamoto (Kyushu University), Dr. Eun Kyung Lee, Dr. Hiroyuki Tanaka, Dr. Guo Xi Zhao, Mr. Hiroyuki Kawanami, Mr. Kai Li, Mr. Takanobu Nobori, Mr. Yu Tahara, Ms. Ayako Yanagida, Ms. Hikari Sato, Ms. Hotaru Matsumoto, Ms. Shoko Toyama, and Mr. Tomohiro Shuno.

I am also grateful to the other members of Katayama laboratory. Ms. Mari Miyazaki's support was kind and emotional in my laboratory life. My junior colleagues also give me cheerful days.

I would particularly like to express their thanks to my colleagues, Mr. Hiroki Otsubo, Mr. Nobukatsu Chijiiwa, Mr. Masayoshi Matsuda, Ms. Hengmin Tang, Ms. HisayoYamauchi for my daily laboratory life.

In particular, I deeply appreciate my parents; Mr. Koji Nakamura, Ms. Reiko Nakamura, and older brother; Mr. Yoshitaka Nakamura of gracious encouragement and constant supporting throughout 9 years college days from undergraduate course to doctoral course.

January 2017

Yuta Nakamura